学位論文

Studies on bioactive compounds from Cameroonian medicinal plants, *Acacia albida* and *Albizia chevalieri*, and Japanese endophytes *Xylaria* sp.

(カメルーン産薬用植物 *Acacia albida* と *Albizia chevalieri* と日本で分離された植物内生菌類 *Xylaria* sp.の生理活性物質に関する研究)

Abdou Tchoukoua

To

My late mom

DJEBBA M. Odile

Acknowledgments

This thesis was successful with the support of a number of people to whom I am greatly indebted.

I would like to express my sincere gratitude to my supervisors, **Prof. Dr. Yoshihito Shiono** (Yamagata University, Japan) and **Prof. Ngadjui T. Bonaventure** (University of Yaounde I, Cameroon) for the guidance, support, and motivation during all the time of my research in their labs. Their help will always be deeply appreciated.

I would also like to thank the **JSPS-Ronpaku Program** for financial support in Japan.

I wish to express my gratitude to **Prof. M. Hashimoto, Prof. Y. Tokuji, Prof. K. Kimura,** and **Prof. T. Koseki**, for their participation as judging committee.

I wish to thank all the people with whom I have worked and contributed to the development of this work.
Great thanks to **Prof. Dr. Özgen Çaliskan** for my sojourn in her lab, and to **Dr. Ibrahim Horo** in offering his expertise in isolation of saponins.

I wish to thank **Prof. K. Kimura** for analyses of biological activities.

I thank **Drs Eunsang Kwon** and **Hiroyuki Momma** for measurements of ESI-MS spectra.

I am particularly grateful to **Dr. T. Tabopda** for his contribution to the success of this investigation. It has been a pleasure working with you.

I thank the **staff members** of the **Department of Organic Chemistry** of the **University of Yaounde I** for my university education.

I wish to thank **Profs. T. Koseki** and **T. Murayama**, for their support and **all my workmates** from Yamagata University, it was great sharing laboratory with all of you during my stay in Japan.

I wish to thank my senior **Dr H. M. Poumale** for having introduced me to Prof. Y. Shiono, and **all my workmates** and **friends** from the University of Yaounde I. Thanks for all your encouragement.

This thesis is dedicated to my grateful dad **H. Tchoukoua**, my late mother **M. O. Djebba**, I forever miss you. To you my **brothers** and **sisters** thank you for your encouragements.

To my loving family, **P. C. Fanta, J. S. Awoudammike** for their unconditional love.

I am thankful to you all who supported me directly or indirectly to complete this research work.

Thank you very much, everyone!

List of abbreviations

$[\alpha]_D$	specific optical rotation
δ	chemical shift value
λ_{max}	wavelength of maximun absorption
1D	1-dimensional
2D	bidimensional
^{13}C-NMR	carbon 13-nuclear magnetic resonance
^{1}H-NMR	proton nuclear magnetic resonance
Ara	arabinose
brs	broad singlet
CC	Column Chromatography
COSY	COrrelation SpectroscopY
d	doublet
dd	double doublet
DEPT	Distortionless Enhancement by Polarisation Transfer
ESI	ElectroSpray Ionization
EtOAc	ethyl acetate
Fuc	fucose
Glc	glucose
GlcNAc	*N*-acetyl-D-glucosamine
HRMS	high-resolution mass spectrometry
H_2O	water
H_2SO_4	sulfuric acid
Hex	hexane
HMBC	Heteronuclear Multiple Bond Correlation
HMQC	Heteronuclear Multipe Quantum Correlation
HPLC	High Performance Liquid Chromatography
HPTLC	High Performance Thin Layer Chromatography
HR	High Resolution
Hz	hertz
IC_{50}	inhibitory concentration of 50%
J	coupling constant

m	multiplet
MeOH	methanol
MPLC	medium pressure liquid chromatography
MS	mass spectroscopy
MTT	3-(4,5-dimethylthiazol-2-yl)-2,5-diphenyltetrazolium bromide
m/z	mass to charge ratio
n.d.	not determined
NOE	Nuclear Overhauser Effect
NOESY	Nuclear Overhauser Enhancement SpectroscopY
ppm	parts per million
Rha	rhamnose
RP	reverse phase
s	singlet
t	triplet
TLC	Thin Layer Chromatography
TMS	TetraMethyl Silane
TOCSY	TOtal Correlation SpectroscopY
VLC	Vacuum Liquid Chromatography
Xyl	xylose

List of figures

List of tables

List of schemes

Abstract

The isolation and characterization of bioactive substances from medicinal plants and endophytes is done using chromatographic and spectroscopic methods.
The polar extracts of *Acacia albida* and *Albizia chevalieri* species (Mimosaceae), and culture filtrates of endophytic fungi of *Xylaria* sp. are investigated. The dissertation consists of the following three parts:

Triterpene saponins from Acacia albida (Mimosaceae)
Chemical investigation of the roots of *A. albida* resulted in the isolation of seven new bidesmosidic triterpenoid saponins named albidosides A – G. Their structures were elucidated using 1D and 2D NMR spectroscopy and mass spectrometry and determined to be bidesmosides of oleanolic acid and 16α-hydroxyoleanolic acid (echinocystic acid). The isolated compounds were assayed for their cytotoxicity against HeLa and HL60 cells using MTT method and microscopic observation. Albidosides E and F showed cytotoxicity against the cell lines studied and induced cytolytic phenotype immediately through membrane damaging effects. Although some saponins showed apoptotic cell death, albidosides E and F did not form apoptotic bodies.

A further detailed investigation of the barks of *Acacia albida* resulted in the isolation of the two additional triterpene saponins named albidosides H and I. These compounds were evaluated for their cytotoxicity against two human cancer cells, HeLa and HL60. Albidoside H exhibited strong cytotoxic effect (IC_{50} 12.7 μM on HL60 and 20.8 μM on HeLa) while albidoside I exhibited weak cytotoxicity.

Two new 5-deoxyflavan-3,4-diol glucosides from the roots of Albizia chevalieri (Mimosaceae)
Phytochemical investigation of the roots of *Albizia chevalieri* led to the isolation of two new 5-deoxyflavan-3,4-diol glucosides, chevalieriflavanosides A and B. Their structures were established by 2D NMR techniques, UV, IR, CD, and mass spectrometry. These compounds were screened for their cytotoxicity against HL60 cells. The antibacterial activities of the new compounds also were evaluated against

Pseudomonas aeruginosa and *Staphylococcus aureus* using the agar diffusion test. However, the tested compounds displayed no significant cytotoxic activity towards HL60 cells at the concentration of 100 μM, but they exhibited weak antibacterial activity at 100 μg/disk.

Metabolites from endophytic fungi of Xylaria sp. (Xylariaceae)

The fungal strain *Xylaria* sp. V-27 was isolated from a dead branch collected in Yamagata, Japan. This strain was then cultured on the steamed unpolished rice medium for four weeks. After cultivation the organic extract was subjected to silica gel and octadecyl silica gel (ODS) column chromatography to afford a new eremophilane sesquiterpene 13,13-dimethoxyintegric acid, together with known compound integric acid as the most abundant constituent of the mycelial extract. The structure of the new compound was established by means of spectroscopic analyses. The isolated compounds indicated growth restoring activity against the mutant yeast strain [*Saccharomyces cerevisiae* (*zds1*Δ *erg3*Δ *pdr1*Δ *pdr3*Δ)] and inhibited degranulation of rat basophilic leukemia RBL-2H3 cells stimulated by IgE+DNP-BSA, Thapsigargin and A23187, respectively.

From endophytic fungus *Xylaria curta*, a new bicyclic lactone was isolated along with two known metabolites, myrotheciumone A and 4-oxo-4H-pyron-3-acetic acid from the ethyl acetate extract. The structures of these compounds were elucidated on the basis of spectroscopic methods (UV, IR, HRESITOFMS, 1D and 2D NMR). The novel lactone isolated from *X. curta* was found to be another rare 5/5 rings-fusion system in a naturally occurring compound. This compound showed moderate antibacterial activity.

Keywords: *Acacia* sp., triterpene saponins, cytotoxicity, *Xylaria* sp., eremophilane, Ca^{2+}-signaling, degranulation, phytotoxicity.

CONTENTS

General Introduction

1. General Introduction

The use of medicinal plants in the treatment of disease dates back several millennia. Plants are for that purpose the major sources used in the treatment of pathologies. The Pharmacopoeia known traditionally is a fast and low cost access to health care. Whereas, despite extraordinary advances in science and technology and their application in the field of modern medicine, the use of plants as an alternative or traditional medicine in the health system seems to be on a rise.

Moreover, several alarming reports from the World Health Organization (WHO, 2002, 2003, 2005) has indicated that the main source and route of access to health care for people in less developing countries in regions without or remote health centers and / or victims of wars, natural catastrophes with more than 60% in Africa and Asia use exclusively traditional plants based medicine. It means that herbal medicine has remained until today the main remedy for treating pathological signs of disease by humanity. This situation pushed laboratories in chemistry, biochemistry, biology and other fields of applied research worldwide to max out traditional medicine in search of new active principles whose application becomes increasingly growing even in developed countries.

However, the main objective of these laboratories and scientific scientists being to find new active molecules that can help to treat a range of diseases such as cancer, leukemia, malaria, HIV/AIDS, that constituted a significant and major challenge for researchers today. Natural substances of vegetable or marine origin are an inexhaustible reservoir of new secondary metabolites with little or no exploration on their activities that may a prerequisite for give hint on the development of new drugs.

Recent trends show that the discovery rate of novel bioactive molecules from plants is declining. Moreover, environmental degradation and loss of biodiversity, also add to problems facing mankind. Therefore, the need to bioprospecting new sources and habitats to maximize the discovery of novel metabolites is great.

Being poorly investigated, endophytes are obviously a rich and reliable source of bioactive and chemically novel compounds with huge medicinal and agricultural potential.

The purpose of this study was aimed to search new secondary metabolites from polar extracts of *Acacia albida* and *Albizia chevalieri* species (Leguminosae-Mimosoideae), and investigate endophytic fungi of two Xylariaceous fungi, *Xylaria* sp. V-27, and *Xylaria curta.*

Chapter 1 reports the isolation and structure elucidation of new saponins from polar extract of *Acacia albida*. Cytotoxicity against HL60 and HeLa cells are reported.

Chapter 2 reports the isolation of new flavan-3,4-diol glucosides from *Albizia chevalieri*. Cytotoxicity against HL60 cells and antibacterial activity are also reported.

Chapter 3 described the isolation, and structure elucidation of biologically active secondary metabolites produced by two Xylariaceous fungi, *Xylaria* sp. V-27, and *Xylaria curta*.

Chapter 1

Triterpene saponins from *Acacia albida* (Mimosaceae)

1.1. Botanical study

1.1.1. Order Fabales

The order Fabales consists of 4 families (Fabaceae, Polygalaceae, Quillajaceae and Surianaceae) and about 19,000 species (Judd et al., 2002).

1.1.1.1. Fabaceae

The legume family (Fabaceae) is the third largest family of flowering plants with more than 18,000 described species. It is surpassed in size only by the orchid family (Orchidaceae) with about 20,000 species and the sunflower family (Asteraceae) with about 24,000 species (Parrotta, 2002).

The family includes herbs, shrubs, trees and vines distributed throughout the world, especially the tropical rain forest.

The **leaves** are usually alternate and compound.

The **flowers** always have five generally fused sepals and five free petals. They are generally hermaphrodite, and have a short hypanthium, usually cup shaped. They are usually arranged in indeterminate inflorescences.

The **fruit** is technically called a legume or pod. It is composed of a single seed-bearing carpel that splits open along two seams (Parrotta, 2002).

The family of Fabaceae (=Leguminosae) is subdivided into three subfamilies: Caesalpinioideae, Faboideae (=Papilionoideae), and Mimosoideae (Judd et al., 2002).

1.1.2. Mimosoideae

The sub-family Mimosoideae comprises about 60 genera and 3000 species worldwide, widespread in tropical and subtropical regions, especially in arid and semi-arid climates.

They are mainly tree, shrubs, lianes or rarely herbs.

The **leaves** alternate, mostly bipinnate, rarely simply pinnate, often with large glands on the rhachis. Stipules mostly present.

The **flowers** in spikes, racemes, are hermaphrodites, actinomorphic and usually 5-merous. Calyx of (3)5(6) sepals, free or united, sometimes reduced or absent. Corolla of (3)5(6) petals, free or joined below to form a tube. Stamens 4-10 or numerous, free or connate below, commonly coloured and long exserted. Carpels 1 or rarely several,

and free.

The **fruit** is a legume, generally a flattened pod.

The **seeds** often with an elongate funicle, with scanty or no endosperm.

The main genera of Mimosoideae are *Acacia, Albizia, Archidendron, Entada, Mimosa,* and *Pithecellobium*.

1.1.2.1. *Acacia*

1.1.2.1.1. Classification

Kingdom: Plantae

Sub-kingdom: Tracheobionta

Division: Magnoliophyta (Angiosperms)

Class: Magnoliopsida (Dicotyledons)

Subclass: Rosidae

Order: Fabales

Family: Fabaceae

Subfamily: Mimosoideae

Genus: *Acacia*

1.1.2.1.1. Botanical aspect and distribution

Acacia is the 2nd largest genus in the Leguminosae family, comprising more than 1200 species worldwide, with members found in almost all habitats. Of the 1200 *Acacia* species worldwide, 700–800 occur in Australia and 129 in Africa, a small number in Asia, and the remainder (about 200 species) in the rest of the world (Doran et al., 1983).

They are trees or shrubs, sometimes spiny.

The **leaves** bipinnate, modified into phyllodes or rarely absent; glands often present.

The **flowers** in spikes are hermaphrodite or male. Calyx usually 4-5-lobed. Corolla 4-5-lobed. Stamens numerous, mostly free.

The **pods** variable, flat to cylindrical, straight, curved, coiled or twisted, dehiscent or indehiscent.

The **seeds** typically with a well developed aril.

1.1.2.2. *Acacia albida*

1.1.2.2.1. Botanical aspect and distribution

Acacia albida is a tree up to 24 m in height, with large straight bole, up to 3 m in girth, and rounded crown. The bark of twigs pale grey, of bole thick, brown, fissured. Spines white straight, thick, up to 1.5 cm long. in pairs, stipular in origin.

The **leaves** are glaucous green, leafless during rainy season.

The **flowers** cream, becoming yellow.

The **fruits** at length sickle-shaped, thick, orange when mature, indehiscent.

A. albida extends throughout the drier parts of northern Africa into Egypt, also in eastern and southern Africa.

Acacia albida (Tree)
Photo Abdou T.

Acacia albida (Flower)
www.royalbotanicgarden.org

1.2. Ethnomedicinal value of *Acacia albida*

In folkloric medicine, a decoction of the bark is used in cleansing fresh wounds, in a manner similar to that of potassium permanganate, used as an emetic in fevers by the Masai people of East Africa, taken for diarrhoea in Tanganyika (Irvine, 1961) and for colds, haemorrhage, leprosy and ophthalmic in West Africa. A liniment, made by steeping the bark, is used for bathing and massage in pneumonia. The bark infusion is

used for difficult delivery, and is used as a febrifuge for cough (Tijani et al., 2009). In northern Nigeria, especially among the cattle rearing nomads, a decoction of the stem bark is taken orally for the management of the sleeping sickness and malaria.

Acacia albida possess anti-pyretic, anti-inflammatory, anti-diarrhoea (Tijani et al., 2008), anti-trypanosomiasis (Tijani et al., 2009) and anti-malarial activity (Tijani et al., 2010). The stem bark is reported to have antibacterial activity (Wurochekke et al., 2013).

1.3. Chemical constituents in the genus *Acacia*

In recent years, there have been studies on the chemical components of several *Acacia* species (Seigler, 2003). A number of secondary metabolites have been reported including diterpenes, triterpenes, flavonoids, and saponins, among other compounds (Seigler, 2003). Our interest will focus towards the triterpene saponins from this genus.

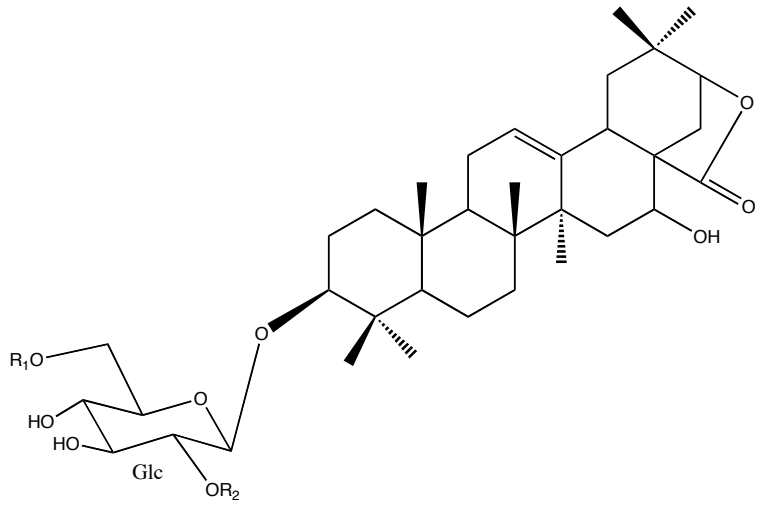

N°	R1	R2	Source	Reference
1.1	Glc	Ara	*Acacia auriculiformis*	Mahato et al., 1989
1.2	Glc	H	*Acacia auriculiformis*	Garai and Mahato, 1997
1.3	H	Ara	*Acacia auriculiformis*	Garai and Mahato, 1997

Fig I.1. Structures of acaciaside and proacasiaside-I & -II

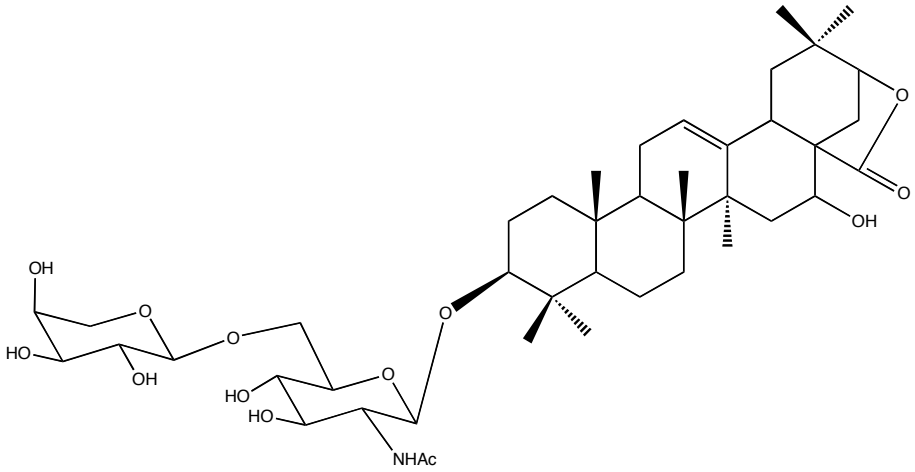

N°	Source	Reference
1.4	*Acacia auriculiformis*	Garai and Mahato, 1997

Fig. I.2. Structure of acaciamine

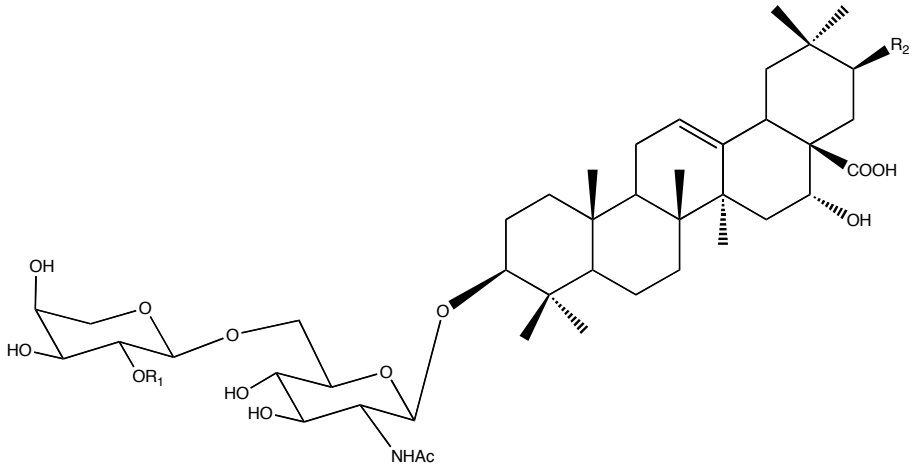

N°	R1	R2	Source	Reference
1.5	Xyl	H	*Acacia tenuifolia*	Seo et al., 2002
1.6	Xyl	OCOCH=CHPH	*Acacia tenuifolia*	Seo et al., 2002
1.7	Ara	OCOCH=CHPH	*Acacia tenuifolia*	Seo et al., 2002

Fig I.3. Structures of acaciosides

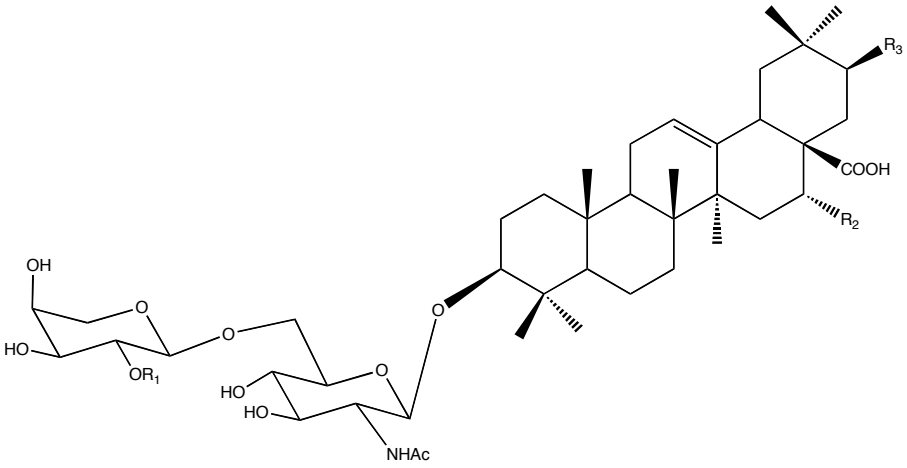

N°	R1	R2	R3	Reference
1.8	Xyl	H	H	Seo et al., 2002
1.9	Ara	H	H	Seo et al., 2002
1.10	Ara	OH	H	Seo et al., 2002

Fig I.4. Structure of compounds from *Acacia tenuifolia*

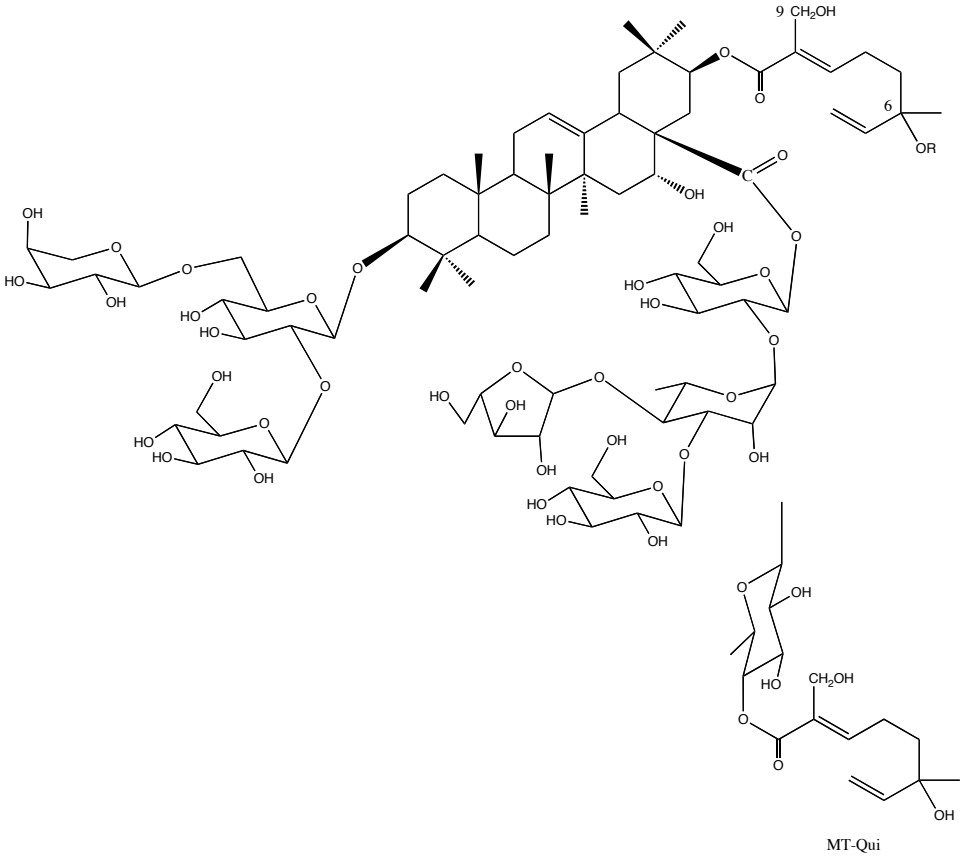

N°	R	Source	Reference
1.11	MT-Qui, 6=R	*Acacia concinna*	Tezuka et al., 2000
1.12	MT-Qui, 6=S	*Acacia concinna*	Tezuka et al., 2000
1.13	H	*Acacia concinna*	Tezuka et al., 2000

Fig. I.5. Structure of kinmoonosides

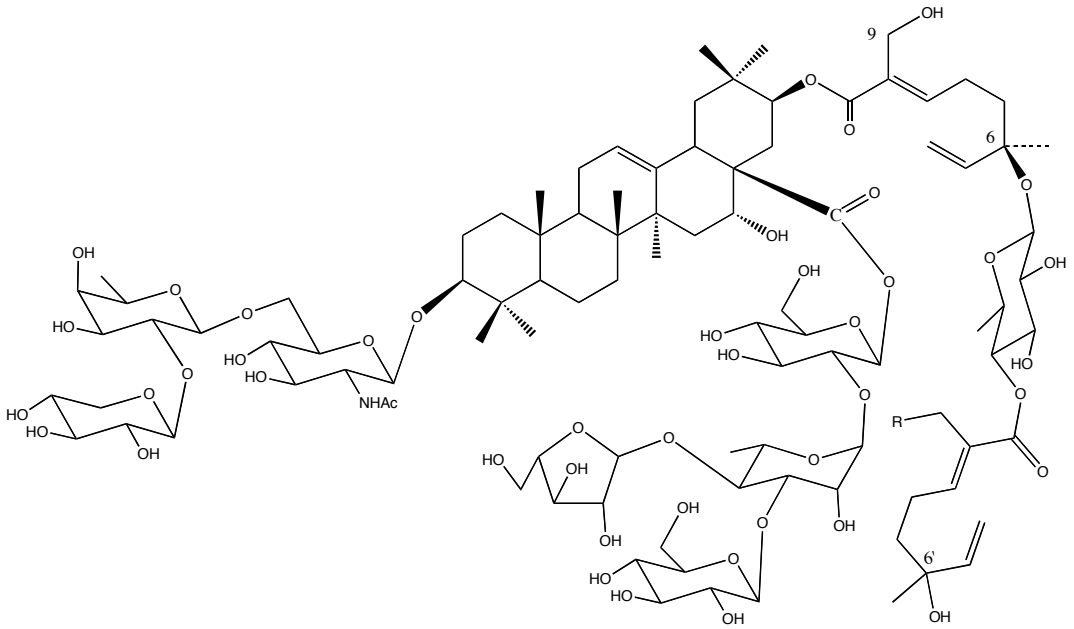

N°	R	Source	Reference
1.14	OH	*Acacia victoriae*	Jayatilake et al., 2003
1.15	H	*Acacia victoriae*	Jayatilake et al., 2003

Fig. I.6. Structure of avicins

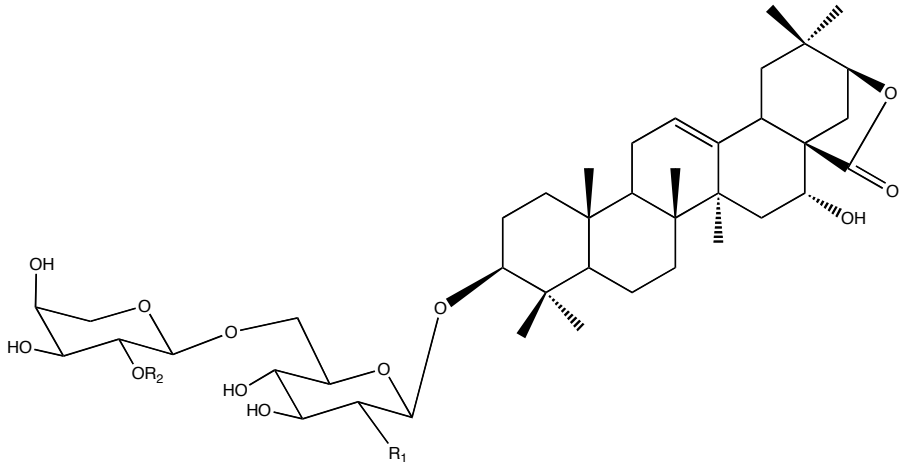

N°	R1	R2	Source	Reference
1.16	NHAc	H	*Acacia concinna*	Gafur M.A. et al., 1997
1.17	NHAc	Ara	*Acacia concinna*	Gafur M.A. et al., 1997
1.18	Glc	Xyl	*Acacia concinna*	Gafur M.A. et al., 1997

1.19	OH	H	*Acacia concinna*	Gafur M.A. et al., 1997

Fig. I.7. Structure of concinnosides (B, D, F and A)

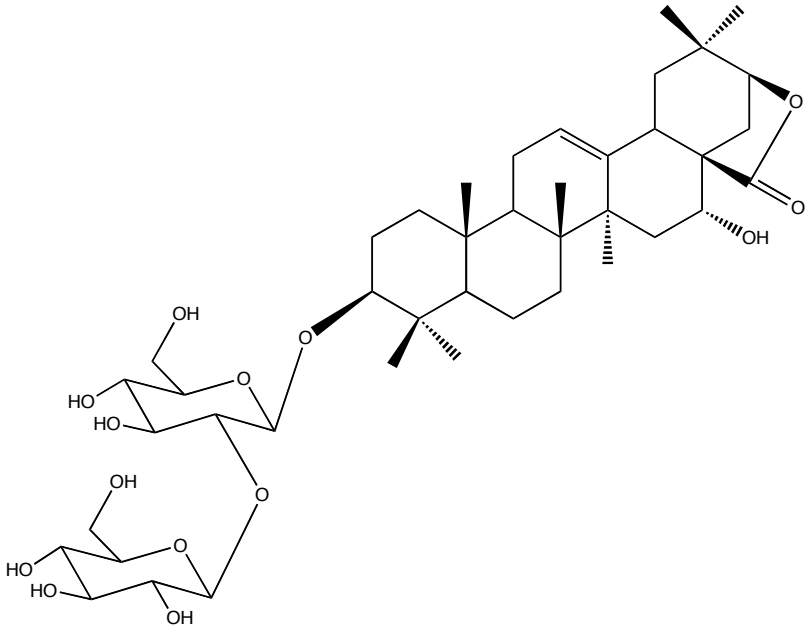

Fig. I.8. Structure of concinnoside C (Source: *Acacia concinna*)

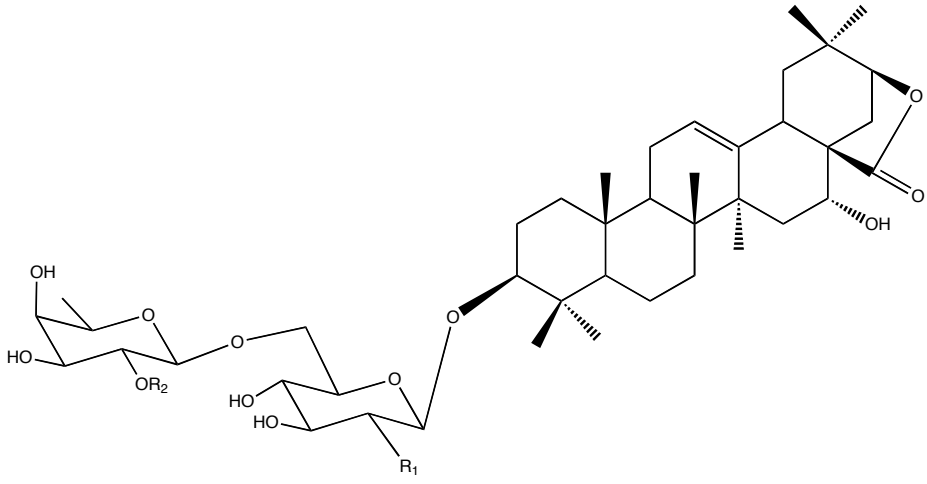

N°	R1	R2	Source	Reference
1.20	Glc	H	*Acacia concinna*	Gafur M.A. et al., 1997
1.21	NHAc	Xyl	*Acacia concinna*	Gafur M.A. et al., 1997

1.22	Glc	Xyl	*Acacia concinna*	Gafur M.A. et al., 1997

Fig. I.9. Structures of concinnoside E and julibroside-A3 & -A1

1.4. Pharmacological properties of saponins from *Acacia*

1.4.1. Introduction

Saponins have been ascribed a number of pharmacological actions (Hostetteman et Marston, 1995; Sparg et al., 2004; Thakur et al., 2011; Lacaille-Dubois et al., 2011).

Cancer-related activity is among the most studied pharmacological property of saponins in the last years. They were shown to be cytotoxic against a large panel of cancer cells and this activity seems to be related to their apoptosis inducing potential (Lacaille-Dubois, 2005).

Plants from the Mimosoideae are known for their medicinal value (Allen and Allen, 1981) and several saponins have been isolated that inhibit the growth of tumor cells in vitro (Abdel-Kader et al., 2000; Mujoo et al., 2001; Seo et al., 2002; Jayatilake et al., 2003; Haddad et al., 2003).

The following section of our dissertation will summarize some of the important recent cancer-related studies on saponins from the genus *Acacia* mainly on cytotoxic/antitumor and apoptosis inducing properties.

1.4.2. Saponins as anti-cancer agents

Plants are a rich source of compounds that can induce apoptosis in premalignant or malignant human cells (Pezzuto, 1997) and most of the cancer-related studies on saponins from Mimosoideae were performed in vitro by using cancer cell culture models.

1.4.3. In the genus *Acacia*

In recent years, there have been studies on the chemical components of several *Acacia* species.

1.4.3.1. *Acacia concinna*

Acacia concinna Wall. (Leguminosae) is a medicinal plant that grows in tropical rainforests of southern Asia, and the fruits of this plant are used for washing hair, for promoting hair growth, as an expectorant, emetic, and purgative.

The MeOH extract of the fruits of *A. concinna* from Myanmar showed significant cytotoxicity against human HT-1080 fibrosarcoma cells (Tezuka et al., 2000). Three new genuine saponins, named kinmoonosides A–C (**fig. I.5)**, have been isolated.

These compounds were found to be significantly cytotoxic against human HT-1080 fibrosarcoma cells with ED_{50} values of 0.70, 0.91, and 2.83 μM, respectively. Their cytotoxicity was greater than that of 5-fluorouracil (ED_{50}, 8.0 μM). ED50 values of < 4 μg/mL are regarded as being significantly cytotoxic.

The ester moiety found at C-21 of the aglycone is not crucial for the cytotoxicity but may rather intensify the activity.

1.4.3.2. *Acacia tenuifolia*

Acacia tenuifolia (L.) Willd., is a climbing shrub, or a small tree distributed in Suriname. The methanol extract was found to show activity against the genetically engineered *Saccharomyces cerevisiae* mutant (1138, 1140, 1353 and Sc-7) yeast strains tested with IC_{12} values of 6000, 5500, 5200, and 4000 μg/ml, respectively (Seo et al., 2002). IC_{12} represents the concentration (in μg/ml) required to produce an inhibition zone of 12 mm diameter around a 100 μl well in the yeast strain in question (Gunatilaka et al., 1994). An extract is considered active if it shows selective activity against one or more repair-deficient yeasts (IC_{12} less than one-third that of the wild-type yeast) and has an IC_{12} less than 2000 μg/ml (Gunatilaka et al., 1994).

Seo et al., 2002, isolated three new saponins (acaciosides A–C, **fig. I.3**) and three known saponins from *Acacia tenuifolia* using bioassay-guided fractionation. The saponins showed weak activity against the mutant yeast strains tested.

Two of the known saponins, which were previously isolated by Abdel-Kader et al., 2001, showed significant cytotoxic activity against the M 109 lung cancer cell line, with IC_{50} values of 1 μM. The new saponins showed weak activity against the A 2780 ovarian cancer cell lines.

1.4.3.3. *Acacia victoria*

Acacia victoriae Benth. (Leguminosae) thrives in semiarid and arid lands, typically along dry waterways (rivers, streams, and arroyos) that are subject to intermittent rains and flooding, and tolerates relatively poor clay-like and sandy soils having potentially high salinity. The traditional use of *Acacia victoriae* as a medicinal plant is not documented.

Efforts to identify plant compounds that may selectively induce apoptosis of cancer cells revealed that an aqueous MeOH extract of the seed pods of *A. victoriae* induced

significant (IC_{50} 0.38 µg/mL) cell cycle arrest in Jurkat cells in vitro (Haridas et al., 2001).

Jayatilake et al., 2003, isolated two new saponins named avicins D and G (**fig. I.6**) from that desert legume plant.

Avicins D and G were found to inhibit the growth of Jurkat cells at lower concentrations, and promoted apoptosis by activation of caspases and cytochrome c release (Haridas et al., 2001).

Avicins induce cell cycle arrest of the human MDA-MB-453 breast cancer cell line and apoptosis of the Jurkat (T-cell leukemia) and the MDA-MB-435 breast cancer cell line. Avicins also partially inhibited signaling through the phosphatidylinositol 3-kinase (PI3K) pathway and phosphorylation in the downstream protein Akt (Mujoo et al., 2001).

Furthermore Avicin G inhibited activation and DNA binding of NF-kB (nuclear transcription factor-kB) (Haridas et al., 2001). This avicin decreased the expression of inducible nitric oxide synthase (iNOS) and cyclooxygenase (COX-2) as described for ginsenosides metabolites (Lee et al., 2005; Oh et al., 2004).

Avicin D induced the expression of nuclear factor erythroid 2-related factor 2, a transcription factor, which mediates the expression of several detoxifying and antioxidant proteins (Haridas et al., 2004).

The protective effect was underlined by UV radiation of mice treated with avicin D, where severe damage and mutations were prevented. A mixture of avicins showed additional protective effects against papilloma-inducing chemicals 7,12-dimethylbenzanthracene (DMBA) and phorbol 12-tetradecanoate 13-acetate (TPA) in mice and reduction of H-*ras* oncogene mutations (Hanausek et al., 2001).

Thus, the avicins may be important for reducing both oxidative and nitrosative cellular stress and thereby suppressing the development of malignancies and related diseases (Hanausek et al., 2001; Haridas et al., 2001).

The pore ability of the avicins D and G at concentrations of 25 µg/mL was demonstrated by Li et *al.* (Li et al., 2005). While pore formation was strongly cholesterol dependent for avicin G, this was not so for the close derivate avicin D. The non-selective pores are too small for proteins but allow ion flux. The authors concluded that the pores might influence the membrane potential of mitochondria. The direct influence on mitochondria was corroborated by studies on rat mitochondria,

where both avicin D and G induced permeabilization leading to decreased respiratory activity (Lemeshko et al., 2006) and ATP efflux after inhibition of the voltage dependent anion channel in the outer mitochondrial membrane (Haridas et al., 2007). This is possibly the main reason for apoptosis induction by avicins and it is likely that further saponins induce pore formation in mitochondrial membranes to induce apoptosis (Bachran et al., 2008).

Avicins were able to perforate the outer mitochondrial membrane and thus induced the release of cytochrome c, which led to inhibited respiration and the induction of apoptosis (Lemeshko et al., 2006).

Avicin D selectively induced apoptosis which was probably dependent on caspase-3, inhibited STAT-3 (signal transducer and activator of transcription-3) activation, and decreased apoptosis inhibitors (bcl-2 and survivin) in CTCL (Cutaneous T-cell lymphomas) cell lines and SS patients' Sézary cells compared with normal CD4+ and activated CD4+ T cells from healthy donors (zhang et al., 2008).

[CTCL cell lines: MJ, Hut78, HH].

Furthermore, recent studies showed that avicin D also induces autophagy, another type of programmed cell death. (Avicin D induced autophagic cell death when apoptosis was inhibited) (Xu et al., 2007).

Avicin D stimulated dephosphorylation of Stat-3 in a number of human tumors cell lines, what lead to a decrease in transcription rate of Stat-3. Avicin D, by the inhibition of Stat-3 activity, suppressed also pro-inflammatory and pro-oxidant stromal environment of tumors. Moreover, avicin D activated PP-1, a cellular economizer, which can lead to redirecting metabolism of tumor cells from growth promoting anabolic to energy sparing pathways. Avicin D inhibited the level of VEGF (vascular endothelial growth factor) and CD31, an endothelial cell marker indicating the microvascular networks within the cells, in mouse skin carcinogenesis model. The compound was applied to the shaved skin of animals. The results suggest its anti-angiogenic potential (Haridas et al., 2009).

1.5. Triterpene saponins from the roots of *Acacia albida* Del. (Mimosaceae)

We report herein the isolation and structural characterization of seven previously undescribed bidesmosidic triterpenoid saponins named albidosides A – G, from a methanol extract of the roots of *Acacia albida*. The isolated compounds were assayed for their cytotoxicity against HeLa and HL60 cells using MTT method and microscopic observation.

1.5.1. Extraction and isolation

The air-dried and powdered roots of *Acacia albida* (558 g) were extracted with MeOH at room temperature. After filtration and evaporation procedures, 32.02 g of MeOH extract was obtained. The crude extract was dissolved in H_2O (400 mL), and successively partitioned with *n*-hexane (3 x 200 mL), EtOAc (3 x 200 mL), and *n*-BuOH (3 x 200 mL) saturated with H_2O. The *n*-BuOH extract (7.26 g), rich in saponins, was chromatographed by repeated medium pressure liquid chromatography (MPLC) over normal and reversed-phase material (Lichroprep RP-18, 25-40 μm) and semi-preparative HPLC over C-18 silica gel to afford seven new bidesmosidic triterpenoid saponins, named albidosides A – G (**1a** – **7a**).

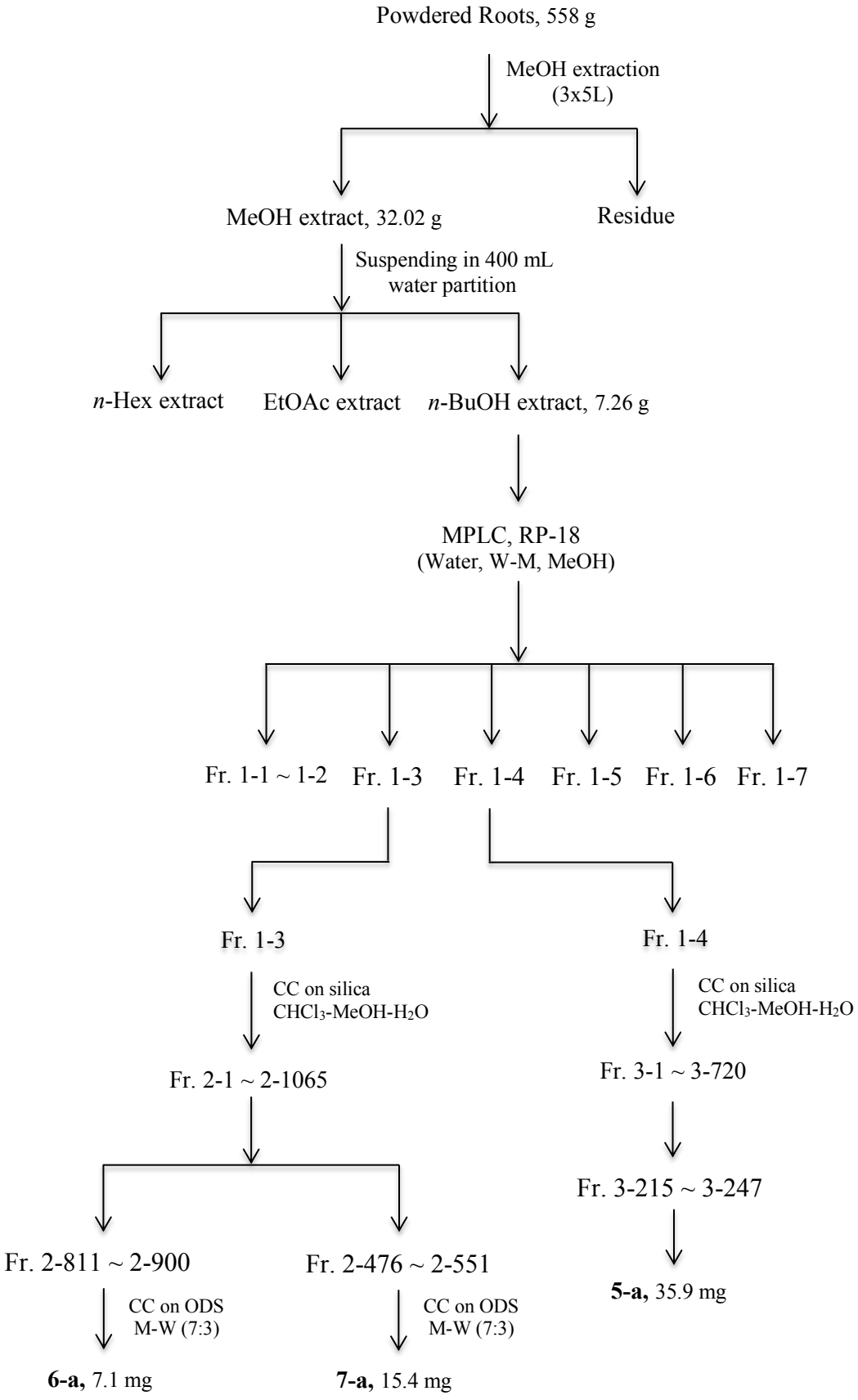

Scheme I.1. Isolation procedure of *Acacia albida* (roots)

Purification of Fr. 1-6

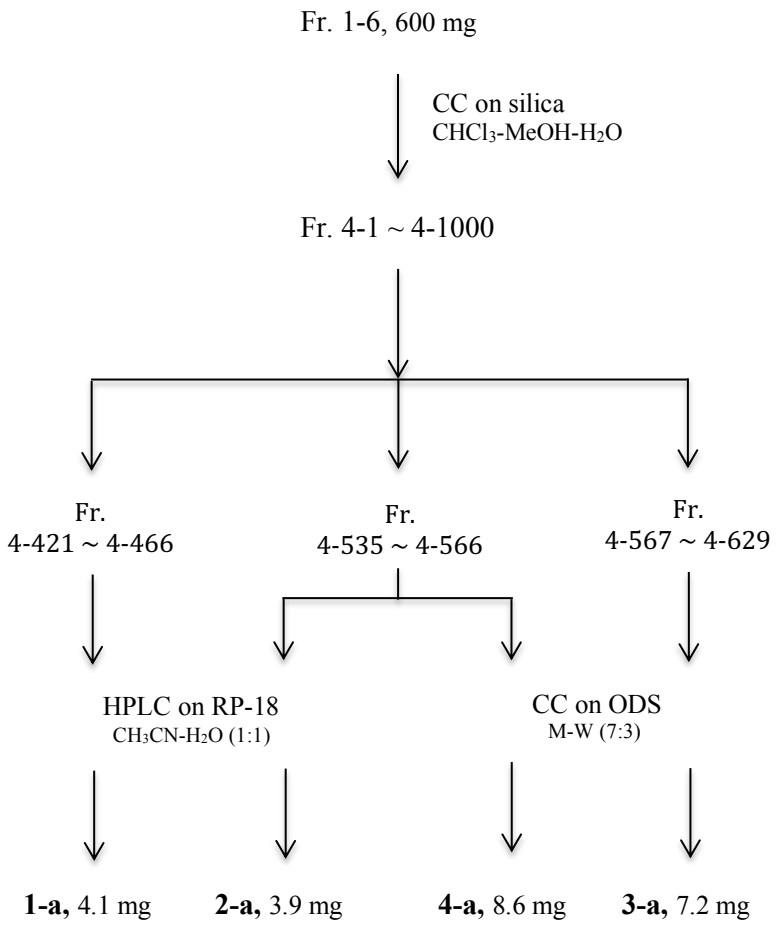

1.5.2. Structure determination

All compounds were obtained as colorless powder. The structures of the aglycones and of the sugar moieties in the saponins were determined from analysis of 1D and 2D NMR experiments and confirmed by HRESIMS.

Nature of the aglycone

The assignments of the proton and the carbon resonances of the aglycone moieties, achieved by analysis of ^{1}H–^{1}H COSY, HMQC, and HMBC experiments, allowed the identification of oleanolic acid in (**1-a – 4-a**) (Nigam et al., 1997) and 16α-hydroxyoleanolic acid (echinocystic acid) in (**5-a – 7-a**) (Mimaki et al., 2004; Melek et al., 2007).

Nature of monosaccharides

Analysis of the ^{1}H-^{1}H COSY, TOCSY, HMBC and NOESY experiments for each monosaccharide in addition with acid hydrolysis and HPLC analysis were used in deducing the nature of the sugar residues.

The D-configuration for 2-acetamido-2-deoxyglucose, glucose, fucose, and xylose, and the L-configuration for arabinose and rhamnose were determined by HPLC analysis (see Experimental). The β-orientation of the anomeric centers of the 2-acetamido-2-deoxyglucose (*N*-acetylglucosamine), glucose, xylose, and fucose moieties in their pyranose form was supported by the relatively large *J* values of their anomeric protons (*J* = 7.2–8.6 Hz) and α-anomeric configurations were determined for the rhamnose and arabinose moieties.

For the rhamnose moiety, the large $^{1}J_{C,H}$ value (165–168 Hz) and three-bond coupled strong HMBC correlations from the anomeric proton to C-3 and C-5 (the dihedral angles between H-1 and C-3, and between H-1 and C-5 about 180°) indicated that the anomeric proton was equatorial, thus possessed an α-pyranoid anomeric form (Jia et al., 1998). The α-anomeric configuration of the arabinose units was deduced from the $^{3}J_{H\text{-}1,\ H\text{-}2}$ value (5.8 – 6.8 Hz) expected for an α-arabinose in rapid $^{4}C_{1}\rightarrow{}^{1}C_{4}$ conformational exchange (Melek et al., 2007; Agrawal, 1992; De Tommasi et al., 2000).

The correlations observed in HMBC spectra indicated that these compounds were bidesmoside saponins. This was also supported by the downfield shift of Agly C-3 and the upfield shift of Agly C-28.

1.5.2.1. Compound 1-a

The HRESIMS (positive-ion mode) exhibited an accurate quasi-molecular ion peak at *m/z* 1254.62429 $[M+Na]^{+}$, in accordance with the molecular formula $C_{60}H_{97}NO_{25}Na$. The ^{1}H NMR spectrum showed characteristic signals of an olean-12-ene skeleton with seven methyl singlet signals at δ_H 0.74 (3H), 0.76 (3H), 0.85 (3H), 0.93 (6H), 0.95 (3H), and 1.34 (3H), an oxymethyne (δ_H 3.08), and a sp^2 proton at δ_H 5.25. The ^{13}C NMR spectrum showed signals of seven angular methyls at δ_C 14.7, 15.4, 16.6, 23.5, 25.8, 27.2, and 32.0, and two sp^2 carbons at δ_H 122.0 and 143.2 (**Table I.1**).

The downfield shift of C-3 signal (by 10 ppm as compared to oleanolic acid) and upfield shifted (*ca* 4 ppm) of C-28, due to the glycosylation shift, suggested that **1-a** was a bidesmoside saponin.

The ^{1}H NMR spectrum data of **1-a** exhibited signals for five anomeric protons at δ_H 4.40 (d, J = 8.3 Hz), 4.55 (d, J = 7.6 Hz), 4.65 (d, J = 7.6 Hz), 5.10 (d, J =1.6 Hz), and 5.45 (d, J = 6.6 Hz), which correlated in the HMQC spectrum to carbons at δ_C 103.5, 103.8, 103.8, 100.0, and 94.2, respectively (**Table I.2**), suggesting the presence of five sugar units.

- One β-glucopyranose at δ_H 4.55 (d, J = 7.6 Hz),
- Two β-xylopyranose at δ_H 4.65 (d, J = 7.6 Hz) and 5.45 (d, J = 6.6 Hz),
- One α-rhamnopyranose at δ_H 5.10 (d, J =1.6 Hz),
- One β-2-acetamido-2-deoxyglucopyranose at δ_H 4.40 (d, J = 8.3 Hz).

The sugar sequence was determined by analysis of 1D and 2D NMR spectra.

At C-3 linked-chain

In the HMBC spectrum, the anomeric proton at δ_H 4.40 (1H, d, J = 8.3 Hz, GlcNHAc H-1) showed correlation with Agly C-3 (δ_C 89.7), hence, GlcNHAc was linked to Agly C-3 through ether linkage. The absence of any glycosylation shift in the ^{13}C NMR spectra suggested a terminal GlcNHAc at C-3 of aglycone.

At C-28 linked-chain

The linkage of the four other sugars at C-28 of aglycone was confirmed by HMBC correlations of Xyl I H-1 (δ_H 5.45) to Agly C-28 (δ_C 176.4), Rha H-1 (δ_H 5.10) to Xyl I C-2 (δ_C 75.4), Glc H-1 (δ_H 4.55) to Rha C-3 (δ_C 81.3), Xyl II H-1 (δ_H 4.65) to Rha C-4 (δ_C 77.6) and supported by the reverse correlations between Rha H-3 (δ_H 3.98) and Glc C-1 (δ_C 103.8), Rha H-4 (δ_H 3.63) and Xyl II C-1 (δ_C 103.8), and Xyl I H-2 (δ_H 3.47) and Rha C-1 (δ_C 100.0). Detailed analysis of the ^{1}H, ^{13}C, TOCSY, HSQC, HMBC, and NOESY data indicated that Xyl II and Glc are terminal sugars and unambiguously supported the sequence of the sugar units.

Conclusion

Based on the above spectral data, the structure of **1-a** was unambiguously established as 3-*O*-β-D-2-deoxy-2-acetamidoglucopyranosyloleanolic acid-28-*O*-β-D-

glucopyranosyl-(1→3)-[*β*-D-xylopyranosyl-(1→4)]-*α*-L-rhamnopyranosyl-(1→2)-*β*-D-xylopyranosyl ester, named albidoside A (A. Tchoukoua et al., 2017a).

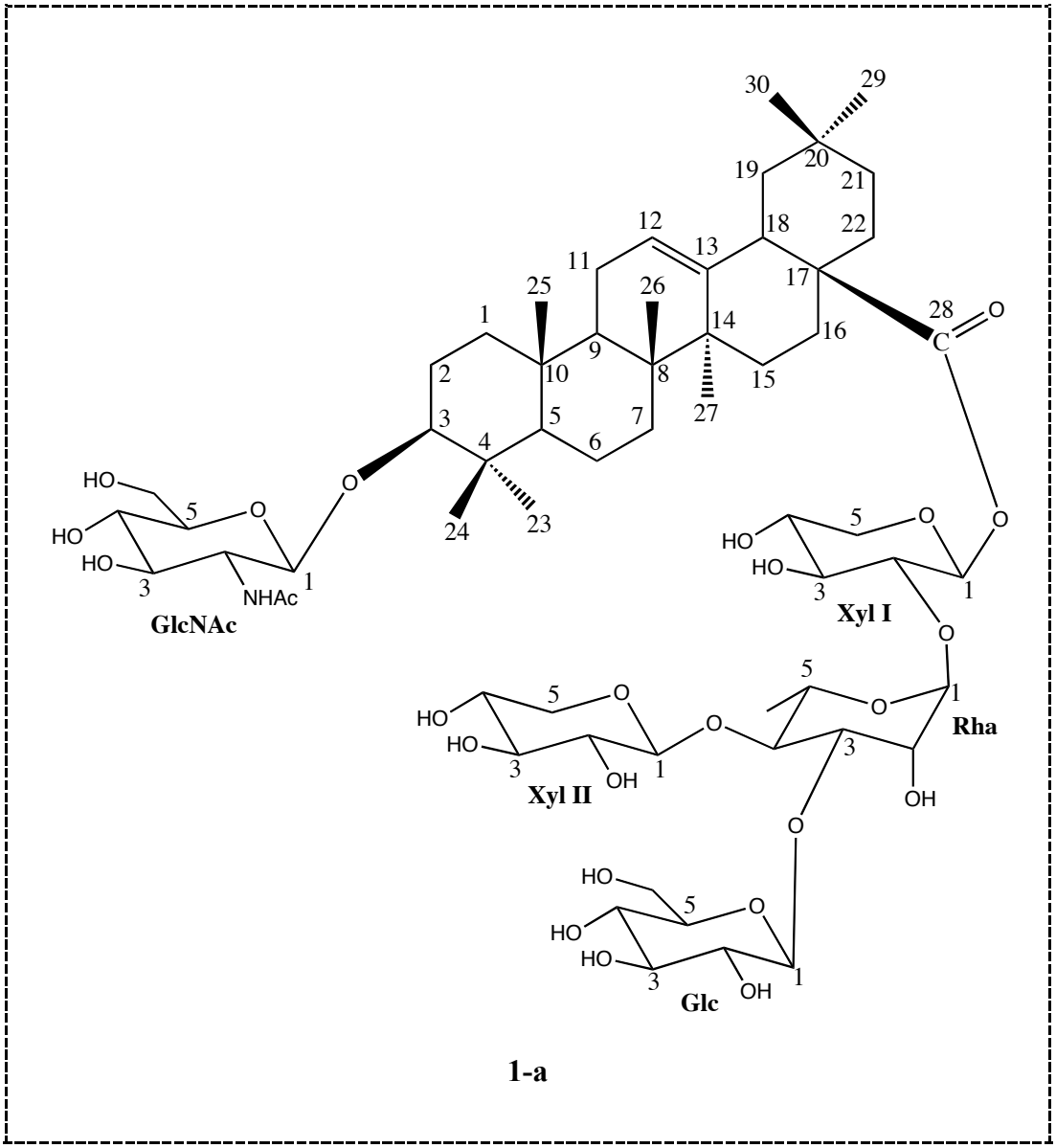

1-a

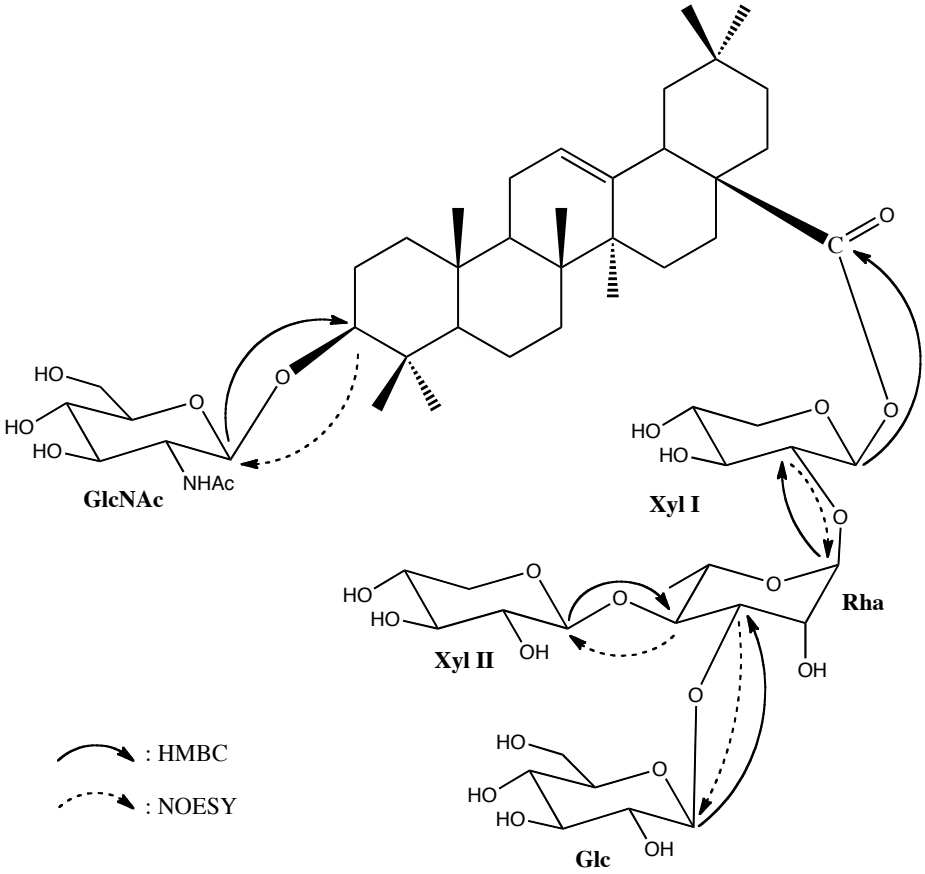

Fig. I.10. Key HMBC and NOESY correlations of compound **1-a**.

Table I.1. ^{1}H and ^{13}C NMR Data for the Aglycone Moiety of **1-a** (MeOH-d_4)

N° C	δ_C	δ_H	N° C	δ_C	δ_H
1	38.6	0.93, 1.59	**16**	22.8	1.62, 2.02
2	25.5	1.64, 1.90	**17**	46.8	-
3	89.8	3.06	**18**	41.7	2.82
4	38.4	-	**19**	45.9	1.10, 1.68
5	55.6	0.74	**20**	30.2	-
6	18.1	1.36, 1.52	**21**	33.5	1.18, 1.35
7	32.7	1.35, 1.46	**22**	31.9	1.51, 1.71
8	39.4	-	**23**	27.3	0.94
9	47.6	1.53	**24**	15.7	0.75
10	36.5	-	**25**	14.7	0.92
11	23.2	0.90, 1.86	**26**	16.4	0.76
12	122.4	5.24	**27**	24.8	1.13
13	143.5	-	**28**	176.4	-
14	41.4	-	**29**	32.2	0.88
15	27.6	1.14, 1.62	**30**	22.7	0.90

Table I.2. ^{1}H and ^{13}C NMR Data for the Sugar Moieties of **1-a** (MeOH-d_4)

Sugars	δ_H	δ_C
3-O-acetamido-2-deoxy-β-D-glucose		
1	4.40 (d, 8.3)	103.5
2	3.63	56.2
3	3.41	74.5
4	3.32	70.5
5	3.29	76.5
6	3.67, 3.83	61.4
$NHCOCH_3$	1.92 (s)	21.8
$NHCOCH_3$		172.1
28-O-β-D-xylose		
1	5.45 (d, 6.6)	94.2
2	3.47	75.4
3	3.51	74.4
4	3.30	69.9
5	3.29	65.0
	3.89 (dd, 4.3, 11.5)	
α-L-rhamnose (at C-2 Xyl)		
1	5.10 (d, 1.6)	100.0
2	4.24	69.7
3	3.98	81.3
4	3.63	77.6
5	3.80	67.8
6	1.26 (d, 6.3)	17.2
β-D-xylose (at C-4 Rha)		
1	4.65 (d, 7.6)	103.8
2	3.05	74.3
3	3.21	76.5
4	3.22	70.4
5	3.13 (t, 11.1)	65.6
	3.79	
β-D-glucose (at C-3 Rha)		
1	4.55 (d, 7.6)	103.8
2	3.26	74.0
3	3.29	76.6
4	3.45	70.0
5	3.21	76.5
6	3.67, 3.83	61.2

1.5.2.2. Compound 3-a

The HRESIMS (positive-ion mode) exhibited a pseudo-molecular ion peak at m/z 1375.65068 [M+Na]+, consistent with the molecular formula $C_{64}H_{104}O_{30}$.

Comparison of the NMR spectra of **3-a** with those of **1-a** showed that the ^{1}H and ^{13}C NMR data of **3-a** due to the aglycone part were superimposable.

The ^{1}H NMR spectrum of **3-a** displayed signals for six anomeric protons at, δ_H 4.40 (1H, d, J = 7.2 Hz), 4.55 (1H, d, J = 8.0 Hz), 4.63 (1H, d, J = 7.6 Hz), 4.65 (1H, d, J = 7.6 Hz), 5.09 (1H, d, J =1.6 Hz), and 5.46 (1H, d, J = 6.3 Hz), which gave correlations in the HMQC spectrum with ^{13}C signals at δ_C 104.3, 104.0, 102.9, 104.3, 100.7, and 94.2, respectively (**Table I.3**) suggesting the presence of five sugar units.

- Three β-glucopyranoses at δ_H 4.40 (d, J = 7.2 Hz), 4.55 (d, J = 8.0 Hz), 4.63 (d, J = 7.6 Hz),
- Two β-xylopyranoses at δ_H 4.65 (d, J = 7.6 Hz) and 5.46 (d, J = 6.3 Hz),
- One α-rhamnopyranose at δ_H 5.09 (d, J =1.6 Hz).

The sugar sequence was determined by analysis of HMBC and NOESY spectra.

At C-3 linked-chain

The sugar units at C-3 of aglycone in **3-a** were identified as two glucose units (Glc I and Glc II). Glycosylation of the Glc I C-2 (δ_C 79.9) was indicated by the downfield shift (*ca* +4 ppm) observed for this carbon resonance. A cross-peak due to the long-range correlation between C-3 (δ_C 90.1) of the aglycone and Glc I H-1 (δ_H 4.40) indicated that Glc I was linked to C-3 of the aglycone, and a cross-peak between Glc I C-2 (δ_C 79.9) and H-1 of the terminal glucose (δ_H 4.63) indicated that Glc II was the second unit of the disaccharide chain at C-3 of the aglycone.

At C-28 linked-chain

Comparison of the NMR spectra of **3-a** with those of **1-a** showed that the ^{1}H and ^{13}C NMR data of **3-a** due to the sugar moieties at C-28 of aglycone were superimposable and suggested the same oligosaccharide chain at C-28.

Conclusion

Hence, the structure of **3-a** was determined as 3-*O*-β-D-glucopyranosyl-(1→2)-β- D-glucopyranosyloleanolic acid-28-*O*-β-D-glucopyranosyl-(1→3)-[β-D-xylopyranosyl-

(1→4)]-α-L-rhamnopyranosyl-(1→2)- *β*-D-xylopyranosyl ester, named albidoside C (A. Tchoukoua et al., 2017a).

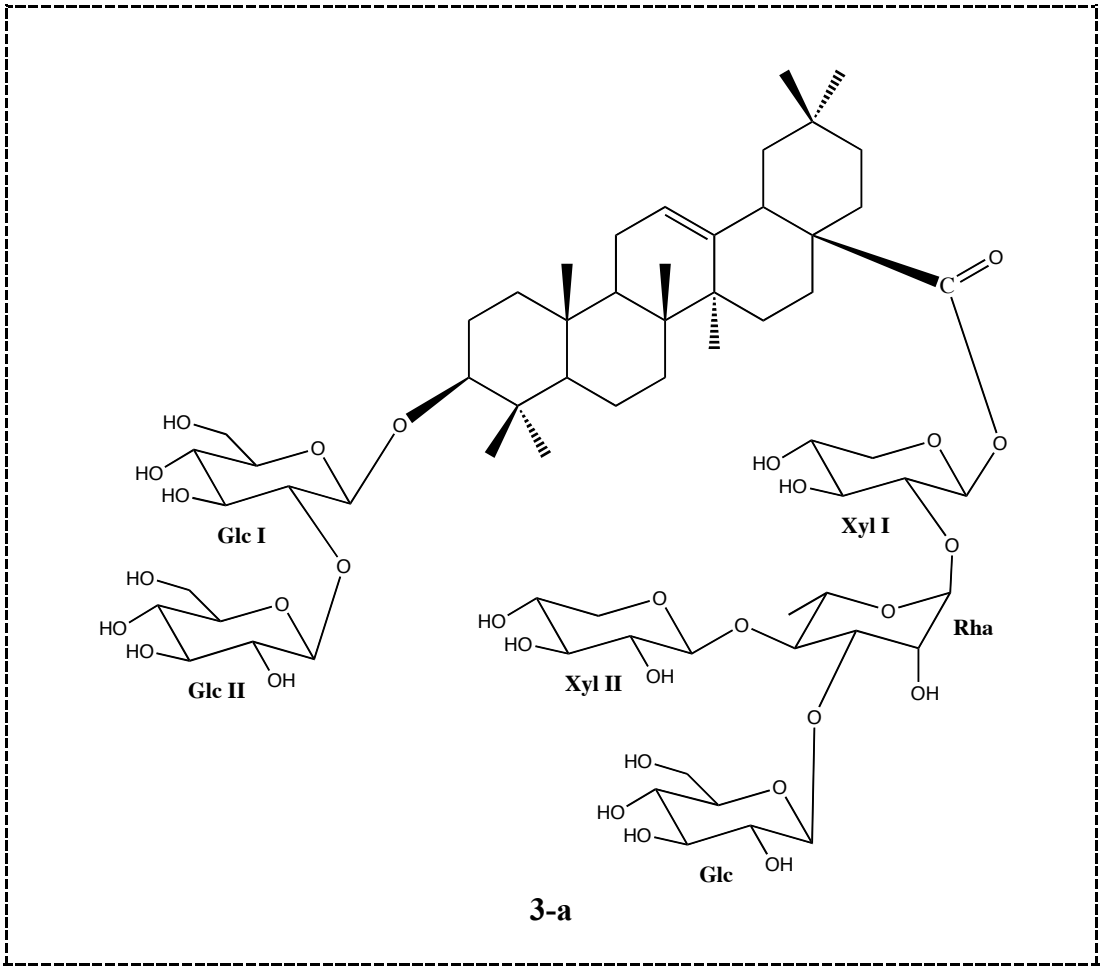

3-a

Table I.3. ^{1}H and ^{13}C NMR Data for the Sugars Moieties of **3-a** (MeOH-d_4)

Sugars	δ_H	δ_C
3-O-β-D-glucose		
1	4.40 (d, 7.2)	104.3
2	3.52	79.9
3	3.43	76.9
4	3.28	70.2
5	3.29	76.7
6	3.58, 3.81	61.8
β-D-glucose (at C-2 Glc)		
1	4.63 (d, 7.6)	102.9
2	3.20	75.3
3	3.53	77.4
4	3.16	71.0
5	3.20	77.2
6	3.61, 3.81	61.5
28-O-β-D-xylose		
1	5.46 (d, 6.3)	94.2
2	3.49	75.4
3	3.51	74.7
4	3.32	70.0
5	3.28 3.89 (dd, 4.3, 11.5)	65.1
α-L-rhamnose (at C-2 Xyl)		
1	5.09 (d, 1.6)	100.7
2	4.24	70.1
3	3.98	81.9
4	3.63	78.1
5	3.78	68.1
6	1.24 (d, 6.3)	17.2
β-D-xylose (at C-4 Rha)		
1	4.65 (d, 7.6)	104.3
2	3.05	74.7
3	3.24	76.8
4	3.26	70.6
5	3.13 (t, 11.1) 3.79	65.6
β-D-glucose (at C-3 Rha)		
1	4.55 (d, 8.0)	104.0
2	3.26	74.1
3	3.29	76.9
4	3.44	70.3
5	3.24	76.8
6	3.66, 3.84	60.8

1.5.2.3. Compound 4-a

The HRESIMS (positive-ion mode) exhibited an accurate pseudo-molecular ion peak at *m/z* 1416.67729 $[M+Na]^+$, in accordance with the molecular formula $C_{66}H_{107}NO_{30}Na$.

Comparison of NMR data of **4-a** with those of **1-a** showed that all signals due to the aglycone were superimposable with those of **1-a** and identified as oleanolic acid.

The ^1H and ^{13}C NMR of **4-a** in the oligosaccharide part displayed signals for six sugar moieties identified as:

- Two β-xylopyranoses at δ_H 5.45 (d, J = 6.5 Hz) and 4.65 (d, J = 8.2 Hz),
- Two β-glucopyranoses at δ_H 4.40 (d, J = 8.2 Hz) and 4.55 (d, J = 7.3 Hz),
- One α-rhamnopyranose at δ_H 5.10 (d, J = 1.3 Hz),
- One β-2-deoxy-2-acetamidoglucopyranose unit at δ_H 4.42 (d, J = 8.6 Hz).

The sugar sequence was determined by analysis of HMBC spectrum.

At C-3 linked-chain

Comparison of NMR data of **4-a** with those of **1-a** showed that all signals due to sugar moieties attached to C-3 were superimposable with those of **1-a** except for the signal of GlcNHAc C-4 (δ_C 79.4) shifted downfield by 9 ppm as compared to that of **1-a**, due to the glycosylation shift. The evident difference was that **4-a** has one additional sugar which was identified as glucose.

In the HMBC spectrum, the long range correlations between H-1 (δ_H 4.40) of the terminal Glc and GlcNHAc C-4 (δ_C 79.3) and H-1 of GlcNHAc and Agly C-3 (δ_C 89.8) and the reverse correlations between GlcNHAc H-4 (δ_H 3.58) and Glc C-1 (δ_C 103.3) and Agly H-3 (δ_H 3.08) and GlcNHAc C-1 (δ_C 103.3) further confirmed the glycosidic chain at C-3 of the aglycone.

At C-28 linked-chain

Comparison of the NMR spectra of **4-a** with those of **1-a** suggested that the two compounds have same oligosaccharide chain at C-28.

Conclusion

Accordingly, **4-a** was elucidated as 3-*O*-β-D-glucopyranosyl-(1→4)-β-D-2-deoxy-2-acetamidoglucopyranosyloleanolic acid-28-*O*-β-D-glucopyranosyl-(1→3)-[β-D-

xylopyranosyl-(1→4)]-α-L-rhamnopyranosyl-(1→2)-β-D-xylopyranosyl ester, named albidoside D (A. Tchoukoua et al. 2017a).

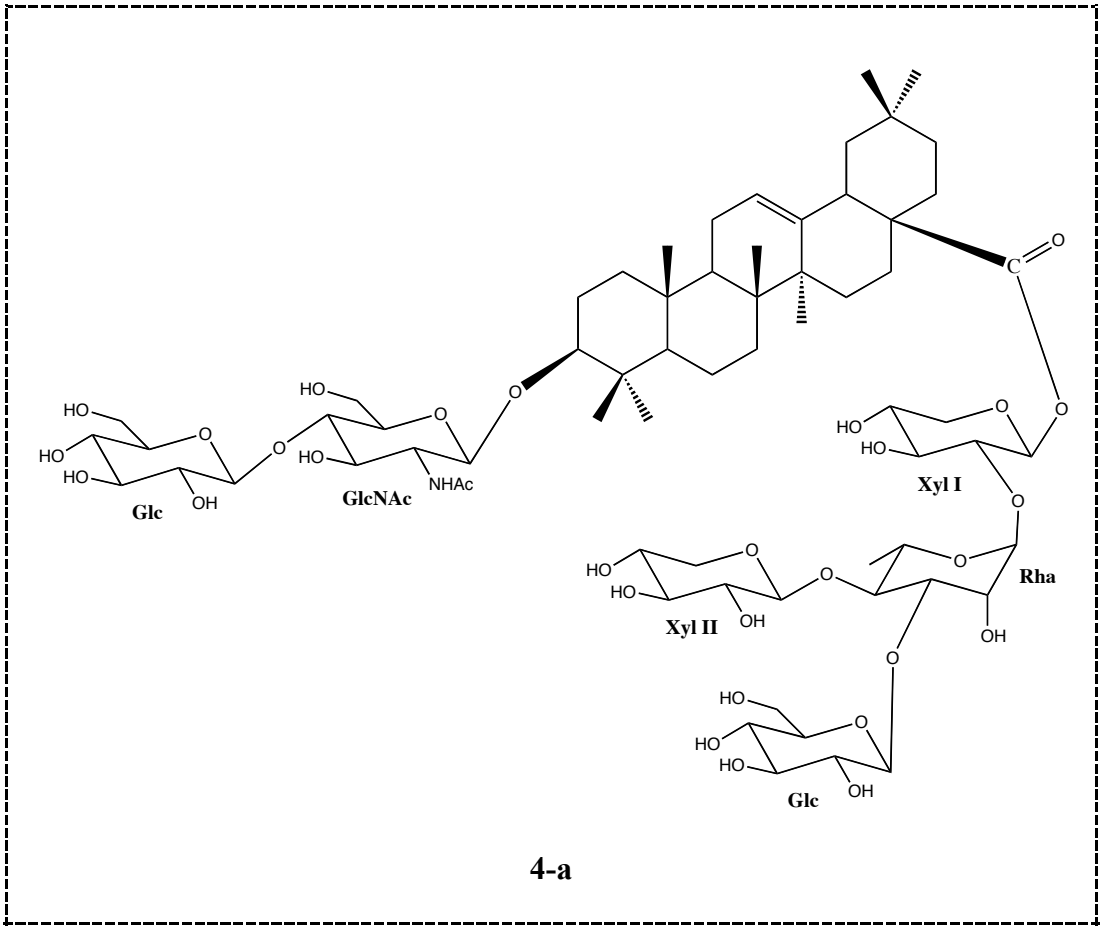

4-a

Table I.4. ^{1}H and ^{13}C NMR Data for the Sugars Moieties of **4-a** (MeOH-d_4)

Sugars	δ_H	δ_C
3-O-acetamido-2-deoxy-β-D-glucose		
1	4.42 (d, J = 8.6)	103.3
2	3.71	55.9
3	3.35	74.8
4	3.58	79.4
5	3.27	76.8
6	3.59, 3.85	61.0
$NHCOCH_3$	1.92 (s)	21.8
$NHCOCH_3$		172.0
β-D-glucose (at C-4 GlcNHAc)		
1	4.40 (d, J = 8.2)	103.3
2	3.20	73.6
3	3.30	76.6
4	3.24	70.0
5	3.33	76.8
6	3.66, 3.85	60.7
28-O-β-D-xylose		
1	5.45 (d, J = 6.5)	94.2
2	3.47	75.3
3	3.51	74.3
4	3.31	69.6
5	3.28 3.89 (dd, J = 4.3, 11.5)	65.0
α-L-rhamnose (at C-2 Xyl)		
1	5.10 (d, J = 1.3)	100.0
2	4.24	69.6
3	3.98	81.2
4	3.61	77.5
5	3.80	67.7
6	1.24 (d, J = 6.2)	17.2
β-D-xylose (at C-4 Rha)		
1	4.65 (d, J = 8.2)	103.8
2	3.07	74.0
3	3.24	77.1
4	3.24	70.0
5	3.13 (t, J = 11.1) 3.80	65.5
β-D-glucose (at C-3 Rha)		
1	4.55 (d, J = 7.3)	103.8
2	3.27	73.6
3	3.29	76.8
4	3.44	70.2

5	3.24	77.1
6	3.66, 3.84	60.8

1.5.2.4. Compound 6-a

The molecular formula, $C_{66}H_{107}NO_{30}$ of **6-a** was obtained from its HRESIMS which showed the pseudo-molecular ion peak at *m/z* 1432.67224 $[C_{66}H_{107}NO_{30}Na]^+$.

The ^1H and ^{13}C NMR spectra of **6-a** were similar to that of **4-a** except for signal of ring D of the aglycone. Comparing the ^{13}C NMR data of ring D of the aglycone part of **6-a** with those of **4-a** indicated that the aglycone of **6-a** should be hydroxylated at C-16. This was supported by the absence of the methylene signal at *ca* 22.5 ppm, replaced by an oxymethine at δ_C 73.4 ppm. Thus, the aglycone of **6-a** was identified as 16α-hydroxyoleanolic acid (echinocystic acid) (**Table I.5**).

The ^1H and ^{13}C NMR of **6-a** in the oligosaccharide part displayed signals for six sugar moieties characterized in the same way as for **4-a**.

- Two β-xylopyranoses at δ_H 5.38 (d, J = 6.3 Hz) and 4.68 (d, J = 7.8 Hz),
- Two β-glucopyranoses at δ_H 4.40 (d, J = 8.0 Hz) and 4.53 (d, J = 7.5 Hz),
- One α-rhamnopyranose at δ_H 5.14 (d, J = 1.6 Hz),
- One β-2-deoxy-2-acetamidoglucopyranose unit at δ_H 4.42 (d, J = 8.6 Hz).

Analysis of 1D and 2D NMR data of **6-a** and **4-a** revealed that the sugar chains at C-3 and C-28 of aglycone were identical.

Conclusion

Hence, **6-a** was elucidated as 3-*O*-β-D-glucopyranosyl-(1→4)-β-D-2-deoxy-2-acetamidoglucopyranosylechinocystic acid-28-*O*-β-D-glucopyranosyl-(1→3)-[β-D-xylopyranosyl-(1→4)]-α-L-rhamnopyranosyl-(1→2)-β-D-xylopyranosyl ester, named albidoside F (A. Tchoukoua et al., 2017a).

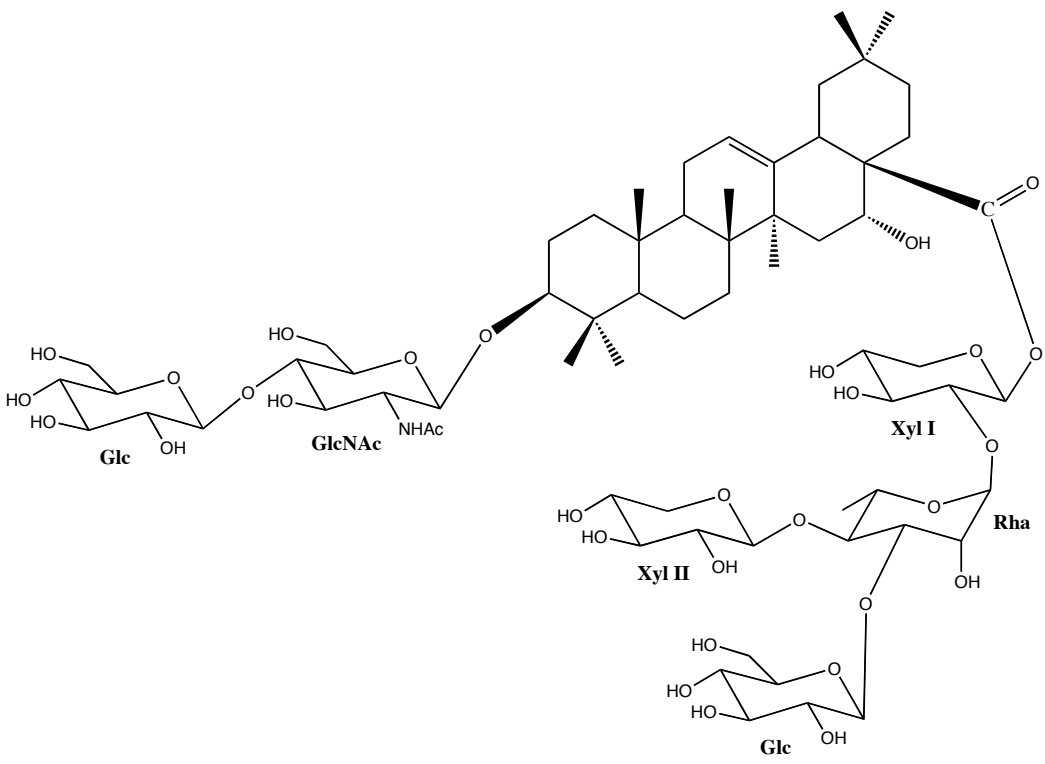
HO
HO
HO
O
OH
Glc
O
HO
HO
NHAc
GlcNAc
O
O
C
O
OH
HO
HO
O
Xyl I
O
HO
HO
O
Xyl II
OH
O
O
Rha
OH
O
HO
HO
HO
O
OH
Glc

6-a

Table I.5. ^{1}H and ^{13}C NMR Data for the Aglycone Moiety of **6-a** (MeOH-d_4)

N° C	δ_C	δ_H	N° C	δ_C	δ_H
1	38.5	0.94, 1.61	**16**	73.4	4.44
2	25.5	1.66, 1.89	**17**	48.9	-
3	89.8	3.06	**18**	41.0	2.93
4	38.5	-	**19**	46.5	1.02, 2.24
5	55.6	0.73	**20**	29.8	-
6	18.0	1.34, 1.53	**21**	35.0	1.13, 1.37
7	33.0	1.35, 1.52	**22**	30.5	1.72, 1.88
8	39.3	-	**23**	27.2	0.94
9	46.7	1.59	**24**	15.5	0.74
10	36.2	-	**25**	14.8	0.93
11	23.2	1.85	**26**	16.5	0.75
12	122.3	5.30	**27**	25.9	1.34
13	143.3	-	**28**	175.6	-
14	41.3	-	**29**	32.0	0.85
15	34.9	1.37, 1.68	**30**	23.6	0.92

1.5.2.5. Compound 7-a

The HRESIMS exhibited a pseudo-molecular ion at *m/z* 1534.70392 ($[M+Na]^+$) in agreement with the molecular formula $C_{70}H_{113}NO_{34}$.

The ^1H and ^{13}C NMR spectra showed signals typical of echinocystic acid and seven sugar units.

- Two α-arabinopyranoses at δ_H 4.50 (d, J = 5.8 Hz) and 4.46 (d, J = 7.2, Hz),
- Two β-xylopyranoses at δ_H 5.39 (d, J = 6.0 Hz) and 4.67 (d, J = 8.2 Hz),
- One β-glucopyranose at δ_H 4.53 (d, J = 7.3 Hz),
- One α-rhamnopyranose at δ_H 5.13 (d, J = 1.3 Hz),
- One β-2-deoxy-2-acetamidoglucopyranose unit at δ_H 4.40 (d, J = 8.6 Hz).

The sugar sequence was determined by analysis of HMBC and NOESY spectra.

At C-3 linked-chain

The ^{13}C NMR data of **7-a** were superimposable to those of **6-a** except for GlcNHAc C-4 and GlcNHAc C-6. The difference was that **6-a** has one sugar at GlcNHAc C-4 while **7-a** has two sugar units linked at GlcNHAc C-6. This was supported by the downfield shifts of GlcNHAc C-6 (δ_C 68.2) in **7-a**. Analysis of NMR data allowed the sequential assignments of the proton and carbon resonances of two arabinose units (Ara I and Ara II) linked to GlcNHAc C-6. Glycosylation shifts were observed for Ara I C-4 (δ_C 79.1) unit. The absence of any ^{13}C NMR glycosylation shift for the Ara II unit suggested that this sugar was a terminal unit. The sequence of the trisaccharide chain was unambiguously defined by the HMBC experiment with cross-peaks between Ara I H-1 (δ_H 4.50) and GlcNHAc C-6 (δ_C 68.2) and between Ara II H-1 (δ_H 4.46) and Ara I C-4 (δ_C 79.1).

The sequencing deduced from HMBC spectrum was confirmed in NOESY spectrum by observation of cross-peaks between GlcNHAc H-1 (δ_H 4.40) and aglycone H-3 (δ_H 3.15), Ara I H-1 (δ_H 4.50) and GlcNHAc H-6 (δ_H 4.02), and Ara II H-1 (δ_H 4.46) and Ara I H-4 (δ_H 3.71).

At C-28 linked-chain

Comparison of the NMR data of **7-a** with those of **6-a**, suggested that the two compounds have same oligosaccharide chain at C-28.

Conclusion

Finally, the structure of **7-a** was determined as 3-*O*-α-L-arabinopyranosyl-(1→4)- α-L-arabinopyranosyl-(1→4)-β-D-2-deoxy-2-acetamidoglucopyranosylechinocystic acid-28-*O*-β-D-glucopyranosyl-(1→3)-[β-D-xylopyranosyl-(1→4)]-α-L-rhamnopyranosyl-(1→2)-β-D-xylopyranosyl ester, named albidoside G (A. Tchoukoua et al., 2017a).

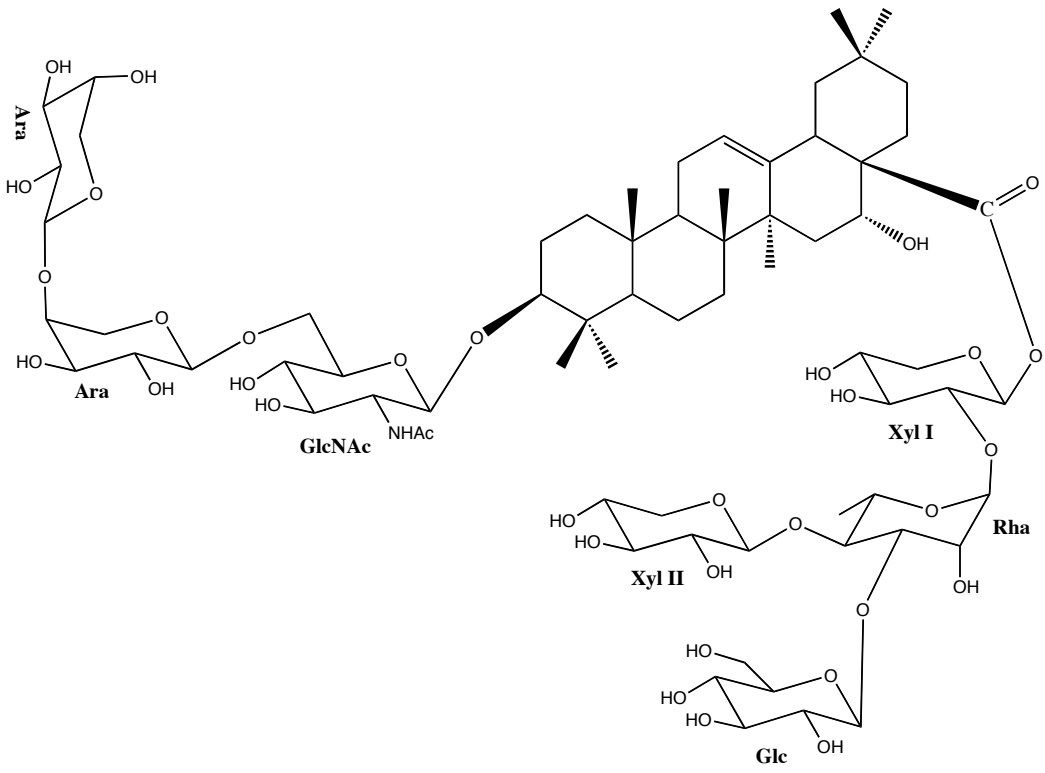

7-a

Table I.6. ^{1}H and ^{13}C NMR Data for the Sugars Moieties of **7-a** (MeOH-d_4)

Sugars	δ_H	δ_C
3-O-acetamido-2-deoxy-β-D-glucose		
1	4.40 (d, J = 8.6)	103.5
2	3.65	56.4
3	3.39	74.2
4	3.40	70.5
5	3.27	76.6
6	3.71, 4.02	68.2
$NHCOCH_3$	1.92 (s)	21.8
$NHCOCH_3$		172.1
α-L-arabinose (at C-6 GlcNHAc)		
1	4.50 (d, J = 5.8)	102.1
2	3.75	72.0
3	3.56	72.7
4	3.71	79.1
5	3.48, 3.83	64.3
α-L-arabinose (at C-4 Ara)		
1	4.46 (d, J = 6.8)	104.5
2	3.62	71.6
3	3.52	72.9
4	3.83	67.4
5	3.55, 3.79	65.7
28-O-β-D-xylose		
1	5.39 (d, J = 6.0)	94.3
2	3.46	75.1
3	3.50	74.7
4	3.31	69.7
5	3.28 3.91 (dd, J = 4.3, 11.4)	65.3
α-L-rhamnose (at C-2 Xyl)		
1	5.13 (d, J = 1.3)	100.0
2	4.20	69.8
3	3.94	81.7
4	3.65	77.3
5	3.78	67.9
6	1.25 (d, J = 6.2)	17.1
β-D-xylose (at C-4 Rha)		
1	4.67 (d, J = 8.2)	103.6
2	3.08	74.3
3	3.24	77.1
4	3.25	70.0
5	3.13 (t, J = 11.1) 3.82	65.7

β-D-glucose (at C-3 Rha)		
1	4.53 (d, *J* = 7.3)	104.0
2	3.26	74.2
3	3.27	76.8
4	3.44	70.1
5	3.21	77.2
6	3.69, 3.82	61.0

1.5.2.6. Compound 2-a

The HRESIMS (positive-ion mode) showed a pseudo-molecular ion peak at *m/z* 1389.66619 $[M+Na]^+$, in accordance with the molecular formula $C_{65}H_{106}O_{30}Na$.

The aglycone was identified as oleanolic acid by comparison of its NMR data with those of albidoside C (**3-a**).

The ^1H NMR spectrum data of **2-a** exhibited signals for six anomeric protons suggesting the presence of six sugar units.

- Three β-glucopyranoses at δ_H 4.40 (d, J = 7.7 Hz), 4.63 (d, J = 7.7 Hz), and 5.35 (d, J = 7.7 Hz),
- One β-xylopyranose at δ_H 4.64 (d, J = 8.0 Hz),
- One α-rhamnopyranose at δ_H 5.17 (d, J = 1.6 Hz),
- One β-fucopyranose at δ_H 4.54 (d, J = 7.7 Hz)

The sugar sequence was determined by analysis of HMBC and NOESY spectra.

At C-3 linked-chain

Similarities of proton and carbon resonances in **2-a** and **3-a** suggested that they have same oligosaccharide chain at C-3 of aglycone: 3-*O*-β-D-glucopyranosyl-(1→2)-β-D-glucopyranoside.

At C-28 linked-chain

The attachment of the glycosidic chain to C-28 of the aglycone was based on a correlation between H-1 (δ 5.35) of glucose and C-28 (δ_C 176.7) of the aglycone. The HMBC spectrum showed interglycosidic correlations for the tetrasaccharidic chain between H-1 (δ 4.64) of the xylose and C-4 (δ_C 77.5) of the rhamnose, H-1 (δ 4.54) of the fucose and C-3 (δ_C 81.3) of the rhamnose, H-1 (δ 5.17) of the rhamnose and C-2 (δ_C 77.0) of the glucose. NOESY observed across the glycosidic bonds confirmed the previous assignments of the HMBC spectrum.

These data agreed with the presence of the β-D-fucopyranosyl-(1→3)-[β-D-xylopyranosyl-(1→4)]-α-L-rhamnopyranosyl-(1→2)-β-D-glucopyranoside as the tetraglycosic ester of **2-a**.

Conclusion

Hence, **2-a** was assigned the structure of 3-*O*-*β*-D-glucopyranosyl-(1→2)-*β*-D-glucopyranosyloleanolic acid-28-*O*-*β*-D-fucopyranosyl-(1→3)-[*β*-D-xylopyranosyl-(1→4)]-*α*-L-rhamnopyranosyl-(1→2)-*β*-D-glucopyranosyl ester, named albidoside B (A. Tchoukoua et al., 2017a).

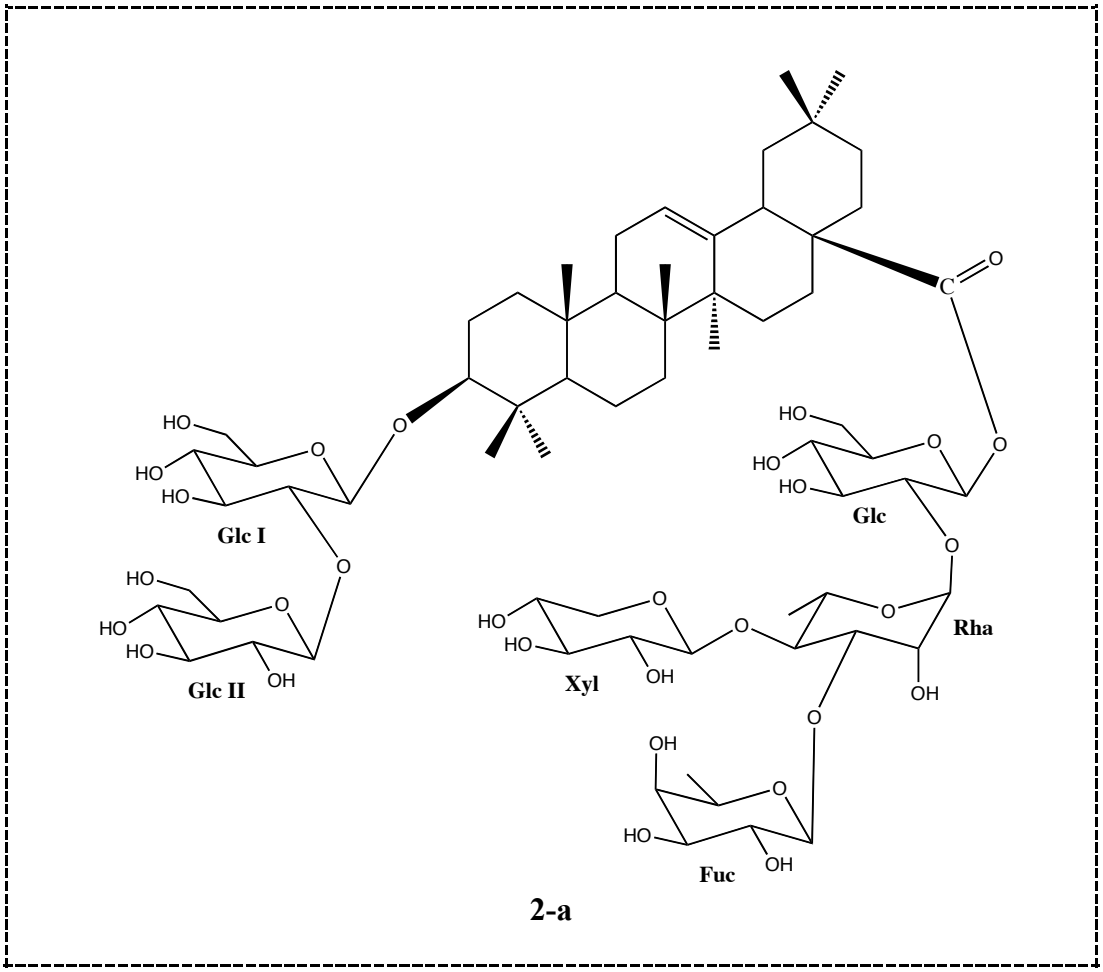

2-a

Table I.7. ^{1}H and ^{13}C NMR Data for the Sugars Moieties of **2-a** (MeOH-d_4)

Sugars	δ_H	δ_C
3-O-β-D-glucose		
1	4.40 (d, J = 7.7)	104.0
2	3.52	79.7
3	3.26	76.3
4	3.16	70.7
5	3.29	76.5
6	3.66, 3.82	61.8
β-D-glucose (at C-2 Glc)		
1	4.63 (d, J = 7.7)	103.0
2	3.19	74.8
3	3.53	77.1
4	3.18	70.7
5	3.21	76.8
6	3.58, 3.80	61.5
28-O-β-D-Glucose		
1	5.35 (d, J = 7.7)	93.6
2	3.53	77.0
3	3.16	77.1
4	3.27	71.2
5	3.62	77.6
6	3.66, 3.82	61.2
α-L-rhamnose (at C-2 Glc)		
1	5.17 (d, J = 1.6)	100.2
2	4.27	69.7
3	3.98	81.3
4	3.60	77.5
5	3.81	67.7
6	1.22 (d, J = 6.0)	17.2
β-D-xylose (at C-4 Rha)		
1	4.64 (d, J = 8.0)	104.1
2	3.04	74.2
3	3.24	76.5
4	3.22	70.0
5	3.13 (t, J = 10.9)	65.6
	3.82	
β-D-fucose (at C-3 Rha)		
1	4.54 (d, J = 7.7)	103.9
2	3.27	73.7
3	3.43	76.8
4	2.99	75.9
5	3.30	72.4
6	1.19 (d, J = 6.3)	16.6

1.5.2.7. Compound 5-a

The HRESIMS (positive-ion mode) showed a pseudo-molecular ion peak at *m/z* 1284.63469 $[M+Na]^+$, in accordance with the molecular formula $C_{61}H_{99}NO_{26}Na$.

The aglycone was identified as echinocystic acid by comparison of its NMR data with those of albidosides F and G.

The ^1H NMR spectrum data of **5-a** showed signals for five sugar units.

- One β-glucopyranose at δ_H 5.45 (d, J = 7.5 Hz),
- One β-xylopyranose at δ_H 4.69 (d, J = 8.5 Hz),
- One α-rhamnopyranose at δ_H 5.09 (d, J = 1.5 Hz),
- One β-fucopyranose at δ_H 4.53 (d, J = 7.1 Hz),
- One β-2-deoxy-2-acetamidoglucopyranose at δ_H 4.40 (d, J = 8.5 Hz).

The sugar sequence was determined by analysis of HMBC and NOESY spectra.

At C-3 linked-chain

The ^1H and ^{13}C NMR data of sugar unit linked to C-3 of aglycone were superimposable to that of albidoside A **(1-a)** and allowed the identification of a 2-deoxy-2-acetamidoglucopyranosyl unit.

At C-28 linked-chain

Similarities of proton and carbon resonances in **2-a** and **5-a** suggested that they have same tetraglycosidic chain at C-28 of aglycone.

Conclusion

Thus, **5-a** was assigned as 3-*O*-β-D-2-deoxy-2-acetamidoglucopyranosylechinocystic acid-28-*O*-β-D-fucopyranosyl-(1→3)-[β-D-xylopyranosyl-(1→4)]-α-L-rhamnopyranosyl-(1→2)-β-D-glucopyranosyl ester, named albidoside E (A. Tchoukoua et al., 2017a).

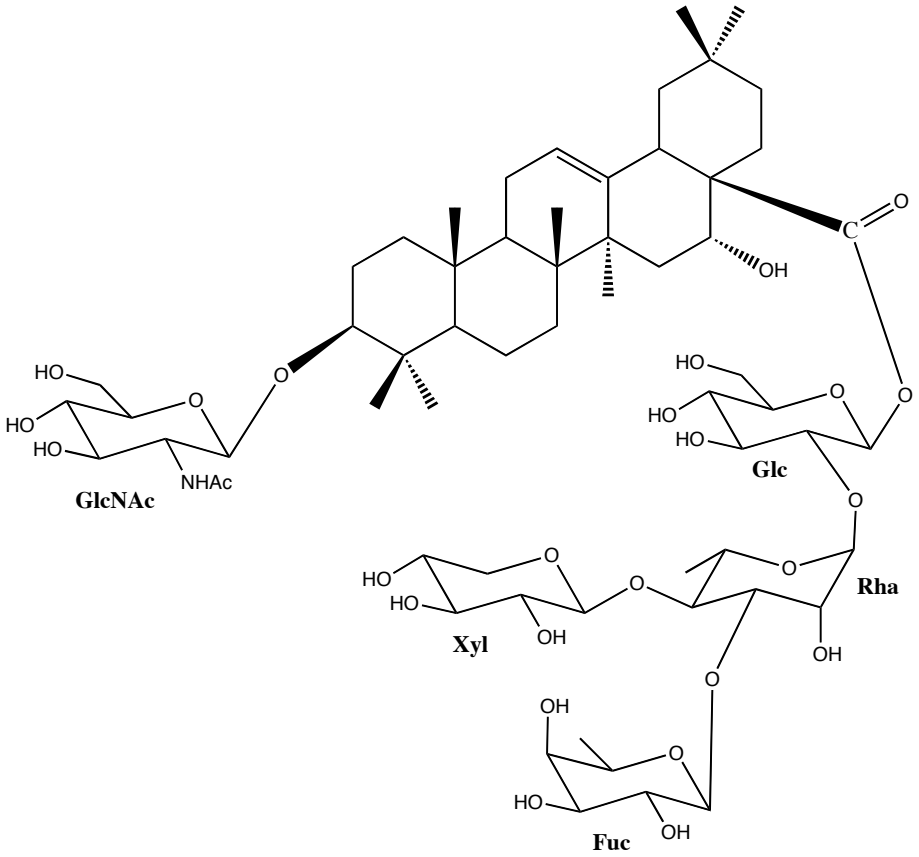
HO
HO
HO
O
NHAc
GlcNAc
O
OH
C
O
HO
HO
HO
O
O
Glc
O
HO
HO
O
O
O
Rha
Xyl
OH
OH
O
OH
HO
O
OH
Fuc

5-a

Table I.8. ^{1}H and ^{13}C NMR Data for the Sugars Moieties of **5-a** (MeOH-d_4)

Sugars	δ_H	δ_C
3-O-acetamido-2-deoxy-β-D-glucose		
1	4.40 (d, J = 8.5)	103.6
2	3.64	56.3
3	3.41	74.5
4	3.26	70.4
5	3.27	76.8
6	3.66	61.1
$NHCOCH_3$		
$NHCOCH_3$		
28-O-β-D-Glucose		
1	5.35 (d, J = 7.7)	93.6
2	3.53	77.0
3	3.16	77.1
4	3.27	71.2
5	3.62	77.6
6	3.66, 3.82	61.2
α-L-rhamnose (at C-2 Glc)		
1	5.17 (d, J = 1.6)	100.2
2	4.27	69.7
3	3.98	81.3
4	3.60	77.5
5	3.81	67.7
6	1.22 (d, J = 6.0)	17.2
β-D-xylose (at C-4 Rha)		
1	4.64 (d, J = 8.0)	104.1
2	3.04	74.2
3	3.24	76.5
4	3.22	70.0
5	3.13 (t, J = 10.9)	65.6
	3.82	
β-D-fucose (at C-3 Rha)		
1	4.54 (d, J = 7.7)	103.9
2	3.27	73.7
3	3.43	76.8
4	2.99	75.9
5	3.30	72.4
6	1.19 (d, J = 6.3)	16.6

1.6. Biological study

1.6.1. Results of cytotoxicity

The isolated compounds were evaluated for their cytotoxicity against two human cancer cells (HeLa and HL60) using MTT method.

Albidosides E (**5-a**) and F (**6-a**) exhibited cytotoxic effect with IC_{50} 18.6 μM and 46.7 μM, respectively on HeLa and 13.3 μM and 15.8 μM, respectively on HL60.

Table I.9. Cytotoxicity (IC_{50}, μM) of **5-a** and **6-a**

Compound	HeLa	HL60
	IC_{50} (μM)	IC_{50} (μM)
5-a	18.6	13.3
6-a	46.7	15.8

The rest of compounds were shown IC_{50}>50 μM on HeLa cells and IC_{50}>20 μM on HL60 cells, respectively. These results show that R=OH, R_1=NHAc and R_2=H on the structure are very important for cytotoxic activity. The rest of compounds were found inactive at 20 μM.

1.6.2. Apoptosis and cytolysis effects

The apoptotic activity of triterpene saponins in leukemia HL60 cells has been demonstrated (Hsu et al., 2000, Zhong et al., 2003, Haddad et al., 2004). Some saponins are able to induce apoptosis and necrosis (Hsu et al., 2000, Gerkens et al., 2007). HL60 cells are known to be highly sensitive to any apoptotic stimuli. Camptothecin is a well-known potent apoptosis inducer in HL60 cells.

We examined whether the cytotoxicity of saponins albidosides E (**5-a**) and F (**6-a**) against HL60 cells is apoptotic or cytolytic cell death compared with camptothecin (apoptotic cell death) and digitonin (cytolytic cell death) by the microscopic observation (**Fig. I.11**).

Compounds **5-a** and **6-a** induced cytolytic phenotype immediately through membrane damaging effects and they are the same phenotype as that of digitonin as a surfactant

(De Groot and Müller-Goymann, 2016). Although some saponins showed apoptotic cell death, **5-a** and **6-a** did not form apoptotic bodies (Gerkens et al., 2007).

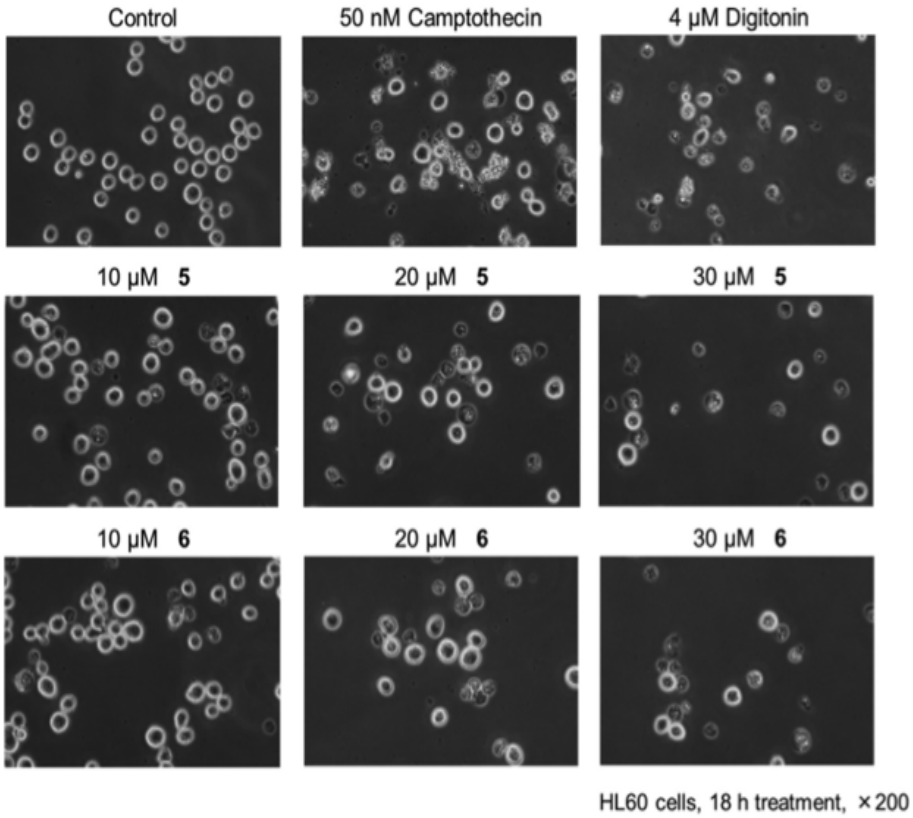

Fig. I.11. Microscopic observation of compounds **5-a** and **6-a**, camptothecin, and digitonin against HL60 cells.

1.7. Triterpene saponins from the barks of *Acacia albida* Del. (Mimosaceae)

A further detailed investigation of the barks of *Acacia albida* resulted in the isolation of the two additional triterpene saponins. Herein, we report the isolation and structure elucidation of these two new triterpene saponins named albidosides H (**1-b**) and I (**2-b**). These compounds were evaluated for their cytotoxicity against two human cancer cells, HeLa and HL60.

1.7.1. Extraction and isolation

The air-dried and powdered barks of *Acacia albida* were extracted with MeOH at room temperature. After filtration and evaporation procedures, the MeOH extract was dissolved in H_2O, and successively partitioned with *n*-Hexane, EtOAc, and *n*-BuOH saturated with H_2O. The *n*-BuOH extract, enriched in saponins, was subjected to open column chromatography by using Sephadex LH-20 and further separated by Flash chromatography over a prepack silica gel phase and repeated open ODS column chromatography to afford two new saponins, albidosides H (**1-b**) and I (**2-b**) together with three known saponins.

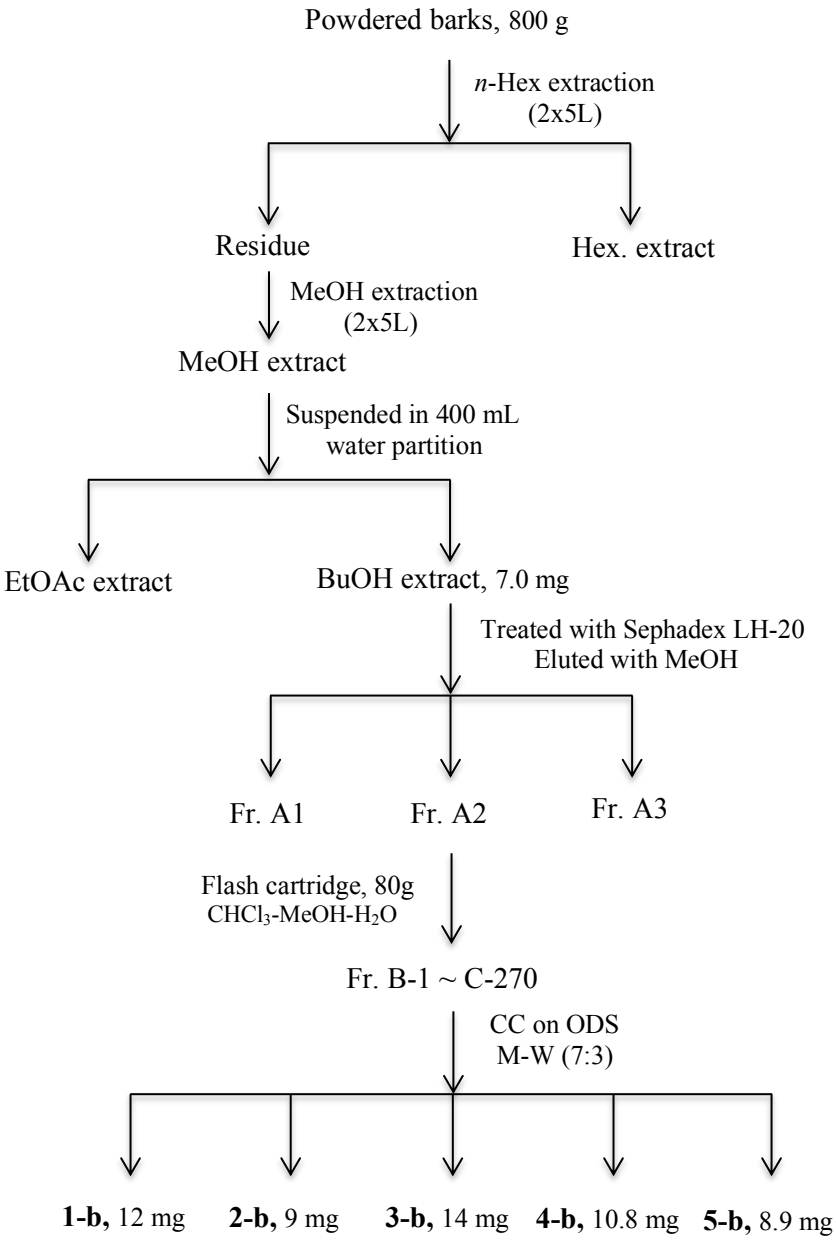

Scheme I.2. Isolation procedure of *Acacia albida* (barks)

1.7.2. Structure determination

Compounds **1-b** and **2-b** were obtained as colorless powder.

1.7.2.1. Compound 1-b

The HRESIMS (positive-ion mode) exhibited an accurate pseudo-molecular ion peak at *m/z* 1446.6879 $[M+Na]^+$, consistent with the molecular formula $C_{67}H_{109}NO_{31}Na$.

The ^1H NMR spectrum showed seven angular methyl signals as singlet at δ_H 0.74, 0.76, 0.85, 0.92, 0.93, 0.94, and 1.34 (each 3H), one olefinic proton signal at δ_H 5.27 (1H, m). The ^{13}C NMR spectrum showed characteristic signals of an olean-12-ene skeleton with seven methyls singlet signals at δ_C 14.7, 15.4, 16.6, 23.5, 25.8, 27.1, and 31.9, two ethylinic carbons at δ_H 122.1 and 143.2.

The HMBC correlations between two angular methyl groups at δ_H 0.74 (3H, s, H_3-24) and δ_H 0.94 (3H, s, H_3-23) with δ_C 89.8 (C-3) confirmed the location of the alcoholic function at C-3. The absolute configuration of C-3 and C-16 was determined by a NOESY experiment between H-3 (δ_H 3.07) and H-5 (δ_H 0.73), and between H-16 (δ_H 4.43) and H-26 (δ_H 0.76). Based on these findings, the aglycone was identified as 3β,16α-hydroxyoleanolic acid (echinocystic acid).

Furthermore, the ^1H and ^{13}C NMR signals due to the aglycone of **1-b** were almost superimposable with those of albidosides E – G, indicating that the aglycone of **1-b** was echinocystic acid (**Table I.10**).

The ^1H NMR spectrum showed six anomeric protons at δ_H 4.41 (1H, d, J = 7.8), 4.43 (1H, d, J = 8.2), 4.52 (1H, d, J = 6.9), 4.68 (1H, d, J = 7.8), 5.22 (1H, d, J = 1.7), and 5.28 (1H, d, J = 7.3) which correlated with six anomeric carbons at δ_C 93.4, 100.0, 103.3, 103.5, 103.6, 103.9 suggesting the presence of six sugar units.

- Two β-glucopyranose at δ_H 5.28 (d, J = 7.3 Hz) and 4.41 (d, J = 7.8 Hz)
- One β-xylopyranose at δ_H 4.68 (d, J = 7.8 Hz),
- One α-rhamnopyranose at δ_H 5.22 (d, J = 1.7 Hz),
- One β-fucopyranose at δ_H 4.52 (d, J = 6.9 Hz),
- One β-2-deoxy-2-acetamidoglucopyranose at δ_H 4.43 (d, J = 8.2 Hz).

The sugar sequence was determined by analysis of HMBC and NOESY spectra.

Glycosylation of the alcoholic function at C-3 and acidic function at C-28 was indicated by the downfield position of C-3 resonance (δ_C 89.8) and upfield position of

C-28 (δ_C 175.8) with reference to the corresponding signal in echinocystic acid (Mimaki et al., 2004; Melek et al., 2007).

At C-3 linked-chain

Detailed comparison of the ^{1}H, ^{13}C, TOCSY, HMQC, HMBC, and NOESY data of **1-b** with those of similar saponins showed that the signals for the sugar chain at C-3 were similar to those of albidosides D and F.

In the HMBC spectrum, the anomeric proton at δ_H 4.43 (1H, d, J = 8.2 Hz, GlcNAc H-1) showed correlation with Agly C-3 (δ_C 89.8), hence, GlcNAc was linked to Agly C-3 through ether linkage. The signal of GlcNAc C-4 (δ_C 79.7) is shifted downfield by 9 ppm as compared to that of albidoside A, due to the glycosylation shift. The long range correlations between H-1 (δ_H 4.41) of the terminal Glc and GlcNAc C-4 (δ_C 79.7) and H-1 of GlcNAc and Agly C-3 (δ_C 89.8) and the reverse correlation between Agly H-3 (δ_H 3.07) and GlcNAc C-1 (δ_C 103.6) further confirmed the glycosidic chain at C-3 of the aglycone.

At C-28 linked-chain

The sugar chain at C-28 was identical to that of albidosides B and E. The attachment of the glycosidic chain to C-28 of the aglycone was based on a correlation between H-1 (δ_H 5.28) of glucose and C-28 (δ_C 175.8) of the aglycone. The HMBC spectrum showed interglycosidic correlations for the tetrasaccharidic chain between H-1 (δ_H 4.68) of the xylose and C-4 (δ_C 77.1) of the rhamnose, H-1 (δ_H 4.52) of the fucose and C-3 (δ_C 81.6) of the rhamnose, H-1 (δ_H 5.22) of the rhamnose and C-2 (δ_C 76.8) of the glucose. NOESY observed across the glycosidic bonds confirmed the previous assignments of the HMBC spectrum.

Conclusion

Therefore, **1-b** was elucidated as 3-*O*-β-D-glucopyranosyl-(1→4)-β-D-2-deoxy-2-acetamidoglucopyranosylechinocystic acid-28-*O*-β-D-fucopyranosyl-(1→3)-[β-D-xylopyranosyl-(1→4)]-α-L-rhamnopyranosyl-(1→2)-β-D-glucopyranosyl ester, named albidoside H (A. Tchoukoua et al., 2017b).

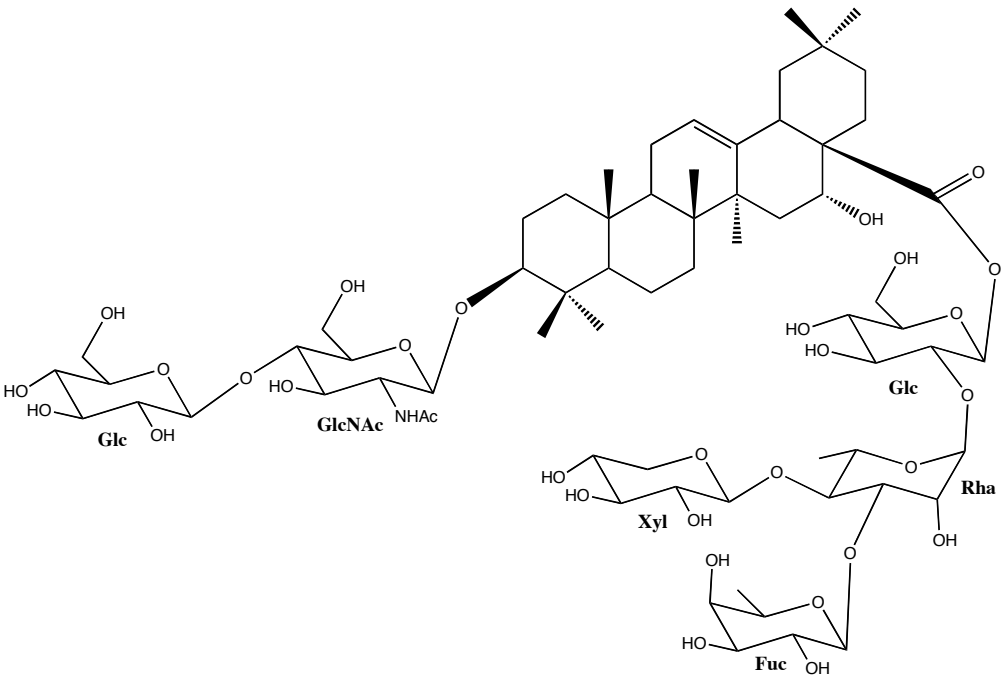
OH
O
OH
O
HO
HO
Glc
OH
O
OH
HO
GlcNAc
NHAc
O
OH
HO
HO
Glc
O
HO
HO
Xyl
OH
O
O
Rha
OH
O
OH
HO
Fuc
OH

1-b

Table I.10. ^{1}H and ^{13}C NMR Data for the Aglycone Moiety of **1-b** (MeOH-d_4)

N° C	δ_C	δ_H	N° C	δ_C	δ_H
1	38.4	0.93, 1.61	**16**	73.3	4.43
2	25.4	1.66, 1.92	**17**	48.5	-
3	89.8	3.07	**18**	40.9	2.89
4	38.4	-	**19**	46.5	1.01, 2.26
5	55.6	0.73	**20**	29.8	-
6	17.8	1.35, 1.54	**21**	35.0	1.14, 1.37
7	33.0	1.35, 1.52	**22**	30.4	1.79, 1.85
8	39.2	-	**23**	27.1	0.94
9	46.6	1.59	**24**	15.4	0.74
10	36.2	-	**25**	14.7	0.92
11	23.0	1.87	**26**	16.6	0.76
12	122.1	5.27	**27**	25.8	1.34
13	143.2	-	**28**	175.8	-
14	41.3	-	**29**	31.9	0.85
15	34.9	1.38, 1.71	**30**	23.5	0.93

Table I.11. ^{1}H and ^{13}C NMR Data for the Sugars Moieties of **1-b** (MeOH-d_4)

Sugars	δ_H	δ_C
3-O-sugars		
GlcNAc		
1	4.43 (d, J = 8.2)	103.6
2	3.70	56.3
3	3.35	75.0
4	3.57	79.7
5	3.29	76.8
6	3.59, 3.85	61.1
$NHCOCH_3$	1.91 (s)	21.7
$NHCOCH_3$		172.1
Glc (at C-4 GlcNAc)		
1	4.41 (d, J = 7.8)	103.3
2	3.18	73.7
3	3.33	76.4
4	3.23	70.1
5	3.46	76.8
6	3.59, 3.85	60.6
28-O-sugars		
Glc		

1	5.28 (d, *J* = 7.3)	93.4
2	3.42	76.8
3	3.22	77.1
4	3.44	70.0
5	3.65	77.3
6	3.66, 3.83	61.0
Rha (at C-2 Xyl or Glc)		
1	5.22 (d, *J* = 1.7)	100.0
2	4.23	69.8
3	3.94	81.6
4	3.66	77.1
5	3.82	67.8
6	1.25 (d, *J* = 6.1)	17.3
Xyl (at C-4 Rha)		
1	4.68 (d, *J* = 7.8)	103.5
2	3.08	74.3
3	3.42	76.9
4	3.44	70.0
5	3.13 (t, *J* = 10.8)	65.7
	3.81	
Fuc (at C-3 Rha)		
1	4.52 (d, *J* = 6.9)	103.9
2	3.28	73.7
3	3.29	76.6
4	2.98 (t, *J* = 8.7)	75.7
5	3.58	72.6
6	1.20 (d, *J* = 6.1)	16.7

1.7.2.2. Compound 2-b

The HRESIMS (positive-ion mode) exhibited an accurate pseudo-molecular ion peak at *m/z* 1518.7088 $[M+Na]^+$, consistent with the molecular formula $C_{70}H_{113}NO_{33}Na$.

The ^1H and ^{13}C NMR spectra showed signals typical of oleanolic acid and seven sugar units.

- Two α-arabinopyranoses at δ_H 4.51 (d, J = 5.9 Hz) and 4.47 (d, J = 6.9 Hz),
- Two β-xylopyranoses at δ_H 5.45 (d, J = 6.1 Hz) and 4.64 (d, J = 7.9 Hz),
- One β-glucopyranose at δ_H 4.55 (d, J = 7.7 Hz),
- One α-rhamnopyranose at δ_H 5.10 (d, J = 1.7 Hz),
- One β-2-deoxy-2-acetamidoglucopyranose at δ_H 4.40 (d, J = 8.4 Hz).

The sugar sequence was determined by analysis of HMBC and NOESY spectra.

At C-3 linked-chain

Detailed comparison of the ^1H and ^{13}C NMR data of **2-b** with those of albidoside G showed that the signals for the sugar residues at C-3 of the two compounds were similar, except for the data due to the GlcNAc linked at C-3 of the aglycone. In **2-b**, GlcNAc C-4 was downfield shifted by 8 ppm compared to reference sugars while in albidoside G, it is GlcNAc C-6 that was downfield shifted by 8 ppm. The sequence of the trisaccharide chain at C-3 of aglycone was unambiguously defined by the HMBC experiment in which long range correlations were observed between H-1 (δ_H 4.40) of GlcNAc and Agly C-3 (δ_C 89.1), H-1 (δ_H 4.47) of Ara I and GlcNAc C-4 (δ_C 79.4) and between H-1 (δ_H 4.51) of Ara II and C-4 (δ_C 67.6) of Ara I.

At C-28 linked-chain

The sequence of the four other sugars linked at C-28 of aglycone was confirmed by HMBC correlations of Xyl I H-1 (δ_H 5.45) to Agly C-28 (δ_C 176.4), Rha H-1 (δ_H 5.10) to Xyl I C-2 (δ_C 75.3), Glc H-1 (δ_H 4.55) to Rha C-3 (δ_C 81.4), Xyl II H-1 (δ_H 4.64) to Rha C-4 (δ_C 77.6).

Conclusion

Consequently, the structure of **2-b** was concluded to be 3-*O*-α-L-arabinopyranosyl-(1→4)-α-L-arabinopyranosyl-(1→4)-β-D-2-deoxy-2-acetamidoglucopyranosyloleanolic acid-28-*O*-β-D-glucopyranosyl-(1→3)-[β-D-

xylopyranosyl-(1→4)]-α-L-rhamnopyranosyl-(1→2)-β-D-xylopyranosyl ester, named albidoside I (A. Tchoukoua et al., 2017b).

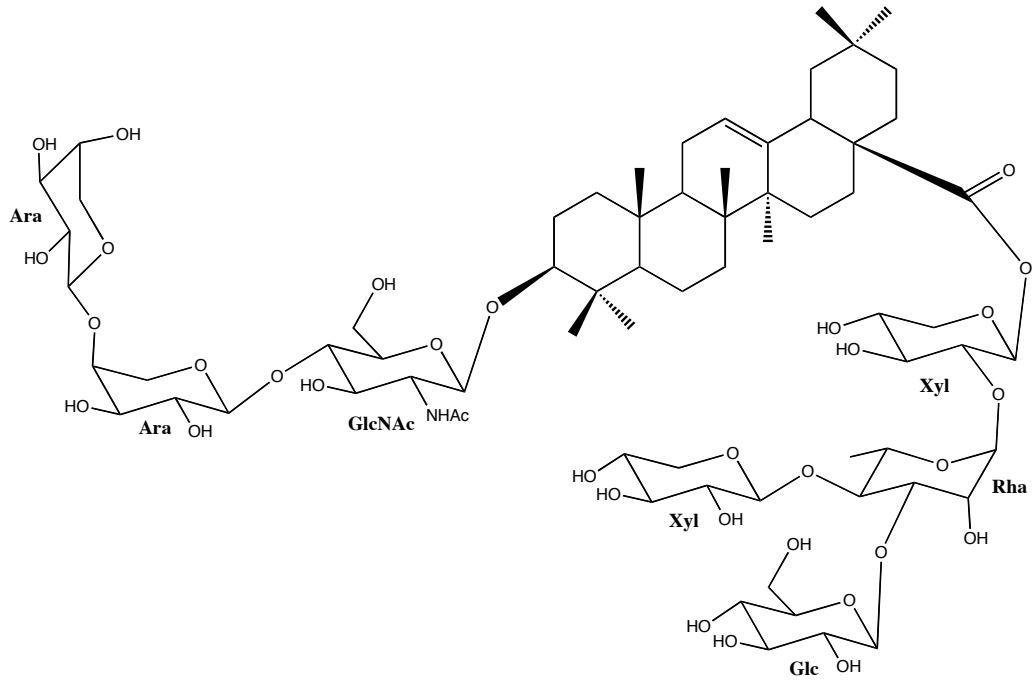

2-b

Table I.12. ^{1}H and ^{13}C NMR Data for the Sugars Moieties of **2-b** (MeOH-d_4)

Sugars	δ_H	δ_C
3-O-sugars		
GlcNAc		
1	4.40 (d, J = 8.4)	103.4
2	3.64	56.4
3	3.35	74.8
4	3.58	79.4
5	3.27	76.8
6	3.59, 3.85	61.0
$NHCOCH_3$	1.92 (s)	21.8
$NHCOCH_3$		172.1
Ara (at C-4 GlcNAc)		
1	4.47 (d, J = 6.9)	104.5
2	3.63	71.7
3	3.54	72.8
4	3.83	67.6
5	3.55, 3.79	65.7
Ara (at C-4 Ara)		
1	4.51 (d, J = 5.9)	102.1
2	3.66	72.2
3	3.56	72.7
4	3.71	79.1
5	3.84, 3.80	64.4
28-O-sugars		
Xyl		
1	5.45 (d, J = 6.1)	94.3
2	3.48	75.3
3	3.51	74.4
4	3.28	69.8
5	3.30, 3.87	65.1
Rha (at C-2 Xyl or Glc)		
1	5.10 (d, J = 1.7)	100.0
2	4.24	69.8
3	3.98	81.4
4	3.63	77.6
5	3.78	67.9
6	1.23 (d, J = 6.4)	17.2
Xyl (at C-4 Rha)		
1	4.64 (d, J = 7.9)	103.9
2	3.07	74.4
3	3.30	76.4
4	3.33	70.0

5	3.12, 3.81	65.8
Glc (at C-3 Rha)		
1	4.55 (d, *J* = 7.7)	103.9
2	3.28	74.0
3	3.29	77.1
4	3.42	70.4
5	3.23	77.2
6	3.66, 3.84	61.2

1.8. Biological study

1.8.1. Results of cytotoxicity

Compounds **1-b** and **2-b** were evaluated for cytotoxicity on two human cancer cell lines (HeLa and HL60) using MTT method. Albidoside H (**1-b**) exhibited strong cytotoxic effect while saponin albidoside I (**2-b**) exhibited weak cytotoxicity.

Table I.13. Cytotoxicity (IC_{50}, μM) of **1-b**

Compound	HeLa	HL60
	IC_{50} (μM)	IC_{50} (μM)
1-b	20.8	12.7

These resulst are in accordance with the previous findings which speculate that in albidosides A – G, the cytotoxicity is greater when the aglycone is echinocystic acid and the sugar linked to aglycone C-3 is GlcNAc unsubstituted at C-6.

1.9. General conclusion and perspectives

The present study was aimed to search new saponin molecules from *Acacia albida* (Leguminosae-Mimosoideae), and evaluate their cytotoxicity activities.

Details regarding the isolation and structure elucidation of saponins from *Acacia albida* have been discussed. By means of modern isolation and chromatographic methods, we isolated and characterized 9 new triterpene saponins:

Five saponins derived from oleanolic acid: albidosides A, B, C, D, and I.

Four saponins derived from echinocystic acid: albidosides E, F, G, and H.

Characteristic physical data of compounds isolated from *Acacia albida* were shown in the experimental section 1.10.3.1 and 1.10.3.2, respectively for its roots and barks. The saponins of *Acacia albida* are bidesmosidic saponins and their aglycones (oleanolic and echinocystic acids) are common in the Mimosaceae family.

All compounds were evaluated for cytotoxicity activities against two human cancer cell lines (HeLa and HL60) using the MTT assay. Some of saponins thereof showed cytotoxicity against the cell lines studied. And two cytotoxic saponins from the roots of *Acacia albida* induced cytolytic phenotype immediately through membrane damaging effects and they are the same phenotype as that of digitonin as a surfactant. Therefore these compounds could be a new type of drug with potential antitumor/anticancer activity due to their ability to induce cytolysis.

Although some saponins from Mimosoideae subfamily showed apoptotic cell death, the tested compounds did not form apoptotic bodies.

Following the investigations described in this dissertation, a further work could be taken up, involving the investigation of the effects of saponins on other types of cancer cells.

1.10. Experimental – I

1.10.1. General

1D and 2D NMR spectra were run on JEOL JNM-ECZ600R/S1 600 MHz NMR spectrometer (600 MHz for ^{1}H and 150 MHz for ^{13}C NMR spectra).

All chemical shifts (δ) are given in ppm, and the samples were solubilized in methanol-d_4. The ^{1}H (600 MHz) and ^{13}C (150 MHz) chemical shifts were referenced to the residual solvent peak of methanol-d_4 at δ_H 3.30 for proton and δ_C 49.0 ppm for carbon. The chemical shifts are given in ppm (δ), relative to TMS as internal standard, and coupling constants are in Hz.

The ESI-MS (ionization voltage 70 eV) was measured on a Varian AAT 311A mass spectrometer, and HRESIMS were taken on a JEOL HX110 mass spectrometer. All sample concentrations ranged from 6 to 10 μg/ml with a total volume of 0.5 ml for each sample.

Column chromatography (CC) was carried out on silica gel (70–230 mesh, Merck) and vacuum liquid chromatography (VLC) on reversed-phase materials (Lichroprep RP-18, 25–40 μm).

TLC was performed on Merck precoated aluminum silica gel 60 F_{254} sheets, and compounds were detected using sulfuric acid spray reagent.

Optical rotations were taken with a Horiba SEPA-300 polarimeter. IR spectra were obtained with a Jasco J-20A spectrophotometer.

Semi-preparative HPLC was carried out with Shimadzu pump and UV LC-10A detector (set at 206 nm) on Mightysil RP-18 column (250 x 6.0 mm i. d.) at the flow rate of 1.5 mL/min.

1.10.2. Plant material

Plants are collected in Cameroon.

Acacia albida was collected in Maroua, Far North Region of Cameroon and identified by Mr. Tapsou, botanist at the Institute of Agricultural Research for Development in December 2013.

A voucher specimen has been deposited at the National Herbarium Cameroon. *Acacia albida* (N° 49880 HNC)

1.10.3. Extraction and isolation of *Acacia albida*

The air-dried and powdered roots and bark of *Acacia albida* were extracted with MeOH. After filtration and evaporation procedures, the MeOH extracts were dissolved in H_2O and successively partitioned with *n*-hexane, EtOAc, and *n*-BuOH saturated with H_2O.

From the roots

The *n*-BuOH extract, rich in saponins, was chromatographed by repeated medium-pressure liquid chromatography (MPLC) over normal and reversed-phase RP-18 silica gel, and semi-preparative HPLC over C-18 silica gel to afford pure saponins, albidosides A – G.

From the bark

The *n*-BuOH extract, enriched in saponins, was subjected to open column chromatography by using Sephadex LH-20 and further separated by Flash chromatography over a prepack silica gel and repeated open ODS column chromatography to afford two new saponins, albidosides H and I together with the known albidosides B, F, and G.

1.10.3.1. Characteristic physical data of isolated compounds from *Acacia albida* (roots)

Compounds	Spectroscopic data
1-a (Albidoside A)	Molecular formula: $C_{60}H_{97}NO_{25}$ HR-ESIMS (positive-ion mode) *m/z* 1254.62429 ($[M+Na]^+$ calcd for $C_{60}H_{97}NO_{25}Na$ 1254.62474) ^1H and ^{13}C NMR data, see Tables I.1 and I.2
2-a (Albidoside B)	Molecular formula: $C_{65}H_{106}O_{30}$ HR-ESIMS (positive-ion mode) *m/z* 1389.66619 ($[M+Na]^+$ calcd for $C_{65}H_{106}O_{30}Na$ 1389.66667) ^1H and ^{13}C NMR data, see Table I.7
3-a (Albidoside C)	Molecular formula: $C_{64}H_{104}O_{30}$ HR-ESIMS (positive-ion mode) *m/z* 1375.65068 ($[M+Na]^+$ calcd for $C_{64}H_{104}O_{30}Na$ 1375.65102). ^1H and ^{13}C NMR data, see Table I.3
4-a (Albidoside D)	Molecular formula: $C_{66}H_{107}NO_{30}$ HR-ESIMS (positive-ion mode) *m/z* 1416.67729 ($[M+Na]^+$ calcd for $C_{66}H_{107}NO_{30}Na$ 1416.67756) ^1H and ^{13}C NMR data, see Table I.4
5-a (Albidoside E)	Molecular formula: $C_{61}H_{99}NO_{26}Na$ HR-ESIMS (positive-ion mode) *m/z* 1284.63469 ($[M+Na]^+$ calcd for $C_{61}H_{99}NO_{26}Na$ 1284.63530) ^1H and ^{13}C NMR data, see Table I.8
6-a (Albidoside F)	Molecular formula: $C_{66}H_{107}NO_{31}$ HR-ESIMS (positive-ion mode) *m/z* 1432.67224 ($[M+Na]^+$ calcd for $C_{66}H_{107}NO_{31}Na$ 1432.67248) ^1H and ^{13}C NMR data, see Table I.5
7-a (Albidoside G)	Molecular formula: $C_{70}H_{113}NO_{34}$ HR-ESIMS (positive-ion mode) *m/z* 1534.70392 ($[M+Na]^+$ calcd for $C_{70}H_{113}NO_{34}Na$ 1534.70417) ^1H and ^{13}C NMR data, see Table I.6

1.10.3.2. Characteristic physical data of isolated compounds from *Acacia albida* (barks)

Compounds	Spectroscopic data
1-b (Albidoside H)	Molecular formula: $C_{67}H_{109}NO_{31}$ HR-ESIMS (positive-ion mode) *m/z* 1446.68786 ($[M+Na]^+$ calcd for $C_{67}H_{109}NO_{31}Na$ 1446.6881) ^1H and ^{13}C NMR data, see Tables I.10 and I.11
2-b (Albidoside I)	Molecular formula: $C_{70}H_{113}NO_{33}$ HR-ESIMS (positive-ion mode) *m/z* 1518.71217 ($[M+Na]^+$ calcd for $C_{70}H_{113}NO_{33}Na$ 1518.7093) ^1H and ^{13}C NMR data, see Table I.12

1.10.4. Chemical analysis

1.10.4.1. Acid hydrolysis and HPLC analysis

Compounds were hydrolyzed in 0.2 M HCl (dioxane-H_2O 1:1, 3 ml) heated at 95°C for 30 min under argon to give the aglycones (oleanolic or echinocystic acids) and the sugars fraction. After the sugar fraction was passed through a Sep-Pak-C_{18} cartridge (Waters, Milford, MA, USA; with 40% MeOH) and Toyopak-IC-SP-M-cartridge (Tosoh; with 40% MeOH), it was analyzed by HPLC (MeCN-H_2O 17:3, fow rate, 0.9 $mL.min^{-1}$; detection, refractive index (RI) and optical rotation (OR): 7.79 (L-rhamnose, negative OR); 8.26 (D-fucose, positive OR); 9.35 (L-arabinose, positive OR), 9.73 (D-xylose, positive OR), 15.37 (D-glucose, positive OR), 14.81 (2-deoxy-2-acetamidoglucopyranose, positive OR).

1.10.5. Cell culture and cytotoxicity

HL60 cells (RCB0041, RIKEN BioResource Center, Tsukuba, Japan) and HeLa cells (RCB0007) were grown in RPMI 1640 medium or DMEM medium (Wako Pure Chemical Industries, Osaka, Japan) supplemented with 10% heat-inactivated FBS (Sigma Aldrich Corp. St. Louis, USA) and penicillin (50 units/ml)-streptomycin (50

μg/ml) (Gibco Corp., Carlsbad, USA) in a humidified atmosphere at 37°C under 5% CO_2. The cytotoxicity of the compounds was examined by MTT assay.

1.10.5.1. MTT assay

HL60 cells ($1x10^5$ cells/mL) or HeLa cells ($2x10^4$ cells/mL) were seeded in 96-well plates and treated with compounds for 2 days. The cells were then incubated for 4 h with 0.5 mg/mL MTT (3-(4,5-dimethylthiazol-2-yl)-2,5-diphenyl tetrazolium bromide, Dojindo Lab., Kumamoto, Japan). Isopropanol containing 0.04 N HCl was added to dissolve the MTT formazan reagent product. Percentages of viable cells were calculated as the ratio of A_{560} values of treated and control cells.

1.10.6. Microscopic observation

HL60 cells (1×10^5 cells/mL) were seeded in 24-well plate and treated with compounds for 18 h. The morphological changes of these cells were observed using optical microscope (CKX41SF, Olympus Corp., Tokyo, Japan).

Appendix – I

Selected spectra for Chapter 1

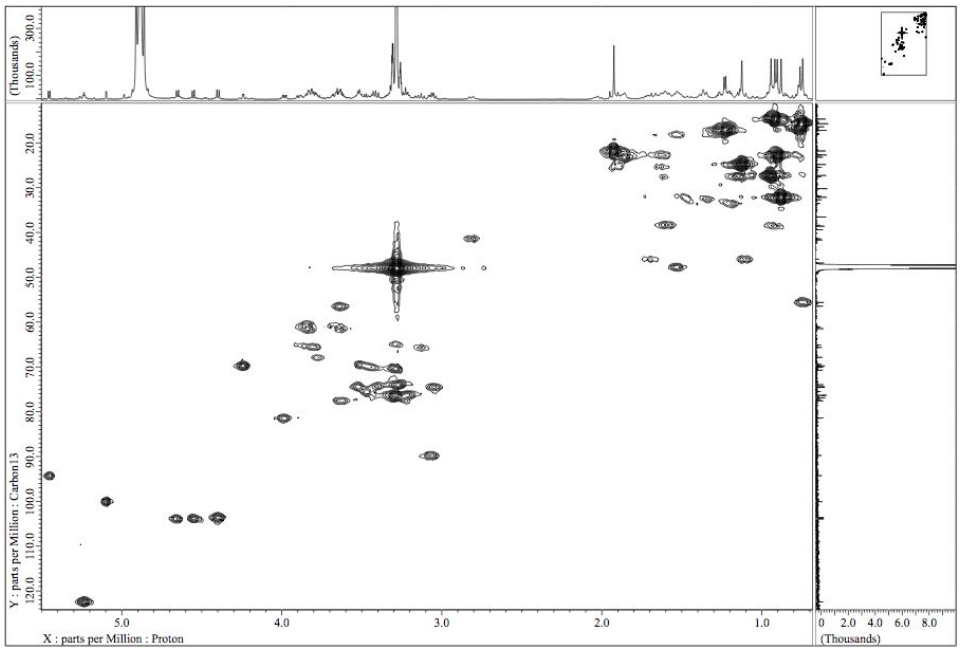

Fig. I.12. HMQC spectrum of compound **1-a** (600 MHz, MeOH-d_4)

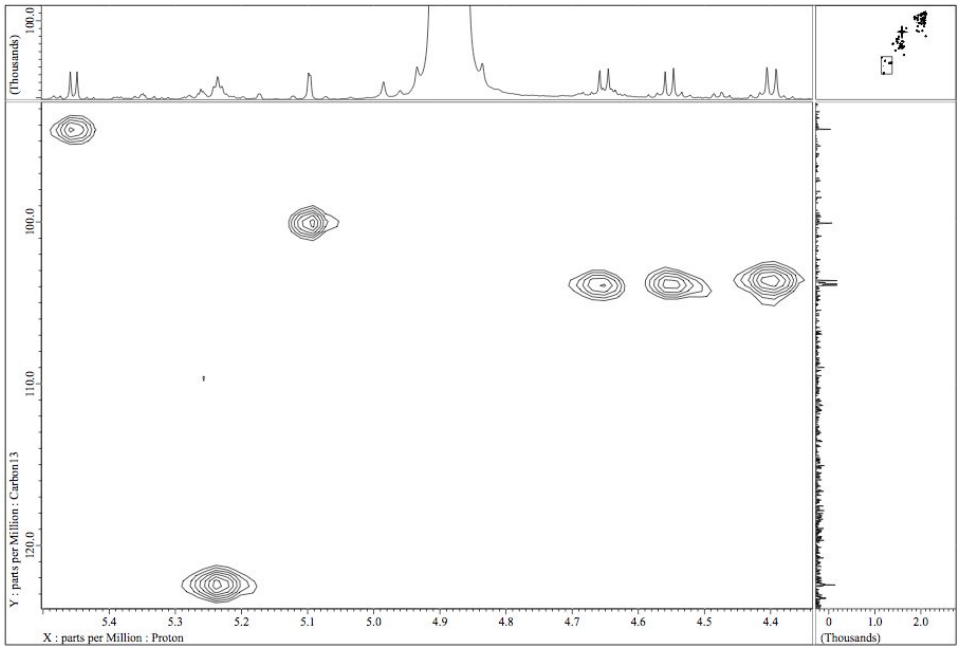

Fig I.13. HMQC spectrum (anomers zone) of compound **1-a** (600 MHz, MeOH-d_4)

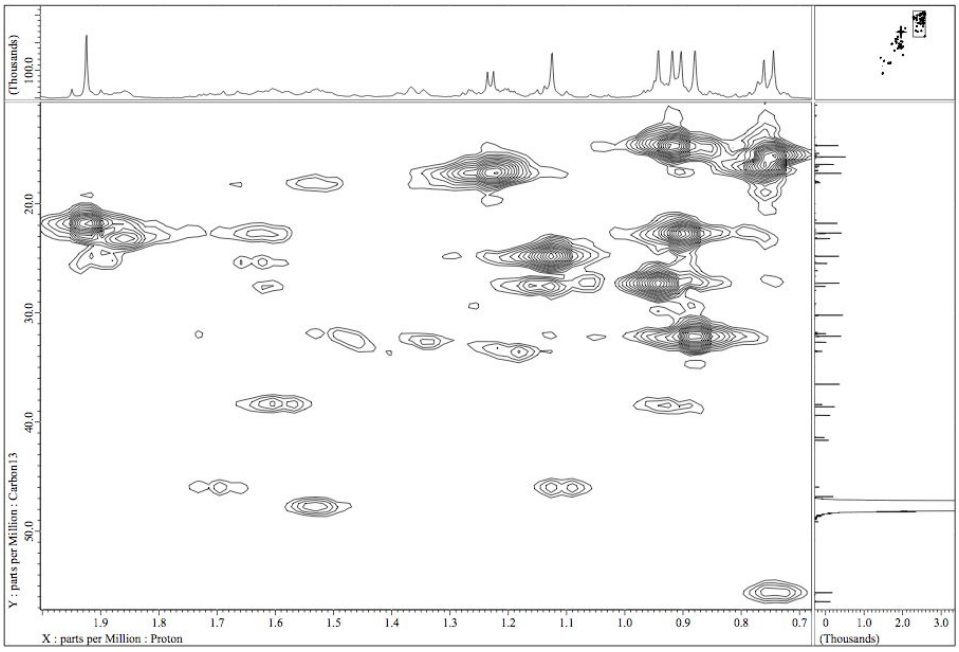

Fig. I.14. HMQC spectrum (methyls zone) of compound **1-a** (600 MHz, MeOH-d_4)

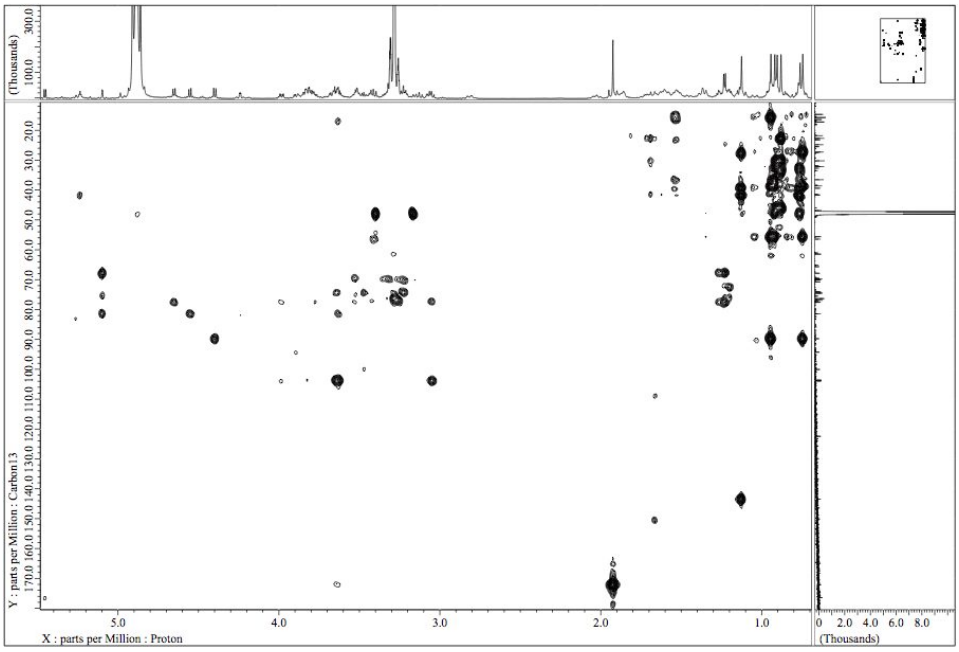

Fig. I.15. HMBC spectrum of compound **1-a** (600 MHz, MeOH-d_4)

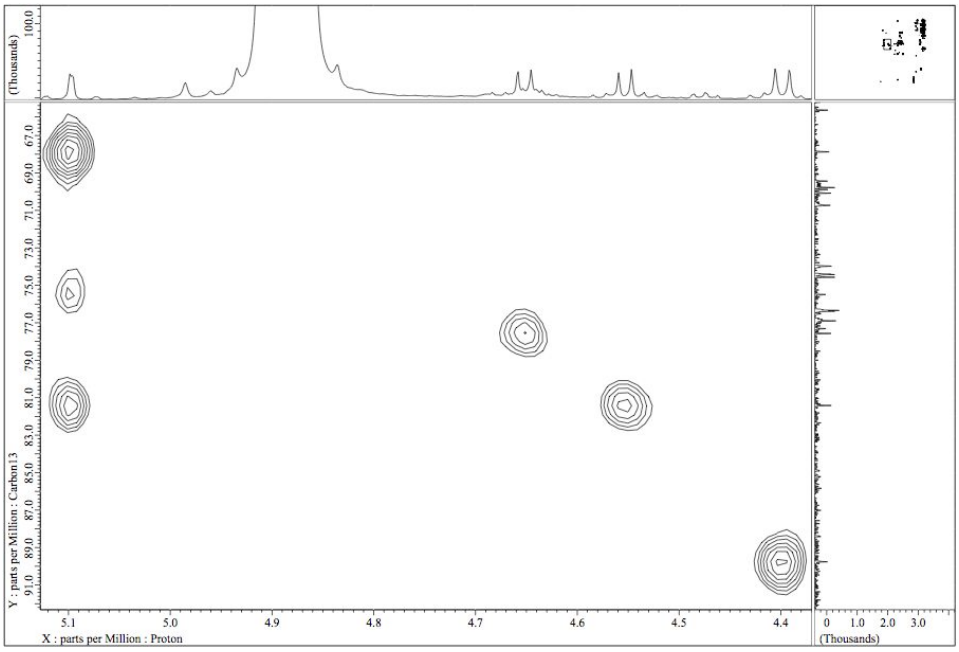

Fig. I.16. HMBC spectrum (anomers zone) of compound **1-a** (600 MHz, MeOH-d_4)

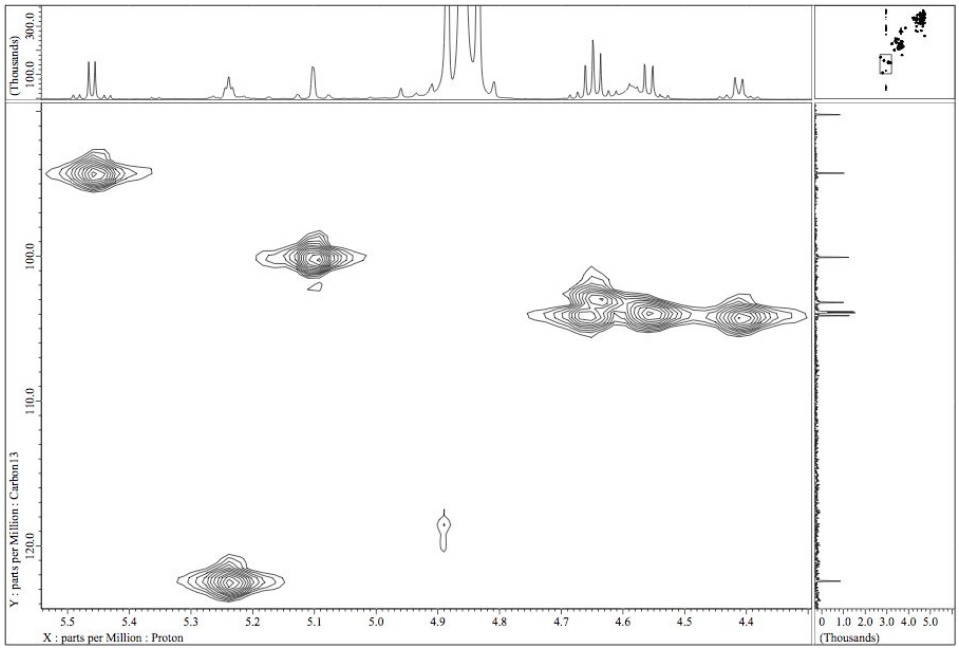

Fig. I.17. HMQC spectrum (anomers zone) of compound **3-a** (600 MHz, MeOH-d_4)

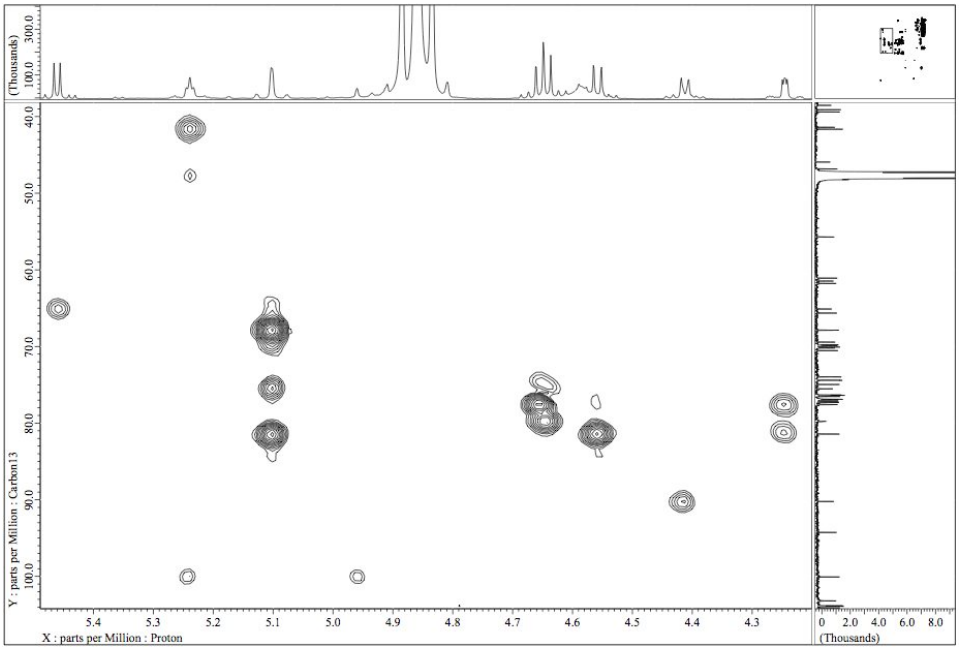

Fig. I.18. HMBC spectrum (anomers zone) of compound **3-a** (600 MHz, MeOH-d_4)

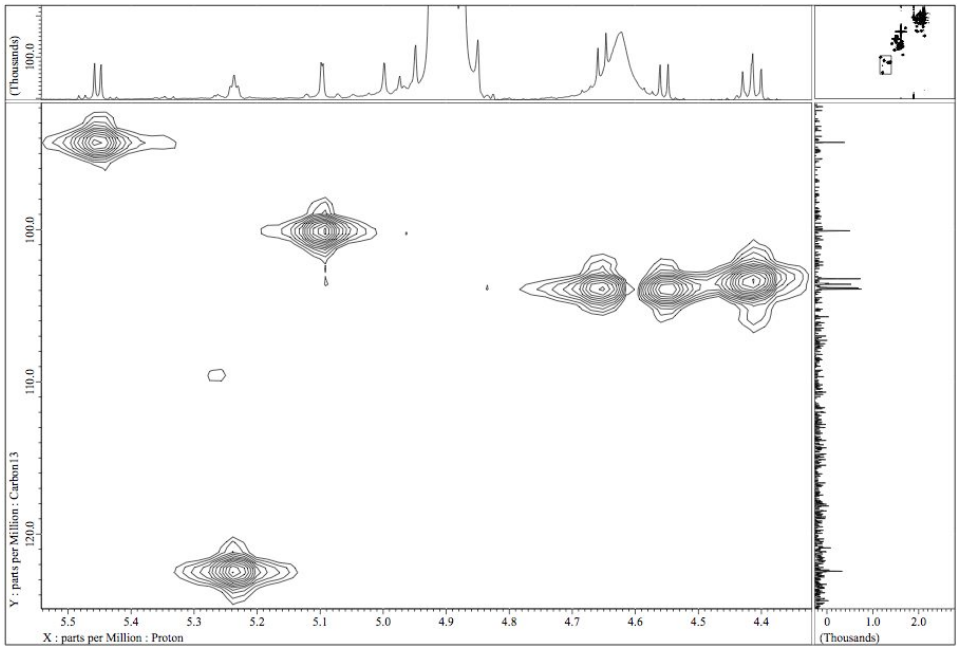

Fig. I.19. HMQC spectrum (anomers zone) of compound **4-a** (600 MHz, MeOH-d_4)

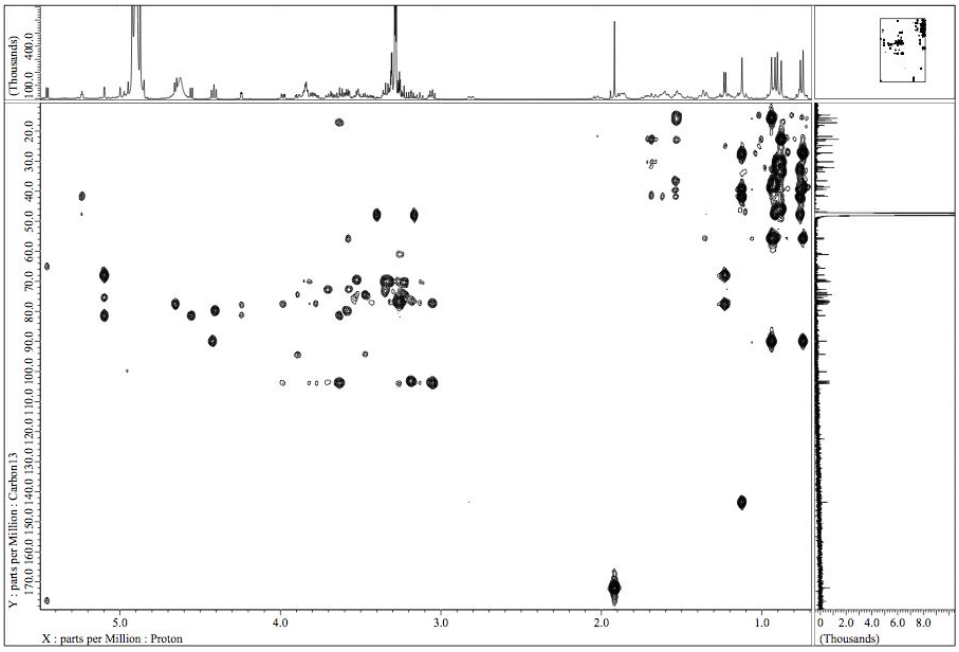

Fig. I.20. HMBC spectrum of compound **4-a** (600 MHz, MeOH-d_4)

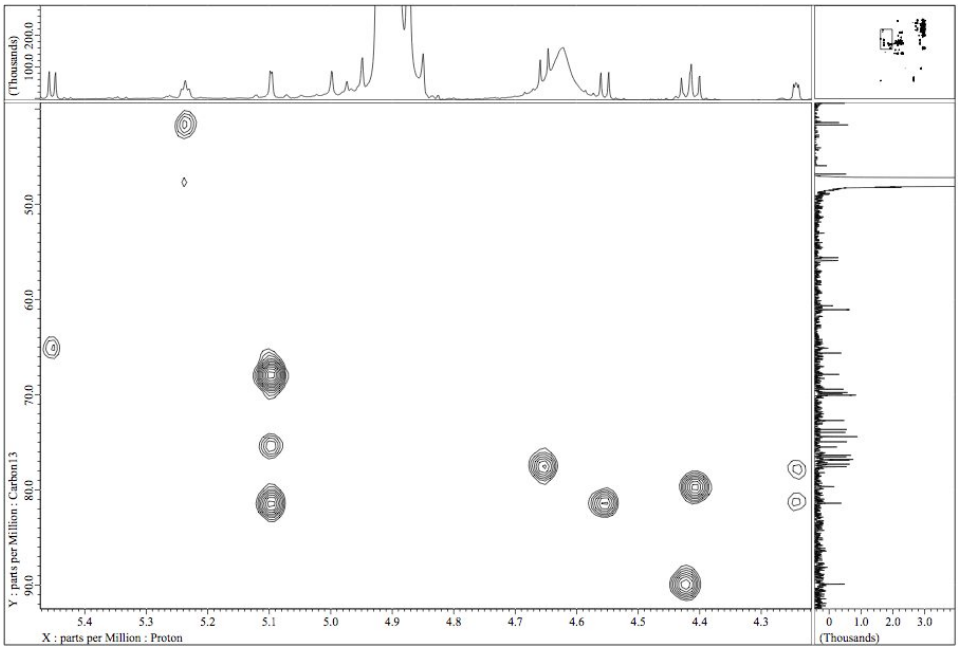

Fig. I.21. HMBC spectrum (anomers zone) of compound **4-a** (600 MHz, MeOH-d_4)

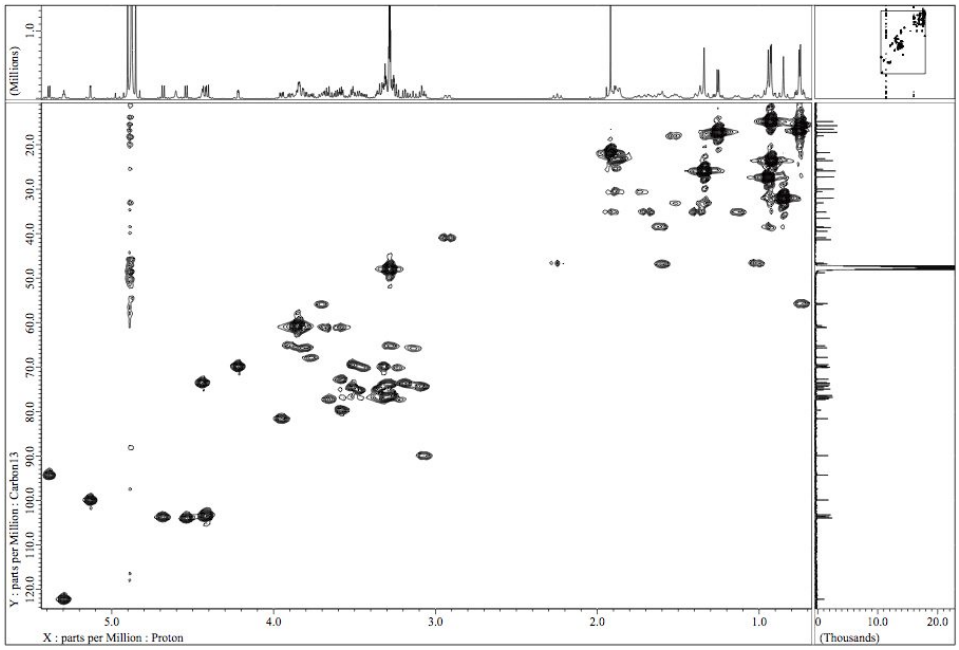

Fig. I.22. HMQC spectrum of compound **6-a** (600 MHz, MeOH-d_4)

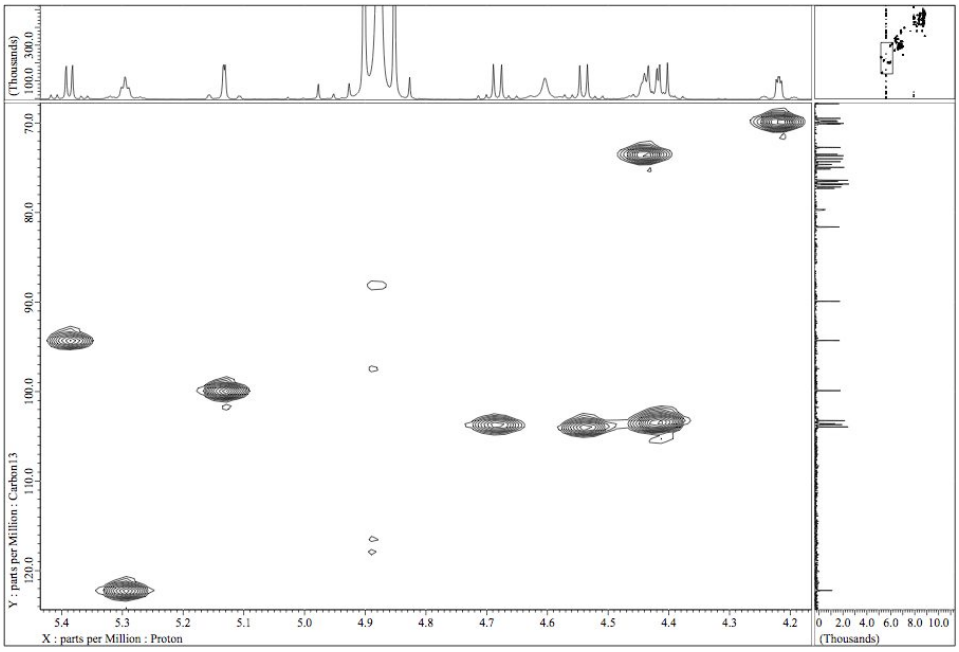

Fig. I.23. HMQC spectrum (anomers zone) of compound **6-a** (600 MHz, MeOH-d_4)

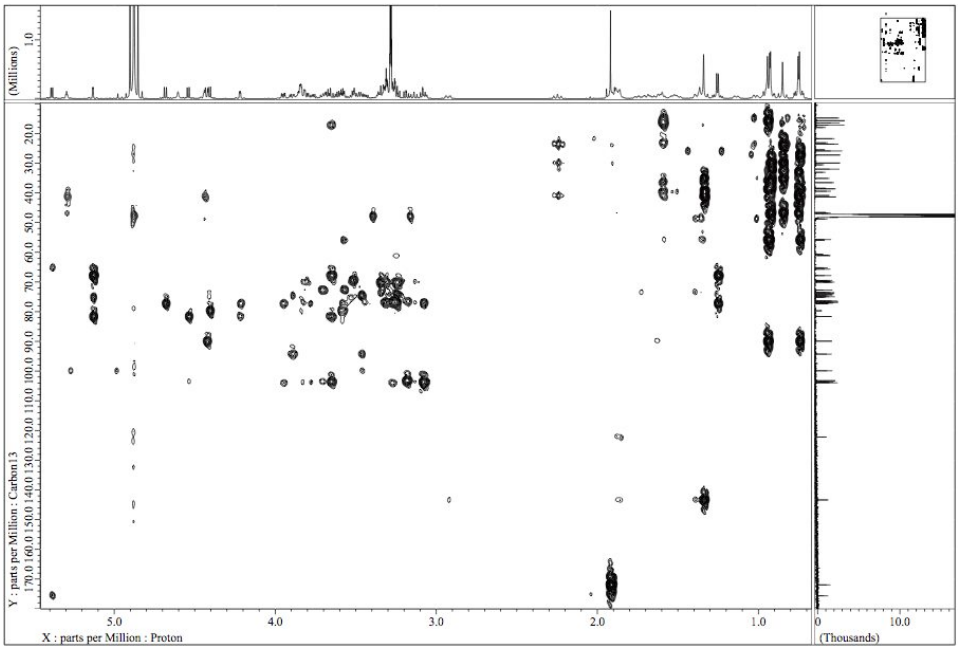

Fig. I.24. HMBC spectrum of compound **6-a** (600 MHz, MeOH-d_4)

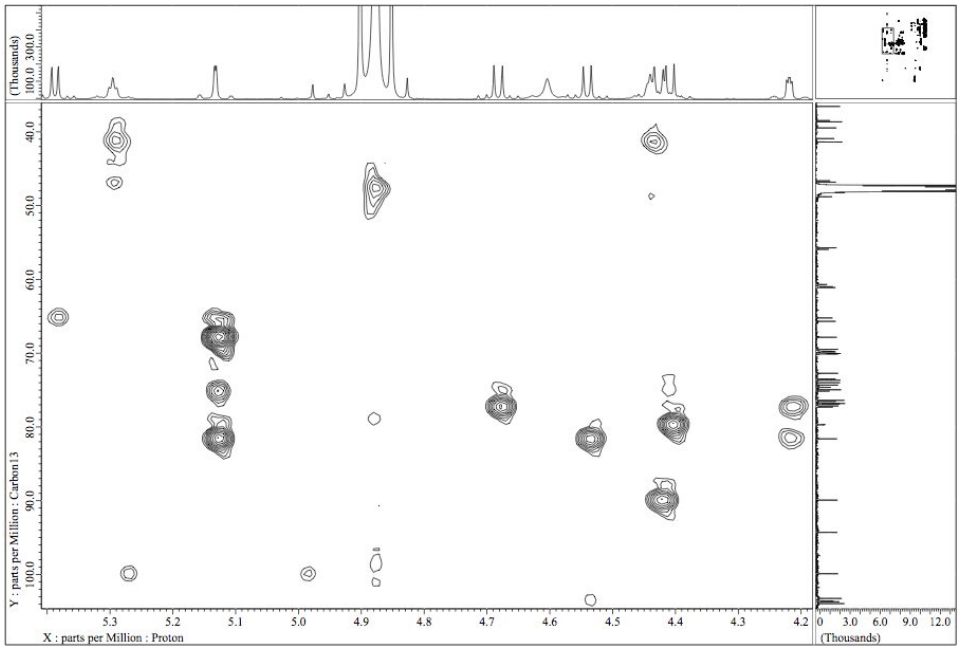

Fig. I.25. HMBC spectrum (anomers zone) of compound **6-a** (600 MHz, MeOH-d_4)

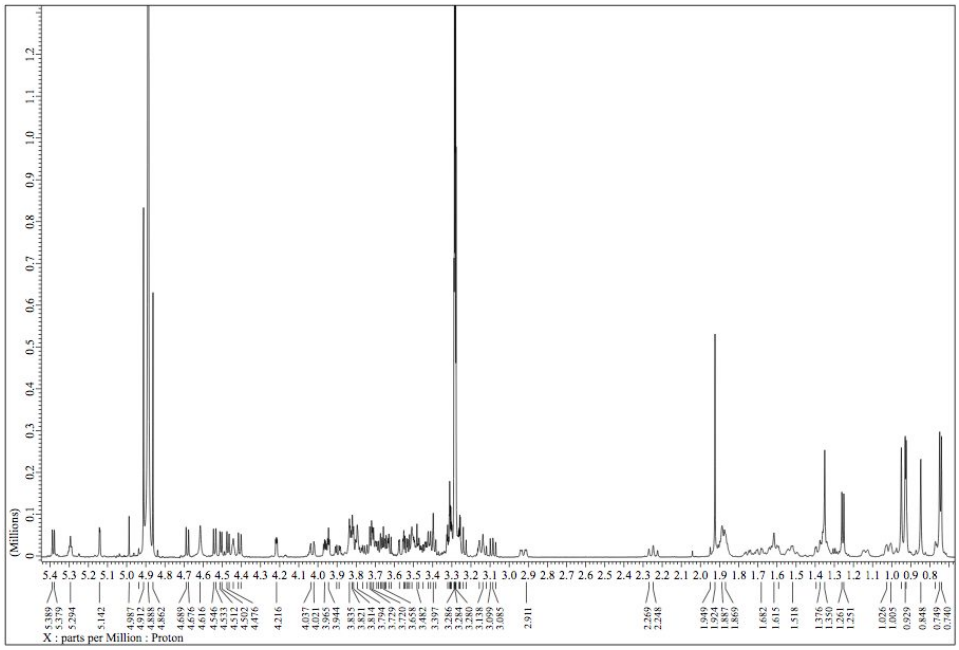

Fig. I.26. ^{1}H spectrum of compound **7-a** (600 MHz, MeOH-d_4)

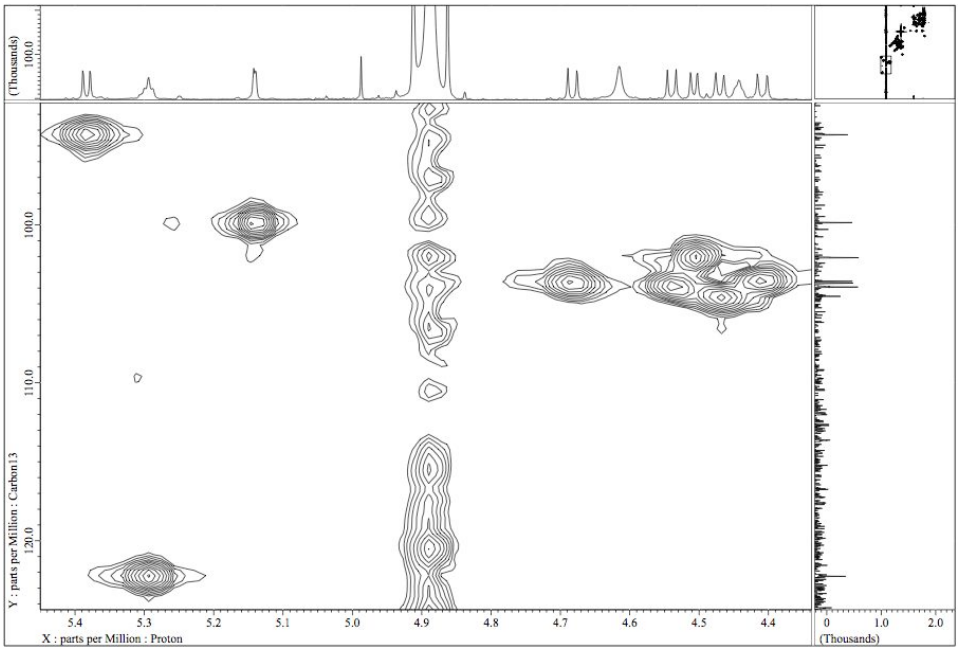

Fig. I.27. HMQC spectrum (anomers zone) of compound **7-a** (600 MHz, MeOH-d_4)

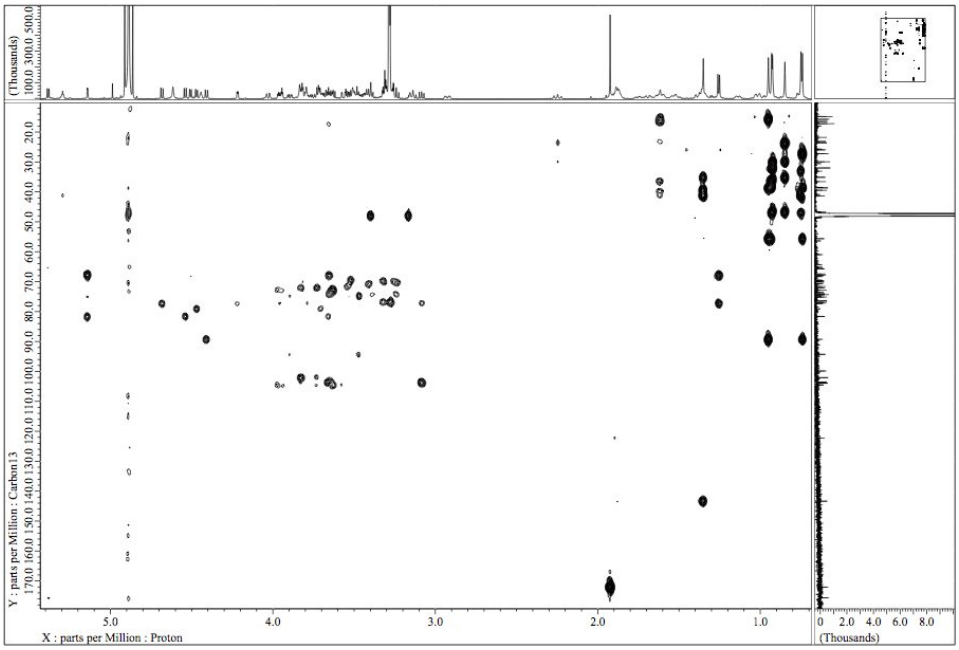

Fig. I.28. HMBC spectrum of compound **7-a** (600 MHz, MeOH-d_4)

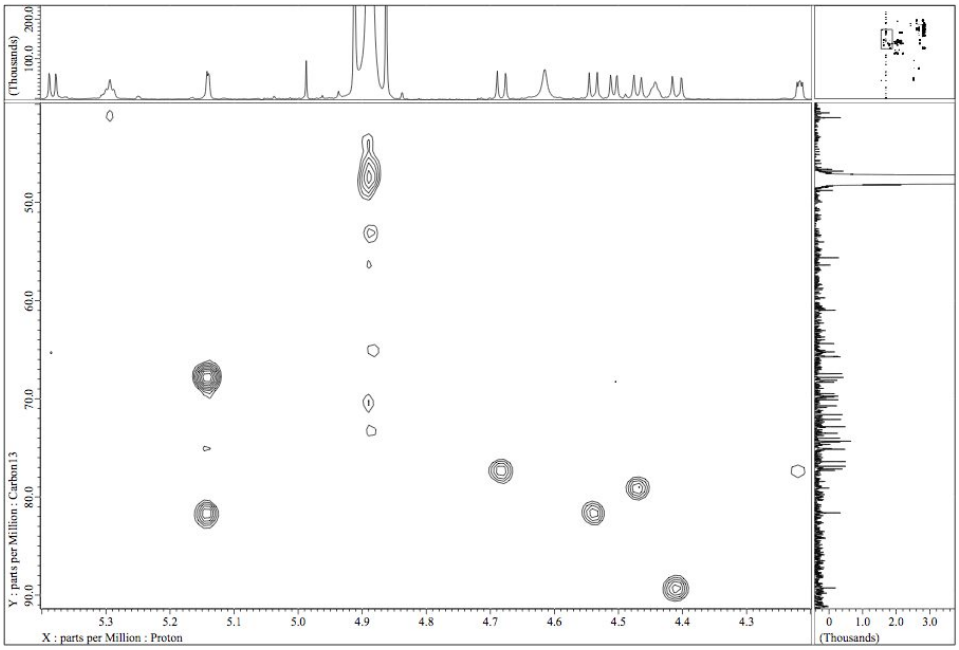

Fig. I.29. HMBC spectrum (anomers zone) of compound **7-a** (600 MHz, MeOH-d_4)

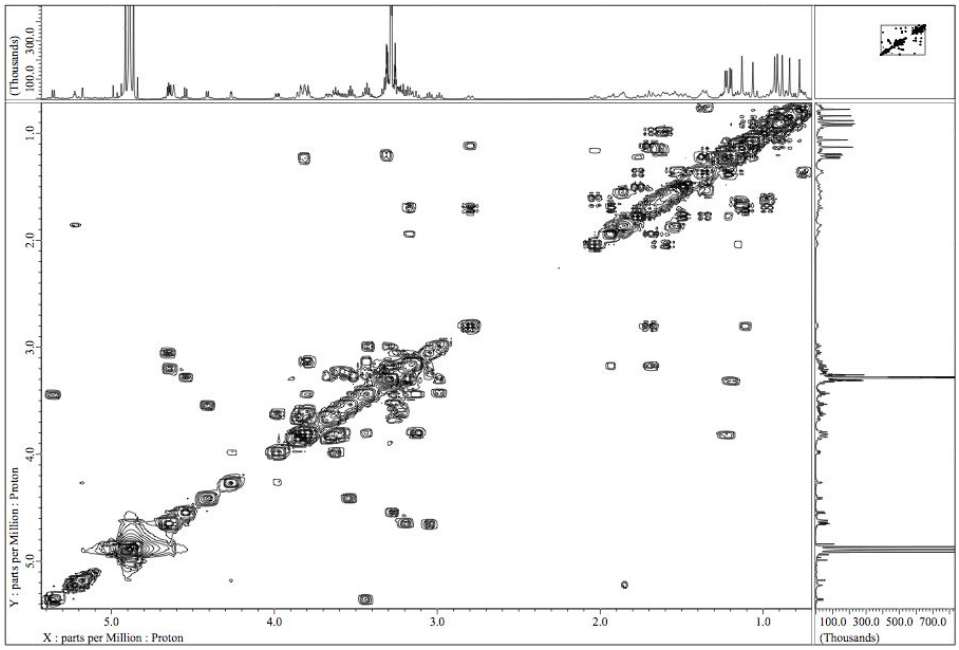

Fig. I.30. COSY spectrum of compound **2-a** (600 MHz, MeOH-d_4)

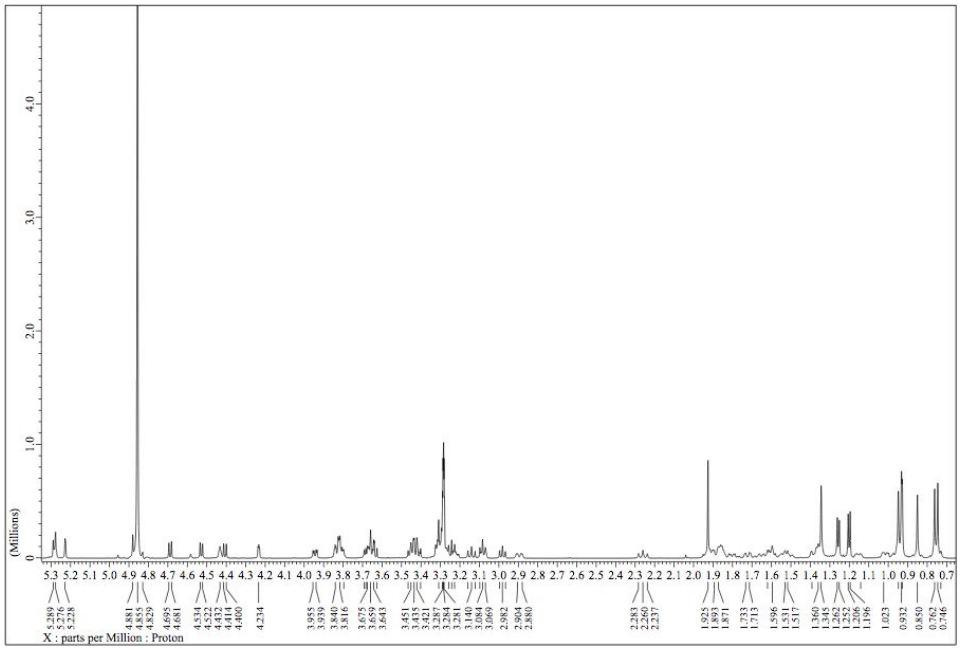

Fig. I.31. ^{1}H spectrum of compound **5-a** (600 MHz, MeOH-d_4)

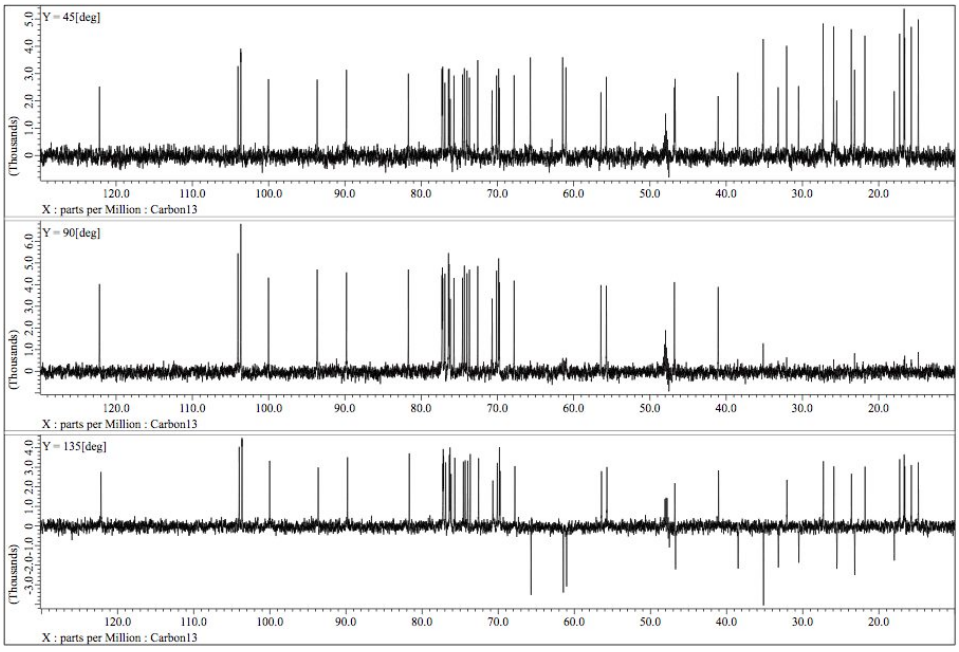

Fig. I.32. DEPT spectra of compound **5-a** (600 MHz, MeOH-d_4)

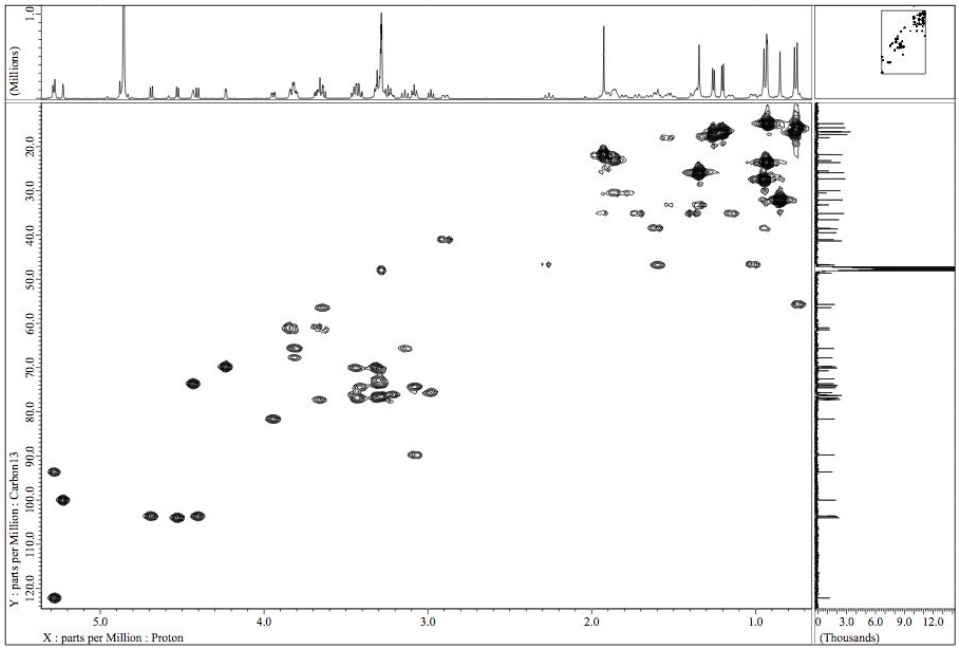

Fig. I.33. HMQC spectrum of compound **5-a** (600 MHz, MeOH-d_4)

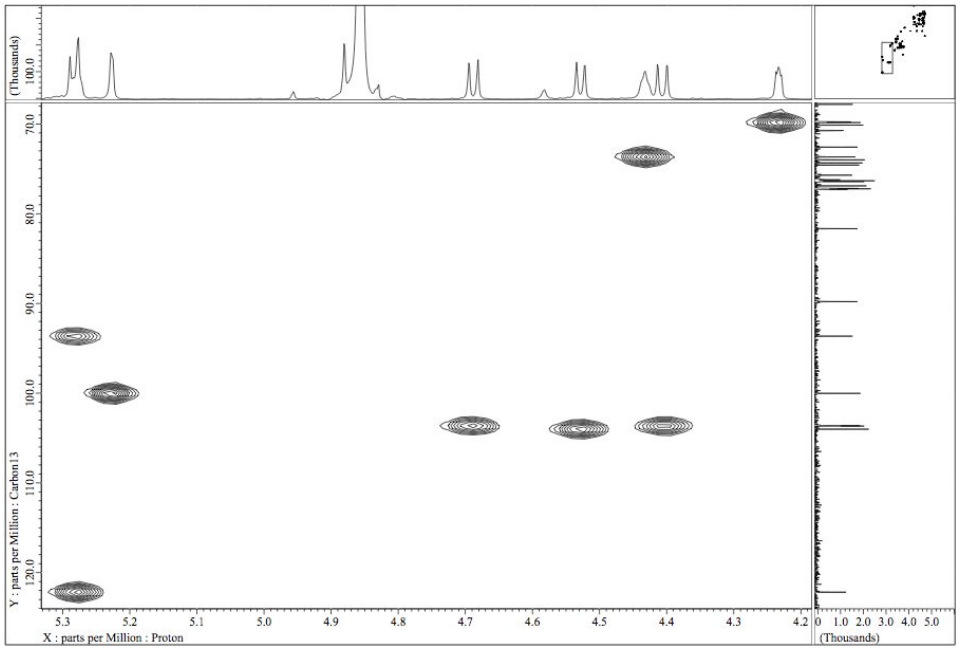

Fig. I.34. HMQC spectrum (anomers zones) of compound **5-a** (600 MHz, MeOH-d_4)

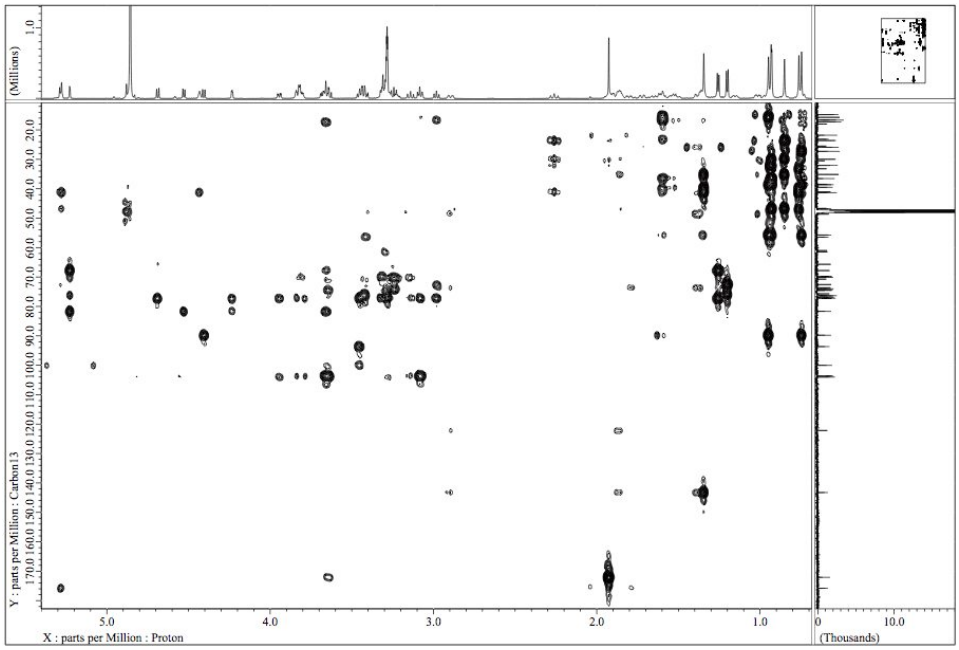

Fig. I.35. HMBC spectrum of compound **5-a** (600 MHz, MeOH-d_4)

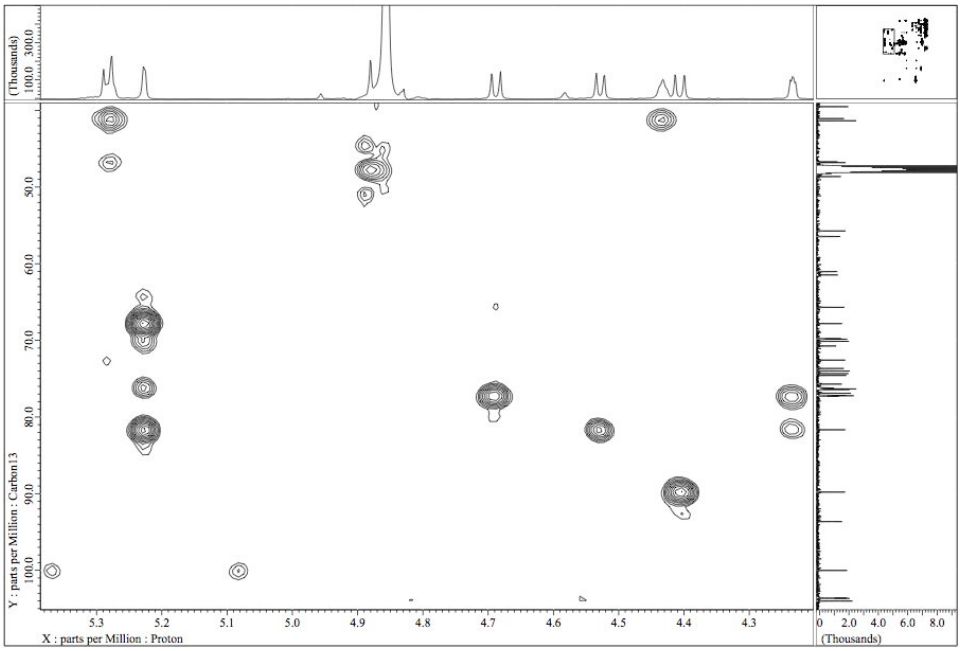

Fig. I.36. HMBC spectrum (anomers zone) of compound **5-a** (600 MHz, MeOH-d_4)

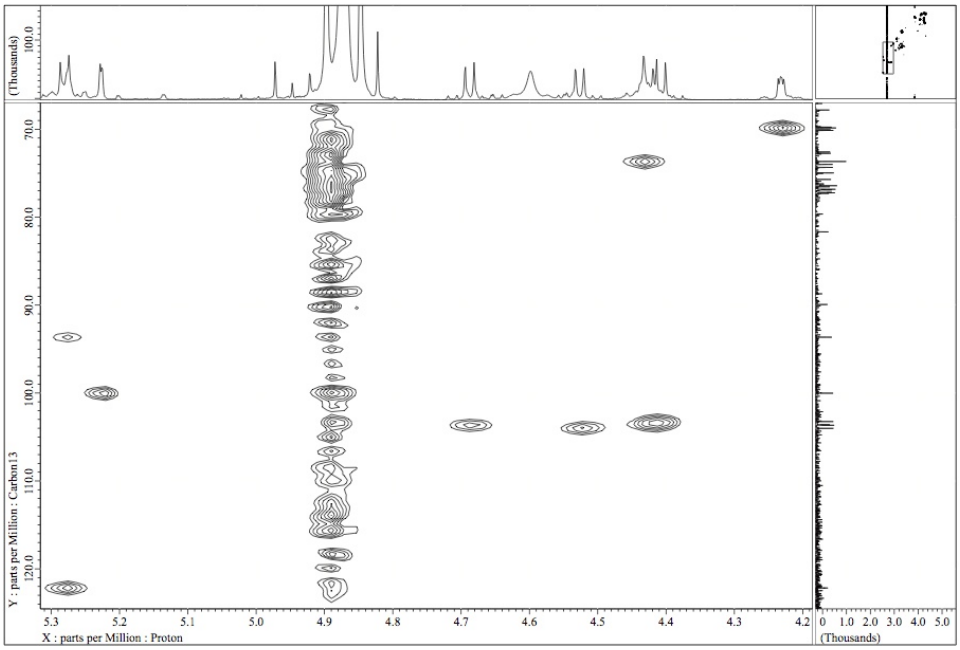

Fig. I.37. HMQC spectrum (anomers zones) of compound **1-b** (600 MHz, MeOH-d_4)

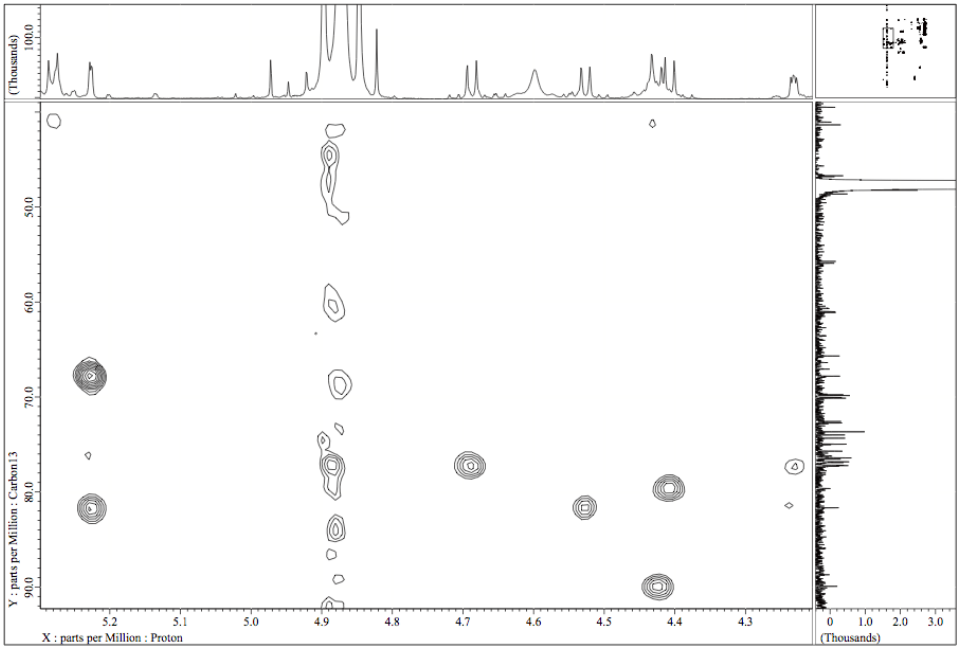

Fig. I.38. HMBC spectrum (anomers zones) of compound **1-b** (600 MHz, MeOH-d_4)

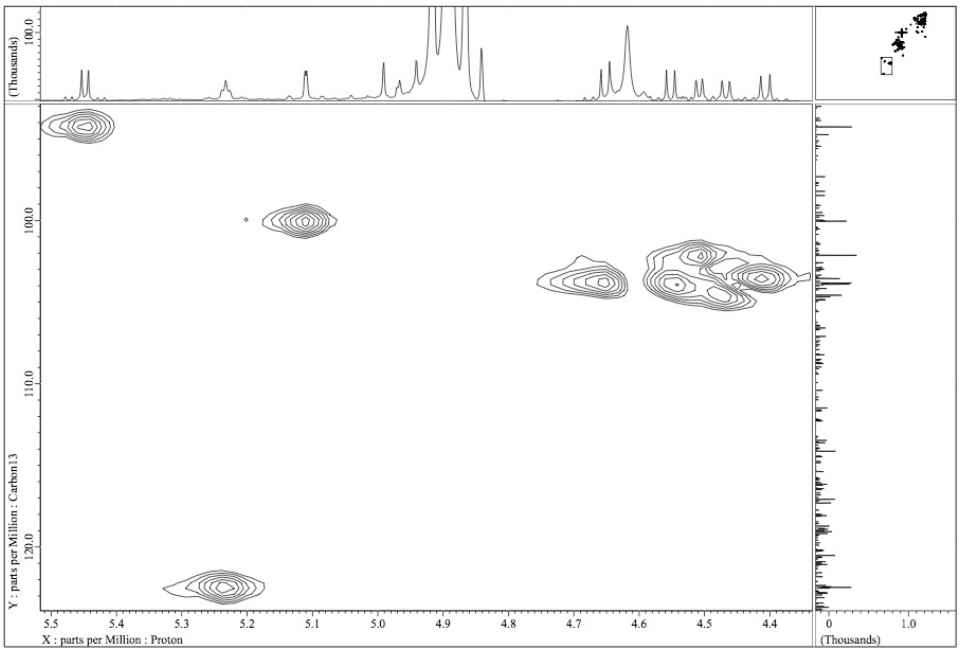

Fig. I.39. HMQC spectrum (anomers zones) of compound **2-b** (600 MHz, MeOH-d_4)

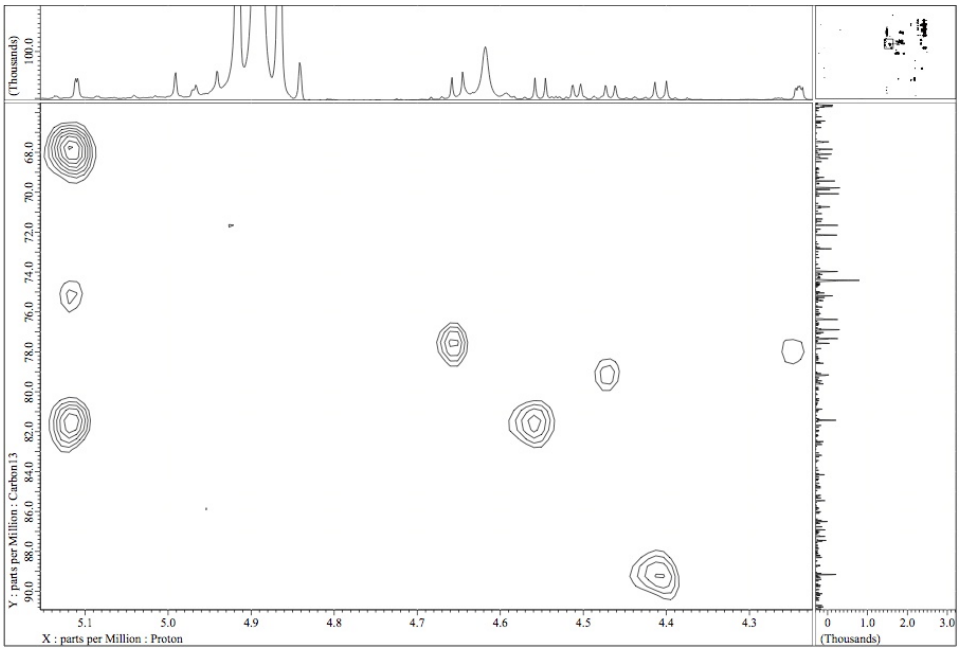

Fig. I.40. HMBC spectrum (anomers zones) of compound **2-b** (600 MHz, MeOH-d_4)

1.11. REFERENCES – I

Abe, I., Rohmer, M., Prestwich, G. C., 1993. Enzymatic cyclization of squalene and oxidosqualene to sterols and triterpenes. *Chem. Rev*., **93**, 2189–2206.

Abdel-Kader, M., Hoch, J., Berger, J. M., Evans, R., Miller, J. S., Wisse, J. H., Mamber, S. W., Dalton, J. M., Kingston, D. G. I., 2001. Two bioactive saponins from *Albizia subdimidiata* from the Suriname rainforest. *J. Nat. Prod*., **64**, 536–539.

Allen O. N., Allen E. K., 1981. The Leguminosae: a source book of characteristics, uses, and nodulation. University of Wisconsin Press, Madison, pp 1–548.

Abdel-Kader, M. S., Bahler, B. D., Malone, S. et al., 2000. Bioactive saponins from *Swartzia schomburgkii* from the Suriname rainforest. *J. Nat. Prod*., **63**, 1461–1464.

Agrawal, P. K., 1992. NMR spectroscopy in the structural elucidation of oligosaccharides and glycosides. *Phytochemistry* **31**, 3307–3330.

Bachran, C., Bachran, S., Sutherland, M., Bachran, D., Fuchs, H., 2008. Saponins in tumor therapy. *Mini Rev. Med. Chem*., **8**, 575–584.

Bruneton, J, 1995. Pharmacognosy, Phytochemistry, Medicinal Plants. Lavoisier Publishing, Paris, pp. 538–544

De Groot, C., Müller-Goymann, C. C., 2016. Saponin interactions with model membrane systems – Langmuir monolayer studies, hemolysis and formation of ISCOMs. *Planta Med*., **82**, 1496–1512.

De Tommasi, N., Autore, G., Bellino, A., Pinto, A., Pizza, C., Sorrentino, R., Venturella, P., 2000. Antiproliferative triterpene saponins from *Trevesia palmata*. *J. Nat. Prod*., **63**, 308–314.

Doran, J. C., Turnbull, J. W., Boland, D. J., Gunn, B. V., 1983. Handbook on seeds of dry zone *Acacias*, pp. 101.

Gafur, M. A., Obata, T., Kiuchi, F., Tsuda, Y., 1997. *Acacia concinna* Saponins. I. Structures of prosapogenols, concinnosides A-F, isolated from the alkaline hydrolysate of the highly polar saponin fraction. *Chem. Pharm. Bull*., **45**, 620–625.

Garai, S., Mahato, S. B., 1997. Isolation and structure elucidation of three triterpenoid saponins from *Acacia auriculiformis*. *Phytochemistry*, **44**, 137–140.

Gerkens, P. C., Dobson, R., Tabatadze, N., Mshviladzade, V., Elias, R., Peulen, O. J., Jolois, O. M., De Pauw-gillet, M.-C. A., 2007. Apoptosis and cytolysis induced by giganteosides and hederacolchisides in HL-60 cells. *Anticancer Res.*, **27**, 2529–2534.

Gunatilaka, A. A. L., Kingston, D. G. I., Johnson, R. K., 1994. Machanism-based isolation and structures of some anticancer active natural products. *Pure Appl. Chem*., **66**, 2219–2222.

Haddad, M., Laurens, V., Lacaille-Dubois, M.-A. 2004. Induction of apoptosis in leukemia cell line by triterpene saponins from *Albizia adianthifolia*. *Bioorg. Med. Chem*., **12**, 4725–4734.

Haddad, M., Miyamoto, T., Laurens, V., Lacaille, M.-A. 2003. Two new biologically active triterpenoidal saponins acylated with salicylic acid from *Albizia adianthifolia*. *J. Nat. Prod*., **66**, 372–377.

Hanausek, M., Ganesh, P., Walaszek, Z., Arntzen, C.J., Slaga, T. J., Gutterman, J. U., 2001. Avicins, a family of triterpenoid saponins from *Acacia victoria* (Benthem), suppress H-ras mutations and aneuploidy in a murine skin carcinogenesis model. *Proc. Natl. Acad. Sci. USA,* **98**, 11551–11556.

Haridas, V., Higuchi, M., Jayatilake, G. S., Bailey, D., Mujoo, K., Blake, M. E., Arntzen, C. J., Gutterman, J. U., 2001. Avicins: triterpenoid saponins from *Acacia victoria* (Bentham) induce apoptosis by mitochondrial perturbation. *Proc. Natl. Acad. Sci. USA,* **98**, 5821–5826.

Haridas, V., Arntzen, C. J., Gutterman, J. U., 2001. Avicins, a family of triterpenoid saponins from *Acacia victoria* (Bentham), inhibit activation of nuclear factor-kappaB by inhibiting both its nuclear localization and ability to bind DNA. *Proc. Natl. Acad. Sci. USA,* **98**, 11557–11562.

Haridas, V., Li, X., Mizumachi, T., Higuchi, M., Lemeshko, V. V., Colombini, M., Gutterman, J. U., 2007. Avicins, a novel plant-derived metabolite lowers energy metabolism in tumor cells by targeting the outer mitochondrial membrane. *Mitochondrion*, **7**, 234–240;

Haridas, V., Hanausek, M., Nishimura, G., Soehnge, H., Gaikwad, A., Narog, M., Spears, E., Zoltaszek, R., Walaszek, Z., Gutterman, J. U., 2004. Triterpenoid electrophiles (avicins) activate the innate stress response by redox regulation of a gene battery. *J. Clin. Invest*., **113**, 65–73.

Haridas, V., Nishimura, G., Xu, Z.-X., Connolly, F., Hanausek, M., Walaszek, Z., Zoltaszek, R., Gutterman, J. U., 2009. Avicin D: a protein reactive plant isoprenoid dephosphorylates Stat 3 by regulating both kinase and phosphatase activities. *PloS ONE,* **5**, e5578.

Hostettmann, K. A., and Marston, A., 1995. Saponins. Chemistry and pharmacology of natural products. Cambridge University Press, Cambridge, UK.

Hsu, M. J., Cheng, J. S., and Huang, H. C., 2000. Effect of saikosaponin, a triterpene saponin, on apoptosis in lymphocytes: association with c-*myc*, *p53*, and *bcl-2* mRNA. *Br. J. Pharmacol*., **131**, 1285–1293.

Irvine, F. R., 1961. Woody plants of Ghana, with special reference to their uses. Oxford University Press. London, pp. 984.

Jayatilake, G. S., Freeberg, D. R., Liu, Z., Richheimer, S. L., Blake, M. E., Bailey, D. T., Haridas, V., Gutterman, J. U., 2003. Isolation and structures of avicins D and G: in vitro tumor-inhibitory saponins derived from *Acacia victoriae*. *J. Nat. Prod*., **66**, 779–783.

Jia, Z., Koike, K., Nikaido, T., 1998. Major triterpenoid saponins from *Saponaria officinalis*. *J. Nat. Prod*., **61**, 1368–1373.

Judd, W. S., Campbell, C. S., Kellog, E. A., et al., 2002. Botanique systématique: une perspective phylogénétique. In: De Boeck Université (ed) Paris, Bruxelles

Lacaille-Dubois, M.-A., Pegnyemb, D. E., Noté, O. P., Mitaine-Offer, A. C., 2011. A review of acacic acid-type saponins from Leguminosae-Mimosoideae as potent cytotoxic and apoptosis inducing agents. *Phytochem. Rev*., **10**, 565–584.

Lacaille-Dubois, M.-A., 2005. Bioactive saponins with cancer related and immunomodulatory activity: recent developments: an update. In: Atta-Ur-Rahman (ed) Studies in natural products chemistry, **32**, Elsevier, Amsterdam, 209–246.

Lee, J. Y., Shin, J. W., Chun, K. S., Park, K. K., Chung, W. Y., Bang, Y. J., Sung, J. H., Surh, Y. J., 2005. Antitumor promotional effects of a novel intestinal bacterial metabolite (IH-901) derived from the protopanaxadiol-type ginsenosides in mouse skin. *Carcinogenesis*, **26**, 359 - 367.

Lemeshko, V. V., Haridas, V., Quijano Perez, J. C., Gutterman, J. U., 2006. Avicins, natural anticancer saponins, permeabilize mitochondrial membranes. *Arch. Biochem. Biophys*., **454**, 114–122.

Li, X. X., Davis, B., Haridas, V., Gutterman, J. U., Colombini, M., 2005. Proapoptotic triterpene elctrophiles (avicins) from channels in membranes: cholesterol dependence. *Biophys. J*., **88**, 2577–2584.

Mahato, S. B., Pal, B. C., Price, K. R., 1989. Structure of acaciaside, a triterpenoid trisaccharide from *Acacia auriculiformis*. *Phytochemistry,* **28**, 207–210.

Melek, F. R., Miyase, T., Ghaly, N. S., Nabil, M., 2007. Triterpenoid saponins with N-acetyl sugar from the bark of *Albizia procera*. *Phytochemistry,* **68**, 1261–1266.

Mimaki, Y., Yokosuka, A., Hamanaka, M., Sakuma, C., Yamori, T., Shibata, Y., 2004. Triterpene saponins from the roots of *Clematis chinensis*. *J. Nat. Prod*., **67**, 1511–1516.

Mujoo, K., Haridas, V., Hoffmann, J. J., Wachter, G. A., Hutter, L. K., Lu, Y., Blake, M. E., Jayatilake, G. S., Bailey, D., Mills, G. B., Gutterman, J. U., 2001. Triterpenoid saponins from *Acacia victoriae* (Bentham) decrease tumor cell proliferation and induce apoptosis. *Cancer Res*., **61**, 5486-5490

Nigam, S. K., Gopal, M., Uddin, R., Yoshikawa, K., Kawamoto, M., Arihara, S., 1997. Pithedulosides A-G, oleanane glycosides from *Pithecellobium dulce*. *Phytochemistry* **44**, 1329–1334.

Oh, G. S., Pae, H. O., Choi, B. M., Seo, E. A., Kim, D. H., Shin, M. K., Kim, J. D., Kim, J. B., Chung, H. T., 2004. 20(S)-Protopanaxatriol, one of ginsenoside metabolites inhibits inducible nitric oxide synthase and cyclooxygenase-2 expressions through inactivation of nuclear factor-kappaB in RAW 264.7 macrophages stimulated with lipopolysaccharide. *Cancer Lett*., **205**, 23–29.

Parrotta, J. A., 2002. *Albizia lebbeck* (L.) Benth. In: Vozzo, J. A., editor. Tropical Tree Seed Manual. Washington, DC.: USDA Forest Service, pp. 274–276.

Pezzuto, J. M., 1997. Plant-derived anticancer agents. *Biochem. Pharmacol*., **53**, 121–133.

Salawu, O. A, Tijani, A. Y, Babayi, H., Nwaeze, A. C., Anagbogu, R. A., Agbakwuru, V. A., 2010. Anti-malarial activity of ethanolic stem bark extract of *Faidherbia Albida* (Del) a. Chev (Mimosoidae) in mice. *Arch. Appl. Sci. Res*., **2**, 261–268.

Sawadogo W. R., Maciuk A., Banzouzi J. T., Champy P., Figadere B., Guissou I. P., Nacoulma O. G., 2012. Mutagenic effect, antioxidant and anticancer activities of six medicinal plants from Burkina Faso, *Nat. Prod. Res.*, **26**, 575–579.

Seigler, D. S., 2003. Phytochemistry of *Acacia–sensu lato*. *Biochem. Syst. Ecol*., **31**, 845–873.

Seo, Y., Hoch, J., Abdel-Kader, M., Malone, S., Derveld, I., Adams, H., Werkhoven, M. C. M., Wisse, J. H., Mamber, S. W., Dalton, J. M., Kingston, D. G. I., 2002. Bioactive saponins from *Acacia tenuifolia* from the Suriname rainforest. *J. Nat. Prod*., **65**, 170–174.

Sparg, S. G., Light, M. E., van Staden, J., 2004. Biological activities and distribution of plant saponins. *J. Ethnopharmacol*., **94**, 219–243.

Tchoukoua, A., Tabopda, T. K., Uesugi, S., Ohno, M., Kimura, K.-I., Kwon, E., Momma, H., Horo, I., Çalişkan, O. A., Shiono, Y., Ngadjui, B. T., 2017a. Triterpene saponins from the roots of *Acacia albida* Del. (Mimosaceae). *Phytochemistry*, **136**, 31–38.

Tchoukoua, A., Tabopda, T. K., Simo, I. K., Uesugi, S., Ohno, M., Kimura, K.-I., Kwon, E., Momma, H., Shiono, Y., Ngadjui, B. T., 2017b. Two new triterpene saponins from the barks of *Acacia albida* Del. (Mimosaceae). *Nat. Prod. Res.*, **32**, 924–932.

Tezuka, Y., Honda, K., Banskota, A. J., Thet, M. M., Kadota, S., 2000. Kinmoonosides A–C, three new cytotoxic saponins from the fruits of *Acacia concinna*, a medicinal plant collected in Myanmar. *J. Nat. Prod*., **63**, 1658–1664.

Thakur, M., Melzig, M. F., Fuchs, H., Weng, A., 2011. Chemistry and pharmacology of saponins: special focus on cytotoxic properties. *Botanics: Targets and Therapy,* **1**, 19–29.

Tijani, A. Y., Uguru, M. O., Salawu, O. A., 2008. Antipyretic, anti-inflammatory, and anti-diarrheal properties of *Faidherbia albida* in rats. *Afr. J. Biotech*., **7**, 696–700.

Tijani, A. Y., Uguru, M. O., Salawu, O. A., Abubakar, A., Onyekwelu, N. O., Akingbasote, J. A., 2009. Effect of *Faidherbia albida* on some biochemical parameters of rats infected with *Trypanosoma brucei brucei*. *Afr. J. Pharm. Pharmacol*., **3**, 26–30.

Wurochekke, A. U., Mahmoud, S. J., Zailani, H. A., 2013. Antimicrobial Activity of stem bark of *Faidherbia albida*. *Br. J. Pharm. Res.*, **3**, 786–794.

Xu, Z. X., Liang, J., Haridas, V., Gaikwad, A., Connolly, F. P., Mills, G. B., Gutterman, J. U., 2007. A plant triterpenoid, avicin D, induces autophagy by activation of AMP-activated protein kinase. *Cell Death Differ*., **14**, 1948–1957.

Zhang, C., Li, B., Gaikwad, A. S. et al., 2008. Avicin D selectively induces apoptosis and downregulates p-STAT-3, bcl-2, and survivin in cutaneous T-cell lymphoma cells. *J. Invest. Dermatol*., **128**, 2728–2735.

Zhong, L., Qu, G., Li, P., Han, J., Guo, D., 2003. Induction of apoptosis and G2/M cell cycle arrest by gleditsioside E from *Gleditsia sinensis* in HL-60 cells. *Planta Med*., **69**, 561–563.

Chapter 2

Two new 5-deoxyflavan-3,4-diol glucosides from the roots of *Albizia chevalieri* (Mimosaceae)

2.1. Botanical study

Members of the subfamily Mimosoideae have flowers with radial symmetry, small, inconspicuous corrollas and numerous, showy stamens. This family includes the genus *Albizia*.

2.1.1. *Albizia*

2.1.1.1. Classification

Kingdom: Plantae
Sub-kingdom: Tracheobionta
Division: Magnoliophyta (Angiosperms)
Class: Magnoliopsida (Dicotyledons)
Subclass: Rosidae
Order: Fabales
Family: Fabaceae
Subfamily: Mimosoideae
Genus: *Albizia*

2.1.1.2. Botanical aspect and distribution

The genus *Albizia* comprises approximately 150 species and includes at least 470 vernacular names. Most species are deciduous woody trees and shrubs.

The **leaves** are bipinnate with leaflets in numerous pairs or larger in fewer pairs. Petiolar glands are conspicuous. Stipules mostly inconspicuous, or caducous.

The **Flowers** are in globose heads or spikes, are hermaphrodite or male. Calyx (4)5(7)-lobed. Corolla (4)5(6)-lobed Stamens elongate and are usually white, filaments basally united into a tube. Corolla is funnel-shaped, connate beyond the middle.

The **Fruit** is broadly linear indehiscent or 2-valved, valves not twisted. Pods oblong, straight, flattened, mostly dehiscent, thin to almost woody.

Albizia has a discontinuous distribution, the most highly diverse in tropical and subtropical regions of Asia, Africa and America. In Africa, there are 36 endemic species and 22 in the Neotropics.

2.1.2. *Albizia chevalieri*

2.1.2.1. Botanical aspect and distribution

The plant *Albizia chevalieri* is a tree that grows up to 12 m high or a shrub under harsher conditions of the dry savannah from Senegal, Niger, Nigeria, and Cameroon. It has a bark pale-greyish, twigs pubescent with white lenticels.

The **leaves** with 8-12 pairs of pinnate and 20-40 pairs of leaflets each. Petals pale crimson with white margins.

The small **flowers** are borne in globular or finger-shaped clusters. Staminal tube included in the corolla-tube or only slightly exserted. Filaments white.

The **fruit** pale brown is a large, strap-shaped pod.

Albizia chevalieri (Tree)
Photo M. Schmidt

Albizia chevalieri (Flower)
Photo J. Tiquet

2.2. Ethnomedicinal value of *Albizia chevalieri*

The leaf extract of *A. chevalieri* is used for the management of diabetes mellitus by traditional medical practitioners in some parts of Niger Republic and Sokoto, Nigeria (Saidu et al., 2007a). The leaf extract has been reported to have a significant hypoglycemic effect (Saidu et al., 2007a), dysentery (Burkill, 1995), hematotoxicity (Saidu et al., 2007b), hypolipidemic (Saidu et al., 2009), and antioxidant activity (Saidu et al., 2009).

The bark is used in Borno-North eastern Nigeria as purgative, taenicide and also remedy for coughs (Aliyu et al., 2009). There are also reports on the local use of the leaves extract for cancer treatment in Zaria city, Kaduna state (Aliyu et al., 2009).

2.3. Chemical constituents in the genus *Albizia*

In prior studies on the genus *Albizia*, saponins and flavonoids were found as the main constituents. A previous phytochemical investigation on *A. chevalieri* stem bark led to the isolation and structure elucidation of three known pentacyclic triterpenoids: friedelin, friedelan-3-ol, and lupeol (Mathias et al., 2016).

Our interest will focus towards the flavonoids from this genus.

Table II.1. Flavonoids from *Albizia* species

Structures	Source	Activity	Ref.
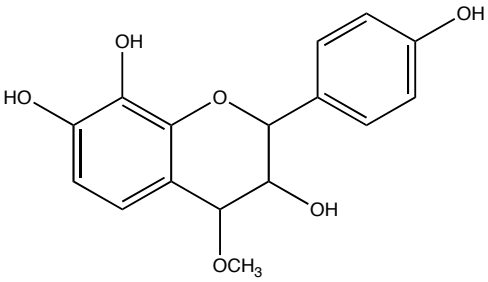 Albiziaflavan A	*A. ferruginea*	Antibacterial	Kamga et al., 2014
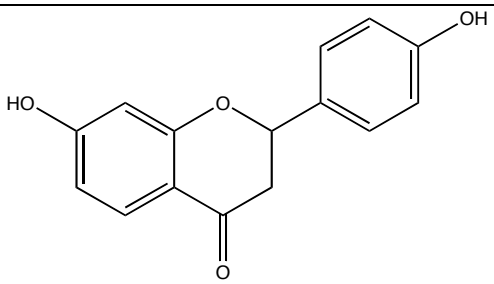 4',7-dihydroxyflavanone	*A. zygia*		Abdalla et al., 2012
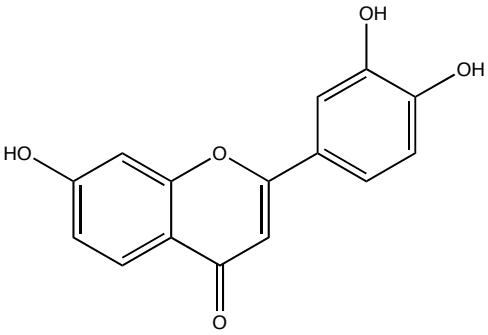 3',4',7-trihydroxyflavone	*A. zygia*	Antimalarial	Abdalla et al., 2012
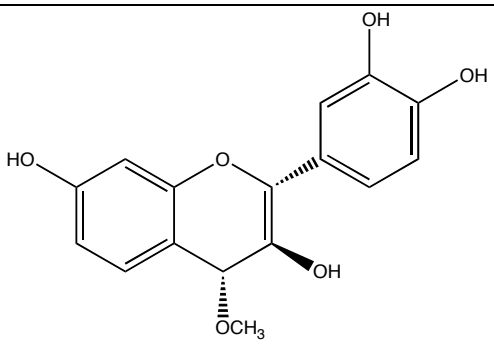 Albiziaflavan B	*A. glaberrima*		Fotso et al., 2017

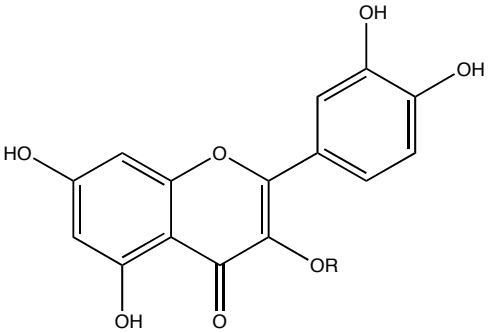 R = Rha(1→6)-Glc(1→6)-Gal Quercetin 3-*O*-α-Rha(1→6)-β-Glc(1→6)-β-Gal	*A. lebbeck*		El-Mousallamy, 1998
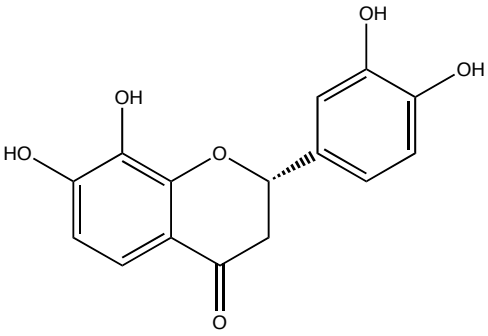 Isookanin	*A. julibrissin*	Antioxidative	Jung et al., 2004
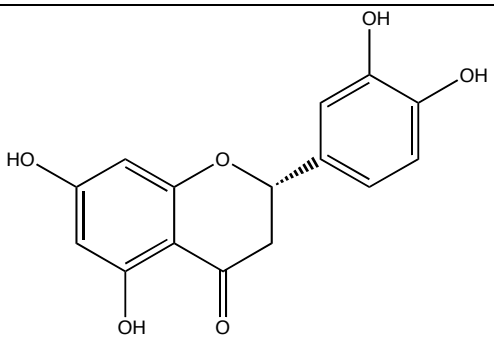 Luteolin	*A. julibrissin*	Antioxidative	Jung et al., 2004
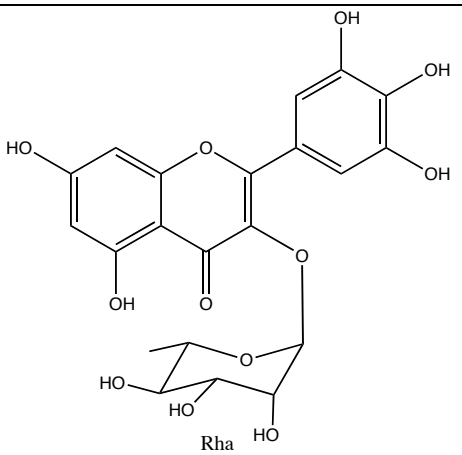 Myricitrin	*A. amara*	DNA protection, modulation of fertility, antioxidant	Kassem et al., 2016

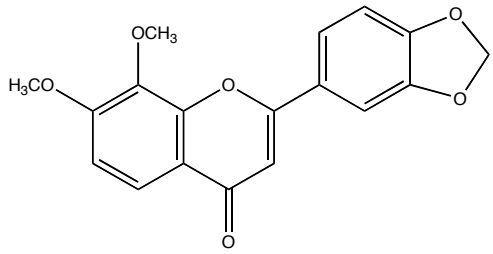 7,8-dimethoxy-3',4'-methyledioxyflavone	*A. odoratissima*	Rao et al., 2002
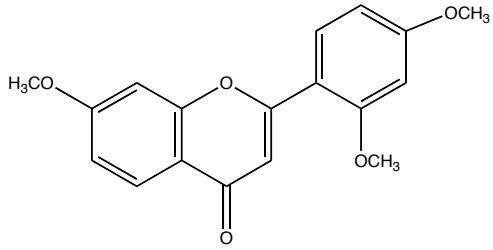 7,2',4'-trimethoxyflavone	*A. odoratissima*	Rao et al., 2002

2.4. Results and discussion

Phytochemical investigation of the roots of *Albizia chevalieri* led to the isolation of two new 5-deoxyflavan-3,4-diol glucosides. Therefore, we report herein the isolation and structure elucidation of these compounds. Furthermore, they were examined for cytotoxicity against HL60 cancer cells lines. Their antibacterial activity was also reported.

2.4.1. Extraction and isolation

The powdered roots of *Albizia chevalieri* were extracted with *n*-hexane, then with MeOH at room temperature. After filtration and evaporation procedures, *n*-hexane and MeOH extracts were obtained respectively. The MeOH extract was dissolved in H_2O, and successively partitioned with EtOAc, and *n*-BuOH saturated with H_2O. The *n*-BuOH extract was subjected to VLC and MPLC using reversed-phase material (RP-18) to afford two new 5-deoxyflavan-3,4-diols glucosides, chevalieriflavanosides A and B.

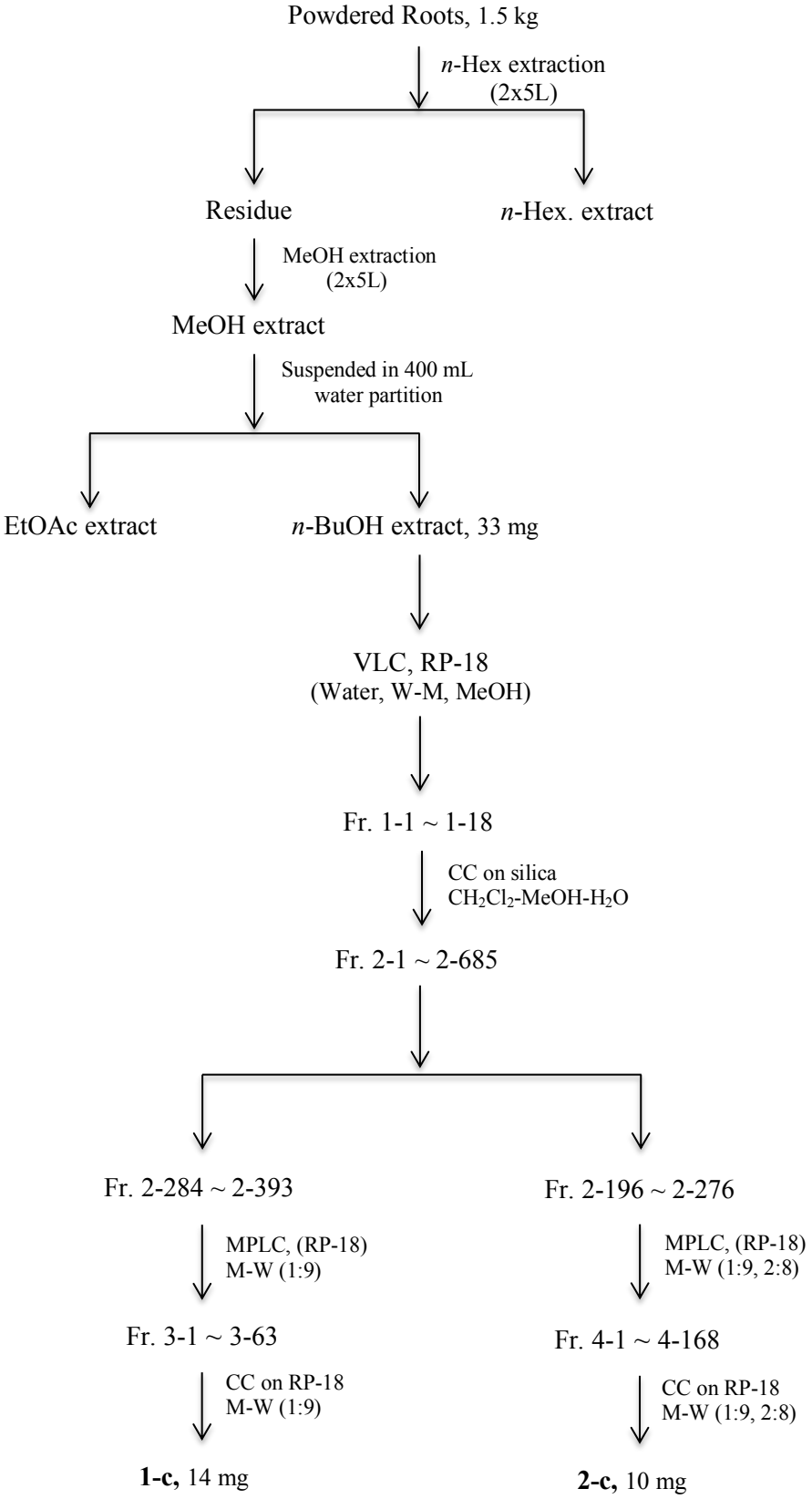

Scheme II.1. Isolation procedure of *Albizia chevalieri* (roots)

2.4.2. Structure determination

Compounds **1-c** and **2-c** were obtained as a brownish amorphous powder and gave a dark blue coloration with $FeCl_3$ reagent. Moreover, they showed a positive Shinoda test, (Sahu et al., 2010) suggesting that **1-c** and **2-c** are flavonoids.

2.4.2.1. Compound 1-c

The molecular formula, $C_{21}H_{24}O_{11}$ was established from the HRESIMS which showed the pseudo-molecular ion peak at *m/z* 475.1210 ($[M+Na]^+$).

The IR spectrum displayed absorption band of hydroxyl groups at ν_{max} 3394 cm^{-1}. The UV spectrum exhibited characteristic absorbance bands of flavan-3,4-diol at λ_{max} 225 and 275 nm (Takahashi et al., 1984).

The ^1H NMR spectrum of **1-c** showed an aromatic AB coupled system at δ_H 6.83 (1H, d, J = 8.3 Hz, H-5) and 6.89 (1H, d, J = 8.3 Hz, H-6), and an AA′BB′ spin system at δ_H 6.81 (2H, d, J = 8.3 Hz, H-3′, H-5′) and 7.42 (2H, d, J = 8.3 Hz, H-2′, H-6′). This observation suggested a tetrasubstituted A-ring and hence the AA'BB' aromatic spin system was located on B-ring. The location of the AB system at H-5 and H-6 was confirmed by the HMBC correlations (**Fig. II.2**) of H-5 with C-6, C-7, C-4, C-4a, and C-8a, and of H-6 with C-4a, C-5, C-7 and C-8. The NMR spectrum of **1-c** further showed signals of a sugar unit at δ_H/δ_C 4.76 (1H, d, J = 7.6 Hz, H-1") / 104.4 (C-1"), 3.49 (1H, t, J = 7.6 Hz, H-2") / 74.9 (C-2"), 3.45 (1H, dd, J = 9.0 Hz, 7.6, H-3") / 77.6 (C-3"), 3.39 (1H, m, H-4") / 71.2 (C-4"), 3.42 (1H, m, H-5") / 78.3 (C-5"), 3.72 (1H, dd, J = 12.5, 4.8 Hz, H-6") and 3.88 (1H, dd, J = 12.5, 2.1 Hz, H-6") / 62.4 (C-6"). Stereochemistry at anomeric position of the sugar moiety of **1-c** was assigned as β on the basis of ^1H-^1H coupling constants ($J_{1",2"}$ = 7.6 Hz) in the ^1H NMR spectrum of **1-c**. The sugar was identified as D-glucopyranosyl by the measurement of optical rotation and retention time and by the evaluation of spin-spin couplings and chemical shifts (Polonsky et al., 1972). The remaining signals in the ^1H and ^{13}C NMR spectra correspond to those of a propan-1,2,3-triol (chroman ring) at δ_H/δ_C 5.11 (1H, br. s, H-2) / 76.4 (C-2), 3.87 (1H, d, J = 2.7 Hz, H-3) / 72.5 (C-3), and 4.48 (1H, d, J = 2.7 Hz, H-4) / 69.2 (C-4). They were assigned to H-2, H-3, and H-4, respectively as H-2 showed HMBC correlations with C-1′, C-2′, C-3, C-4, and C-8a, and the H-4, correlations with C-2, C-3, C-4a, C-5, and C-8a.

Acid hydrolysis of **1-c** afforded a free sugar moiety and (−)-teracacidin (Clark-Lewis et al., 1961). The HMBC correlation between the anomeric proton of the glucose unit and C-7 (δ_C 147.0) suggested that the glucose is fixed at C-7 through an ether linkage. The *R*-configuration of C-2 was deduced from the CD spectra which showed a negative cotton effect within the ^1L_b transition ($[\theta]_{278}$ = – 4,000) (Ferreira et al., 2004). The coupling constants ($J_{2,3}$ = nearly 0 Hz and $J_{3,4}$ = 2.7 Hz) of between H-2 and H-3, and between H-3 and H-4 of C-ring, confirmed the 2,3-*cis*-3,4-*cis* relative configurations. The trend of small coupling constants compared to their *trans* isomers (^3J = 7.0 Hz-10.0 Hz) has been well established in closely related 2,3-*cis*-3,4-*cis*-flavan-3,4,7,3',4'-pentaol ($J_{2,3}$ = 1.0 Hz, $J_{3,4}$ = 4.0 Hz) and 2,3-*cis*-3,4-*cis*-4-methoxyflavan-3,7,8,3',4'-pentaol ($J_{2,3}$ = 1.0 Hz, $J_{3,4}$ = 2.8 Hz) (Kim et al., 2013, Wu et al., 2008).

Thus the absolute configuration of the flavan moiety of **1-c** was elucidated to be 2*R*,3*R*,4*R* as shown in **Fig. II.1**, named chevalieriflavanoside A (A. Tchoukoua et al., 2016).

2.4.2.2. Compound 2-c

The molecular formula, $C_{21}H_{24}O_{11}$ was established from the HRESIMS which showed the pseudo-molecular ion peak at *m/z* 475.1210 ($[M+Na]^+$).

The ^1H and ^{13}C NMR spectra of **2-c** (**Table II.2**) were similar to those of **1-c** with the differences being the chemicals shifts and coupling patterns of C-2 [δ_H 5.00 (1H, d, *J* = 9.0 Hz); δ_C 78.3], C-3 [δ_H 3.97 (1H, dd, *J* = 9.0, 3.4 Hz); δ_C 72.0] and C-4 [δ_H 4.57 (1H, d, *J* = 3.4 Hz); δ_C 67.8] in **2-c** compared to those of corresponding carbons in **1-c**. This suggested that **2-c** has different configurations at the C-ring from those of **1-c**. The gross structure of **2-c** was clearly elucidated by analyzing 2D NMR experiments (COSY, HMQC, and HMBC) (**Appendix–II**).

Furthermore, the absolute configuration of **2-c** was determined by comparing their coupling constants and CD data. The CD data of **2** ($[\theta]_{270}$ = – 1,000) established its absolute configuration to be 2*R*. By contrast, the large coupling constant between H-2/H-3 in **2-c** meant that H-3 must be pseudo-equatorial, and so the 4-hydroxy must be *β*. The small coupling constants between H-3 and H-4 of the C-ring suggested the 3,4-*trans* configuration. 2,3-*trans*-3,4-*cis*-orientation was further supported by previously reported compound, 2,3-*trans*-3,4-*cis*-7,4'-dimethoxyflavan-3,4-diol ($J_{2,3}$ = 9.7 Hz,

$J_{3,4}$ = 3.6 Hz) (Benavides et al., 2007), ($J_{2,3}$ = 9.5 Hz, $J_{3,4}$ = 3.5 Hz) (du Preez et al., 1970).

On the basis of the evidence, the absolute configuration of the flavan moiety was established as 2*R*,3*S*,4*S* as shown in **Fig. II.1**, named chevalieriflavanoside B (A. Tchoukoua et al., 2016).

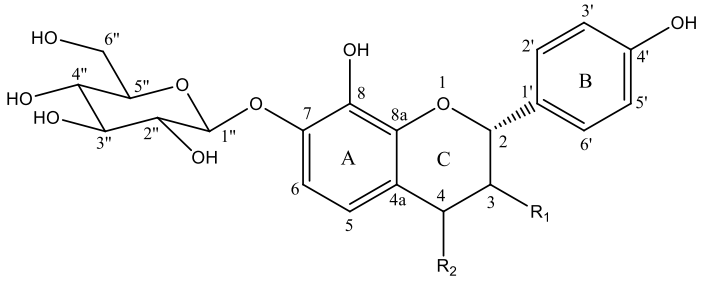

1: R_1= OH , R_2= OH

2: R_1= OH , R_2= OH

Fig. II.1. Structures of compounds **1-c** and **2-c**.

Table II.2. ^{1}H and ^{13}C NMR data of **1-c** and **2-c**

Position	**1-c**[a]		**2-c**[a]	
	δ_C	δ_H (m, *J* in Hz)	δ_C	δ_H (m, *J* in Hz)
2	76.4	5.11 (br. s)	78.3	5.00 (d, 9.0)
3	72.5	3.87 (d, 2.7)	72.0	3.97 (dd, 9.0, 3.4)
4	69.2	4.48 (d, 2.7)	67.8	4.57 (d, 3.4)
4a	119.0	-	120.4	-
5	122.6	6.83 (d, 8.3)	119.8	6.70 (d, 8.9)
6	111.3	6.89 (d, 8.3)	111.6	6.82 (d, 8.9)
7	147.0	-	147.7	-
8	136.4	-	138.5	-
8a	145.2	-	145.1	-
1'	130.7	-	130.5	-
2', 6'	129.5	7.42 (d, 8.3)	130.2	7.29 (d, 8.3)
3', 5'	115.9	6.81 (d, 8.3)	116.3	6.78 (d, 8.3)
4'	158.2	-	159.3	-
1"	104.4	4.76 (d, 7.6)	104.6	4.74 (d, 7.6)
2"	74.9	3.49 (t, 7.6)	74.9	3.36 (m)
3"	77.6	3.45 (dd, 9.0, 7.6)	77.6	3.42 (m)
4"	71.2	3.39 (m)	71.3	3.44 (m)
5"	78.3	3.42 (m)	78.3	3.36 (m)
6"	62.4	3.72 (dd, 12.5, 4.8)	62.5	3.69 (dd, 12.4, 4.8)
		3.88 (dd, 12.5, 2.1)		3.85 (d, 12.4)

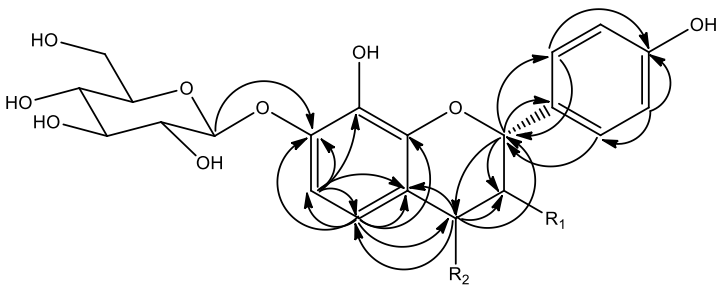

Fig. II.2. Selected HMBC (H→C) correlations of **1-c** and **2-c**.

2.5. Biological study

2.5.1. Results of cytotoxicity

Compounds **1-c** and **2-c** were evaluated for their cytotoxic activities against human cancer. Unfortunately, they exhibited no activities towards HL60 cells at the concentration of 100 μM.

2.5.2. Antibacterial activities

The antibacterial activities of **1-c** and **2-c** also were evaluated against *Pseudomonas aeruginosa* and *Staphylococcus aerus* using the agar diffusion test, and the **1-c** and **2-c** showed marginal activity at 100 μg/disk.

2.6. General conclusion

The study carried out on roots of *Albizia chevalieri* led to the isolation and identification of two new flavan-3,4-diol glucosides, chevalieriflavanosides. Characteristic physical data of isolated compounds from *Albizia chevalieri* were shown in the experimental section 2.7.3.1. They exhibited weak antibacterial activity. Catechins which have the same skeleton with the chevalieriflavanosides are reported to have antibacterial activity (Borris, 1996, Moerman, 1996). Because of the minimal activity of the chevalieriflavonosides, one might assume that the absence of hydroxyl group at C-5 on A-ring decrease the antibacterial activity, and the occurrence of a glycosidic unit at C-7 also makes them weaker due to their high polarity (Kumar et al., 2013).

2.7. Experimental – II

2.7.1. General procedures

CD spectra were recorded on a JASCO 302-A spectrophotometer in MeOH.

Optical rotation was measured with a Horiba SEPA-300 polarimeter (HORIBA, Kyoto, Japan). IR spectrum was recorded with a Jasco J-20A (JASCO Cooperation, Tokyo, Japan) and Shimadzu UV mini-1240 (SHIMADZU, Kyoto, Japan) spectrophotometers.

The ESI-MS was measured on a Varian AAT 311A mass spectrometer, and the HRESIMS was taken on a JEOL HX110 mass spectrometer (JEOL, Tokyo, Japan).

1D and 2D NMR spectra were run on JEOL JNM-ECZ600R/S1 600 MHz NMR spectrometer. The ^{1}H (600 MHz) and ^{13}C (150 MHz) chemical shifts were referenced to the residual solvent peak of methanol-d_4 at δ_H 3.30 for proton and δ_C 49.0 ppm for carbon. Coupling constants (J) are in hertz. The ^{1}H sweep width was set at 11282 Hz for all experiments with a 45° pulse for ^{1}H and a 30° pulse for ^{13}C.

The pulse programs of the COSY, HMQC, and HMBC experiments were taken from the Varian Software Library and standard pulse sequences were used for 2D spectra.

Semipreparative HPLC was carried out with Shimadzu pump and UV LC-10A detector (set at 210 nm) on Mightysil RP-18 column (250 x 6.0 mm i.d.) at the flow rate of 0.8 and 1.0 mL/min^{-1}. Column chromatography was conducted on silica gel 60 (Kanto Chemical Co., Inc., Japan).

TLC was carried out on Merck precoated silica gel plates (silica gel 60 F_{254}, 20 x 20 cm, Merck, Darmstadt, Germany), and spots were detected by spraying with H_2SO_4 followed by heating.

2.7.2. Plant material

A. chevalieri was collected in Maroua, Far North Region of Cameroon and identified by Mr. Tapsou, botanist at the Institute of Agricultural Research for Development in December 2013 and a voucher specimen N° 36696 HNC has been deposited at the Cameroon National Herbarium.

2.7.3. Extraction and isolation

The powdered roots of *Albizia chevalieri* were extracted with *n*-hexane, then with MeOH at room temperature. After filtration and evaporation procedures, *n*-hexane and MeOH extracts were obtained respectively. The MeOH extract was dissolved in

H_2O, and successively partitioned with EtOAc, and *n*-BuOH saturated with H_2O. The *n*-BuOH extract was subjected to vacuum liquid chromatography (VLC) using reversed-phase material (RP-18), MPLC and column chromatography over normal and reverse phase RP-18 silica gel to afford pure flavonoids, chevalieriflavanosides A and B.

2.7.3.1. Characteristic physical data of isolated compounds from *Albizia chevalieri*

Compounds	Spectroscopic data
1-c (Chevalieriflavanoside A)	Molecular formula: $C_{21}H_{24}O_{11}$ HR-ESIMS (positive-ion mode) *m/z* 475.1210 ($[M+Na]^+$ calcd for $C_{21}H_{24}O_{11}Na$ 475.1215) CD (c 0.1, MeOH) [θ] (λ) – 4000 mol. ellip. (278 nm) (neg. max.), +7000 mol. ellip. (235 nm) (pos. max.) ^1H and ^{13}C NMR data, see Table II.2
2-c (Chevalieriflavanoside B)	Molecular formula: $C_{21}H_{24}O_{11}$ HR-ESIMS (positive-ion mode) *m/z* 475.1210 ($[M+Na]^+$ calcd for $C_{21}H_{24}O_{11}Na$ 475.1215) CD (*c* 0.1, MeOH) [θ] (λ) – 1000 mol. ellip. (270 nm) (neg. max.), – 10000 mol. ellip. (224 nm) (neg. max.) ^1H and ^{13}C NMR data, see Table II.2

2.7.4. Chemical analysis

2.7.4.1. Acid hydrolysis and HPLC analysis

Each solution of **1-c** (5 mg) and **2-c** (5 mg) in 0.2 M HCl (dioxane-H_2O 1:1, 3 ml) was heated at 95°C for 30 min under argon. After cooling, the mixture was neutralized by passage through an Amberlite-IRA-93ZU (Organo, Tokyo, Japan) column and chromatographed (Diaion HP-20, 40% MeOH followed by Me_2CO-EtOH 1:1) to give aglycone fractions (2.5 mg) and a sugar fraction (1.7 mg). After the sugar fraction was passed through a Sep-Pak-C_{18} cartridge (Waters, Milford, MA, USA; with 40% MeOH) and Toyopak-IC-SP-M-cartridge (Tosoh; with 40% MeOH), it was analyzed by HPLC (MeCN-H_2O 17: 3, flow rate, 0.9 $mlmin^{-1}$; detection, refractive

index (RI) and optical retention (OR): D-glucose (t_R 15.84, $[\alpha]_D^{25}$ +53.3 º in **1-c** and **2-c** (lit. (Schaffer, 1972) +52.7 º).

2.7.5. Cell culture and cytotoxicity

HL60 cells (RCB0041, RIKEN BioResource Center, Tsukuba, Japan) was grown in RPMI 1640 medium supplemented with 10% heat-inactivated FBS (BioWest, Canada) and penicillin (50 units/ml)-streptomycin (50 µg/ml) (Gibco Corp., Carlsbad, USA) in a humidified atmosphere at 37°C under 5% CO_2. The cytotoxicity of the compounds was examined by MTT assay, as described previously (Arayama et al., 2016).

2.7.6. Assay for antimicrobial activity

Antimicrobial activities were determined using the agar diffusion test using paper disks (8mm in diameter, thin, ADVANTEC) against *S. aureus* NBRC 13276, *P. aeruginosa* ATCC 15442. An antibiotic paper disk was loaded with a sample soln. and then dried for 2h *in vacuo* to remove the solvent. Each test sample-loaded disk was placed on the agar plates inoculated with tester strains, which were incubated at 25°C. Antimicrobial activities were estimated by measuring the diameter of inhibition zone formed on the agar (Shiono et al., 2005).

Appendix – II

Selected spectra of chapter 2

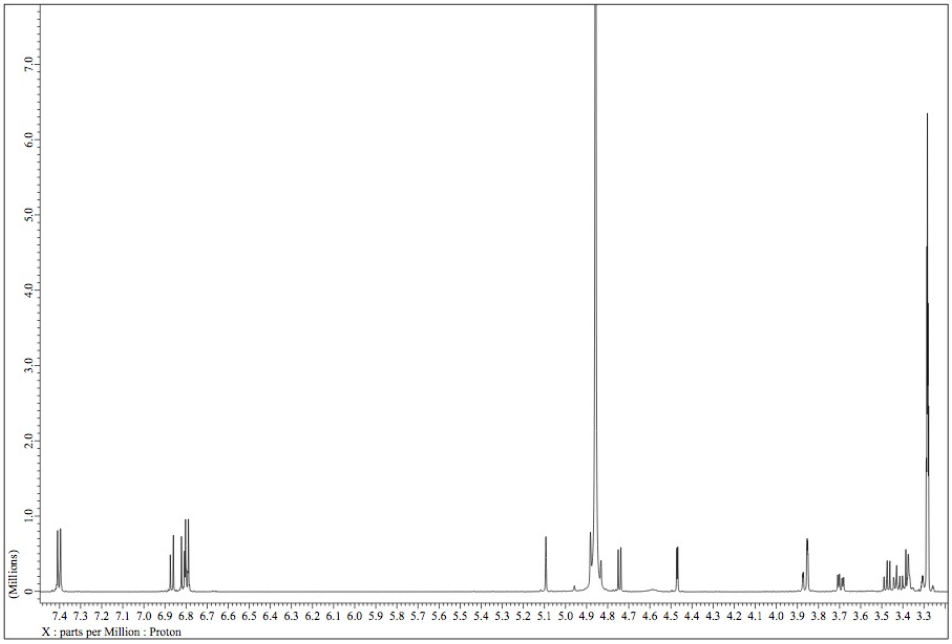

Fig. II.3. ^{1}H spectrum of compound **1-c** (600 MHz, MeOH-d_4)

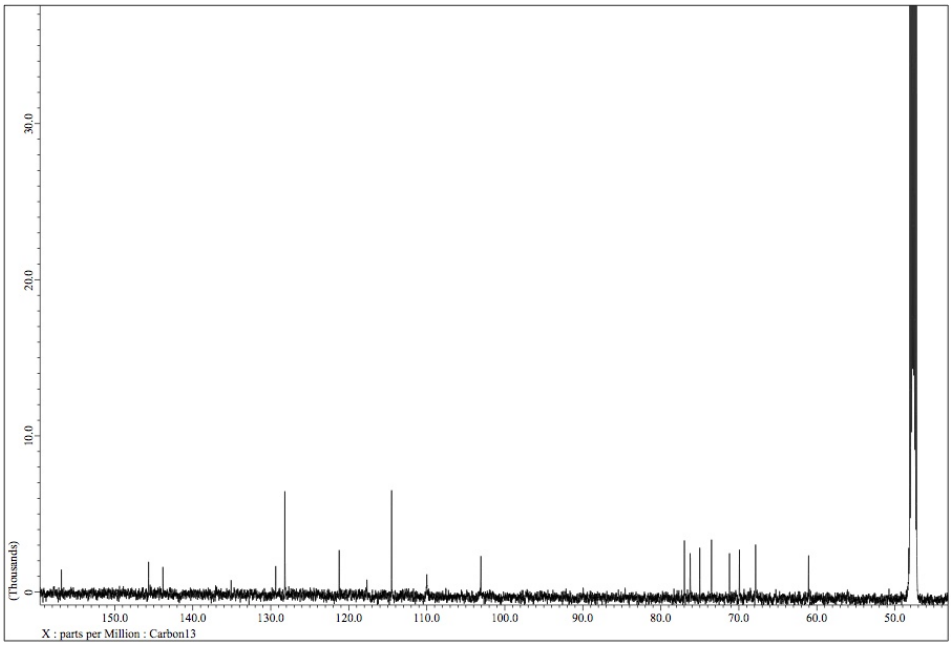

Fig. II.4. ^{13}C spectrum of compound **1-c** (150 MHz, MeOH-d_4)

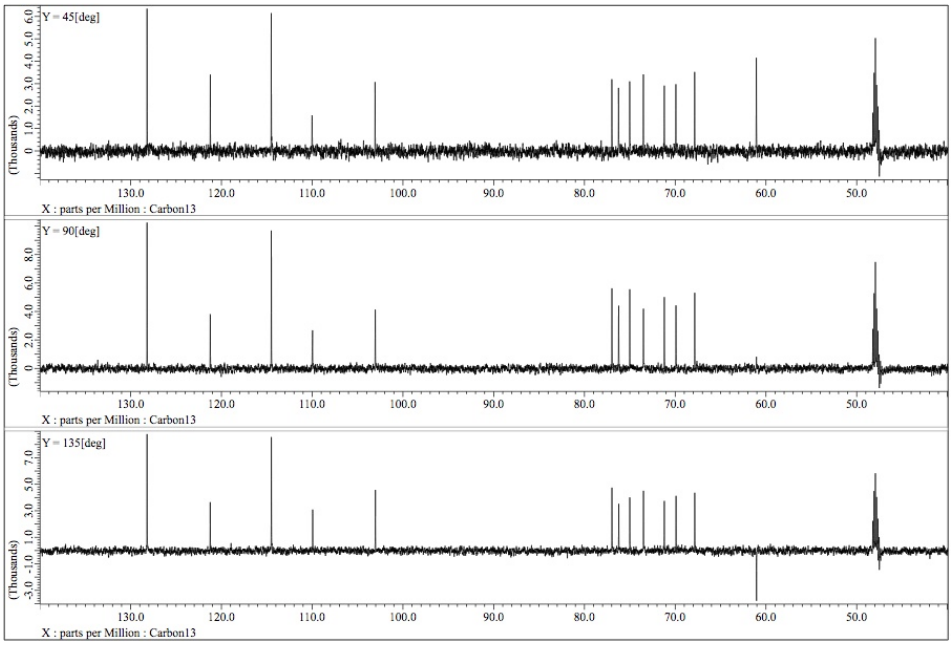

Fig. II.5. DEPT spectra of compound **1-c** (600 MHz, MeOH-d_4)

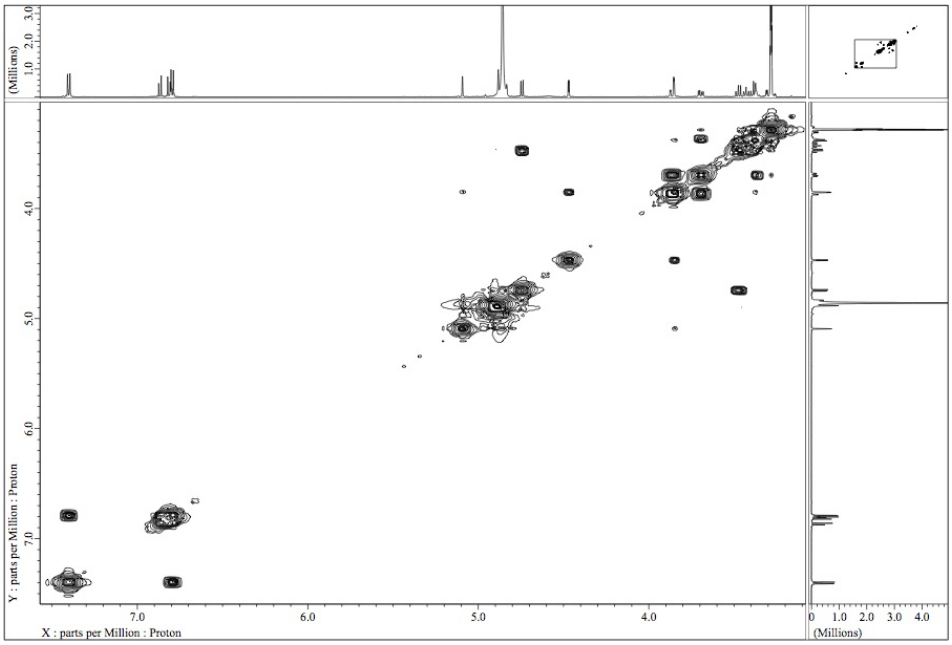

Fig. II.6. COSY spectrum of compound **1-c** (600 MHz, MeOH-d_4)

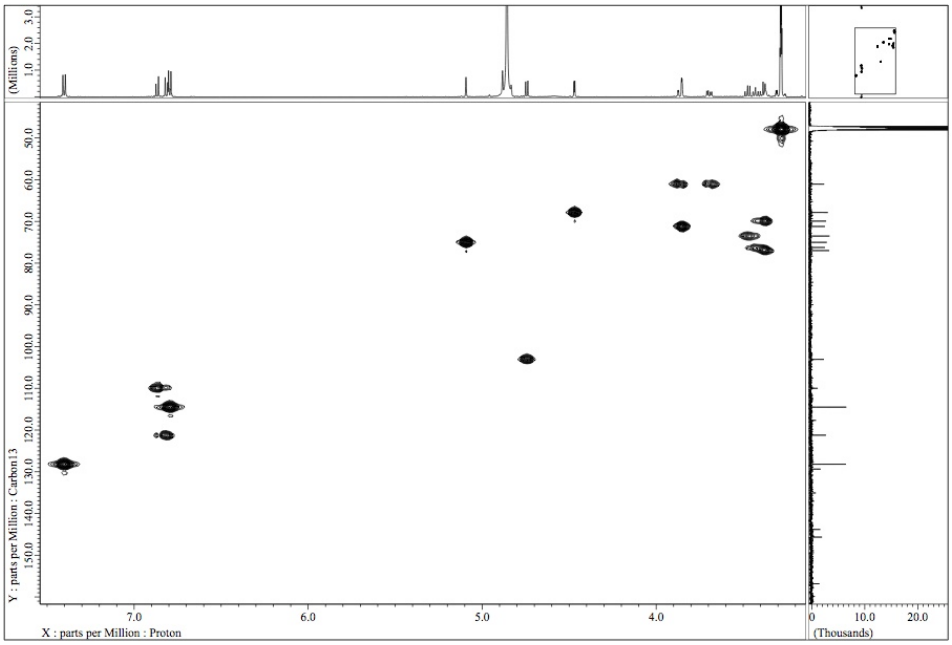

Fig. II.7. HMQC spectrum of compound **1-c** (600 MHz, MeOH-d_4)

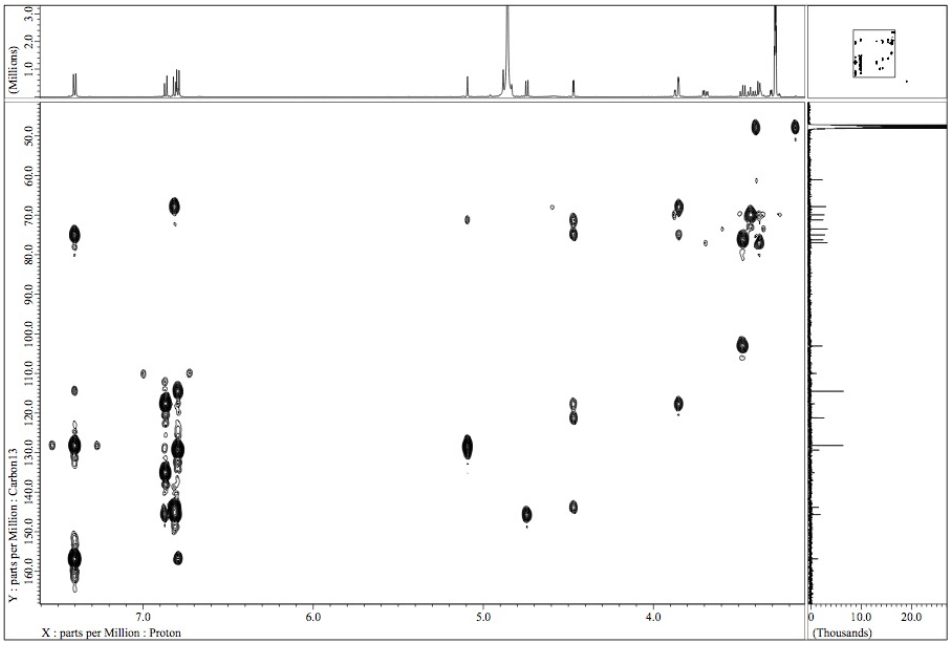

Fig. II.8. HMBC spectrum of compound **1-c** (600 MHz, MeOH-d_4)

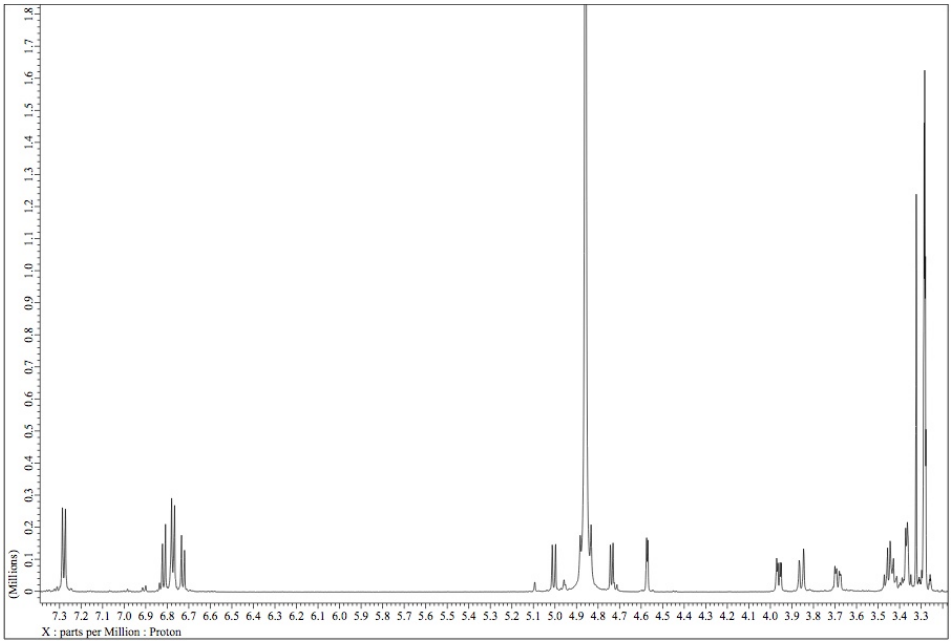

Fig. II.9. ^{1}H spectrum of compound **2-c** (600 MHz, MeOH-d_4)

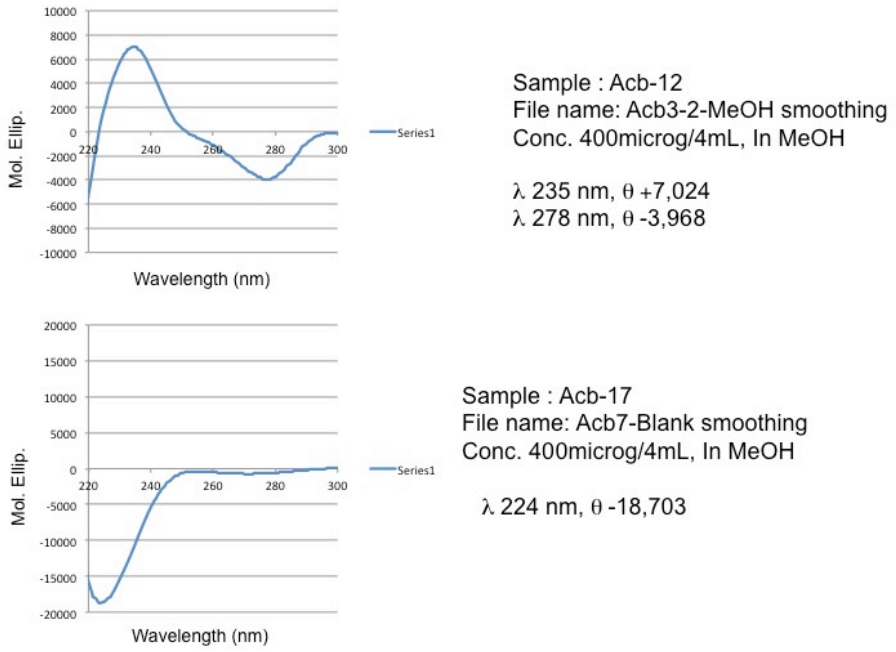

Fig. II.10. CD spectrum of compounds **1-c** and **2-c**

2.8. References – II

Abdalla, M. A., Laatsch, H., 2012. Flavonoids from Sudanese *Albizia zygia* (Leguminosae, subfamily Mimosoideae), a plant with antimalarial potency. *Afr. J. Tradit. Complement. Altern. Med*., **9**, 56–58.

Aburai, N., Yoshida, M., Ohnishi, M., Kimura, K., 2010. Pisiferdiol and pisiferic acid isolated from *Chamaecyparis pisifera* activate protein phosphatase 2C *in vitro* and induce caspase-3/7-dependent apoptosis via dephosphorylation of Bad in HL60 cells. *Phytomedicine,* **17**, 782–788.

Aliyu, A. B., Musa, A. M., Ibrahim, M. A., Ibrahim, H., Oyewale, A. O. 2009. Preliminary phytochemical screening and antioxidant activity of leave extract of *Albizia chevalieri* Harms (Leguminosae-Mimosoideae). *Bajopas*, **2**, 149–153.

Benavides, A., Bassarello, C., Montoro, P., Vilegas, W., Piacente, S., Pizza, C. 2007. Flavonoids and isoflavonoids from *Gynerium sagittatum*. *Phytochemistry*, **68**, 1277–1284.

Borris, R. P., 1996. Natural products research: perspectives from a major pharmaceutical company. *J. Ethnopharmacol*., **51**, 29–38.

Burkill, H. M., 1995. The useful plants of West Tropical Africa. *Royal Botanical Gardens, Kew*., **3**, 207–208.

Clark-Lewis, J. W., Katekar, G. F., Mortimer, P. I. 1961. Flavan derivatives. Part IV. Teracacidin, a new leucoanthocyanidin from *Acacia intertexta*. *J. Chem. Soc.***,** **99**, 499–503.

El-Mousallamy, A. M. D. 1998. Leaf flavonoids of *Albizia lebbeck*. *Phytochemistry,* **48**, 759–761.

Ferreira, D., Marais, J. P. J., Slade, D., Walker, L. A., 2004. Circular dichroic properties of flavan-3,4-diols. *J. Nat. Prod.*, **67**, 174–178.

Fotso, G. W., Kamga, J., Ngameni, N., Uesugi, S., Ohno, M., Kimura, K.-I., Momma, H., Kwon, E., Furuno, H., Shiono, Y., Ingrid, S. K., Yeboah, S. O., Ngadjui, B. T., 2017. Secondary metabolites with antiproliferative effects from *Albizia glaberrima* var glaberscens Oliv. (Mimosoideae). *Nat. Prod. Res*., **31**, 1981–1987.

Jung, M. J., Kang, S. S., Jung, H. A., Kim, G. J., Choi, J. S., 2004. Isolation of flavonoids and a cerebroside from the stem bark of *Albizia julibrissin*. *Arch. Pharm. Res.*, **27**, 593–599.

Kamga, J., Sandjo, L. P., Böke-Sarikahya, N., Kirmizigül, S., Kuete, V., Ngadjui, B. T., 2014. Albiziaflavane A: a new flavane from *Albizia ferruginea* (Mimosoideae). *Nat. Prod. Res.,* **28**, 1574–1578.

Kassem, M. E. S., Ibrahim, L. F., Hussein, S. R., El-Sharawy, R., El-Ansari, M. A., Hassanane, M. M., Booles, H. F., 2016. Myricitrin and bioactive extract of *Albizia amara* leaves: DNA protection and modulation of fertility and antioxidant-related genes expression. *Pharm. Biol.*, **54**, 2404–2409.

Kim, K. H., Moon, E., Choi, S. U., Kim, S. Y., Lee, K. R. 2013. Polyphenols from the bark of *Rhus verniciflua* and their biological evaluation on antitumor and anti-inflammatory activities. *Phytochemistry,* **92**, 113–121.

Kumar, S., Pandey, A. K., 2013. Chemistry and biological activities of flavonoids: An overview. *Tswj*, 1–16.

Mathias, S. N., Abubakar, M. S., October, N., 2016. Pentacyclic triterpenoids from the stem-bark of *Albizia chevalieri* Hams (Mimosaceae). *Int. J. Pharm. Pharm. Sci.,* 8, 261–265.

Moerman, D. E., 1996. An analysis of the food plants and drug plants of native North America. *J. Ethnopharmacol.*, **52**, 1–22.

Polonsky, J., Baskevitch, Z., Cagnoli-Bellavita, N., Ceccherelli, P., Buckwalter, B. L., Wenkert, E., 1972. Carbon-13 NMR spectroscopy of naturally occurring substances. XI. Biosynthesis of the virescenosides. *J. Am. Chem. Soc.*, **94**, 4369–4370.

du Preez, I. C., Roux, D.G., 1970. Novel flavan-3,4-diols from *Acacia aucultriformis*. *J. Chem. Soc.*, 1800–1804.

Rao, Y. K., Reddy, M. V. B., Rao, C. V., Gunasekar, D., Blond, A., Caux, C., Bodo, B., 2002. Two new 5-deoxyflavones from *Albizia odoratissima*. *Chem. Pharm. Bull.,* **50**, 1271–1272.

Sahu, V. K., Irchhaiya, R., Shashi, A., Gurjar, H., 2010. Phytochemical investigation and chromatographic evaluation of the ethanolic extract of whole plant extract of *dendrophthoe falcate* (L.F.) ettingsh. *Int. J. Pharm. Sci. Res.*, **1**, 39–45.

Saidu, Y., Bilbis, L. S., Isezuo, S. A., Habibullah, S. A., Ladan, M. J., Lawal, M., 2009. The hypolipidaemic effects of the partially puriiified "Hypoglycaemic agent" of aqueous leaf extract of *Albizzia chevalieri* Harms. *Cameroon J. Exp. Biol.,* **5**, 37–43.

Saidu, Y., Lawal, M., Isezuo, S. A., Shehu, R. A., Sahabi, D. M. A., Bilbis, L. S., 2007. Partial purification and elucidation of mechanism of hypoglycaemic agent of aqueous leaf extract of *Albizzia chevalieri* Harms (Leguminosae). *J. Pharmacol. Toxicol.***, 2**, 513–523.

Saidu, Y., Bilbis, L. S., Lawal, N., Isezua, S. A., Hassan, S. W., Abbas, A. Y., 2007. Acute and sub-chronic toxicity studies of crude aqueous extract of *Albizzia chevalieri*. *Asian J. Biochem.,* **2**, 224–236.

Shiono, Y., Murayama, T., Takahashi, K., Okada, K., Katohda, S., Ikeda, M., 2005. Three oxygenated cyclohexanone derivatives produced by an endophytic fungus. *Biosci. Biotechnol. Biochem.,* **69**, 287–292.

Schaffer, R., 1972. Occurrence, properties and preparation of naturally occurring monosaccharides (including 6-deoxy sugars). In W. Pigman, D. Horton (eds). "The Carbohydrates: Chemistry and Biochemistry, Academic Press, New York, **1**, 69–111.

Takahashi, H., Kubota, Y., Miyazaki, H., Onda, M., 1984. Heterocycles. XV. Enantioselective synthesis of chiral flavonols and flavan-3,4-diols. *Chem. Pharm. Bull.,* **32**, 4852–4857.

Tchoukoua, A., Tabopda, T. K., Uesugi, S., Kimura, K.-I., Kwon, E., Momma, H., Ngadjui, B. T., Koseki, T., Shiono, Y., 2016. Two new 5-deoxyflavan-3,4-diol glucosides from roots of *Albizia chevialieri*. *Magn. Reson. Chem.*, **54**, 893–896.

Wu, J.-H., Tung, Y.-T., Chien, S.-C., Wang, S.-Y., Kuo, Y.-H., Shyur, L.-F., Chang, S.-T., 2008. Effect of phytocompounds from the heartwood of *Acacia confusa* on inflammatory mediator production. *J. Agric. Food. Chem.,* **56**, 1567–1573.

Chapter 3

Metabolites from Endophytic Fungi of *Xylaria* sp. (Xylariaceae)

3.1. Endophytes

3.1.1. Introduction

Endophytes are microbes that colonize living, internal tissues of plants without causing any immediate negative effects (Bacon and White, 2000). They reside inside the tissues of nearly all healthy plants.

It appears that all higher plants are hosts to one or more endophytic microbes. These microbes include the fungi, bacteria, and actinomycetes.

In the last few decades, plant scientists have begun to realize that plants may serve as a reservoir of untold numbers of organisms known as endophytes (Bacon and White, 2000).

Endophytic fungi are a very promising source of novel biologically active compounds, and have proven to yield a considerable hit-rate of novel compounds when screening larger strain numbers for biological activities (Schulz *et al.*, 2002).

3.1.2. The Xylariaceae

The Xylariaceae are a family of mostly small ascomycetous fungi that is found throughout the temperate and tropical regions of the world. This family comprises of nearly 70 genera (Lumbsch and Huhndorf, 2007). These saprophytic fungi can be found on decayed wood, litter, fruits, seeds, dung and leaves and on insects. Members of Xylariaceae occur as endophytes (Petrini et al., 1985).

3.1.2.1. The genus *Xylaria*

Xylaria is a genus of ascomycetous fungi commonly found growing on dead wood. The name comes from the Greek xýlon meaning wood (xylem).

Xylaria is the largest genus of the family Xylariaceae and presently includes ca. 300 accepted species of stromatic pyrenomycetes (Kirk et al., 2008). *Xylaria* species are widespread from the temperate to the tropical zones of the earth (Abate et al., 1997). The traditional view of *Xylaria* sp. as saprotrophic wood-destroyers had to be emended, since it was found that members of this genus occur ubiquitously as endophytes of vascular plant (Petrini et al., 1995).

Fungi of the genus *Xylaria* have been shown to be potential sources of novel secondary metabolites, and many of them possess biological activities relevant for drug discovery (Pittayakhajonwut et al., 2005), including cytotoxic, antimalarial, and antimicrobial activities. In this part of our thesis, we compile the most important secondary metabolites isolated from the genus *Xylaria* recentely.

3.1.2.2. Secondary metabolites from *Xylaria* sp.

The secondary metabolites from *Xylaria* sp. include sesquiterpenoids, diterpenoids, diterpene glycosides, triterpene glycosides, steroids, N-containing compounds, aromatic compounds, pyrone derivatives, and polyketides.

Table III.1. Secondary metabolites from *Xylaria* species

N°	Structures	Source	Activity	Ref.
3.1	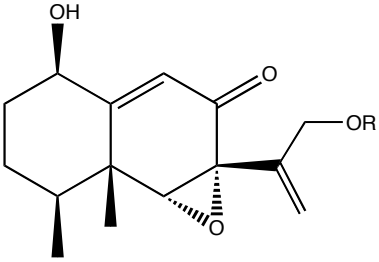 R = H, Xylarenone A R = Ac, Xylarenone B	*X.* sp. NCY2	Antibacterial Antitumor	Hu et al., 2008
3.2	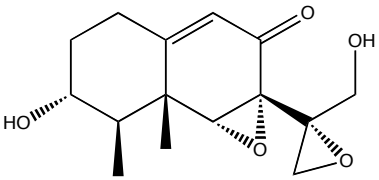 Phaseolinone	*X.* sp. PA-01	Cytotoxic	Silva et al., 2010
3.3	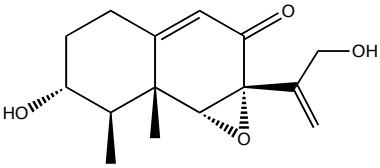 Phomenone	*X.* sp. PA-01	Antifungal	Silva et al., 2010
3.4	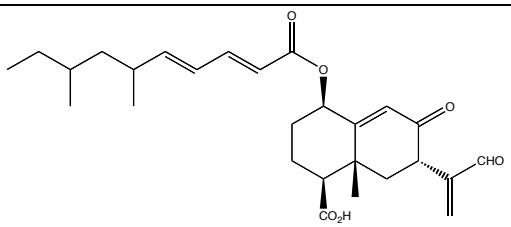 07H239-A	*X.* sp. LL-07H239	Cytotoxic Inhibitory activity	McDonald et al., 2004 Song et al., 2012
3.5	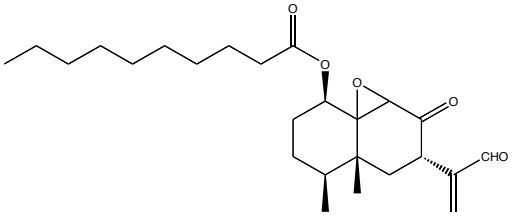 Xylarenal B	*X. persicaria*		Smith et al., 2002

3.6	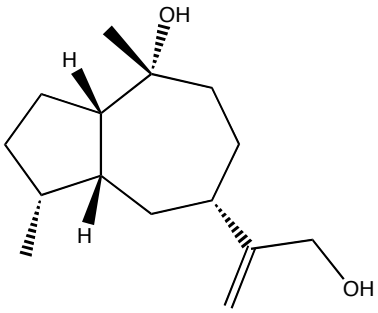 Xylaranol A	*X.* sp. 101		Li et al., 2010
3.7	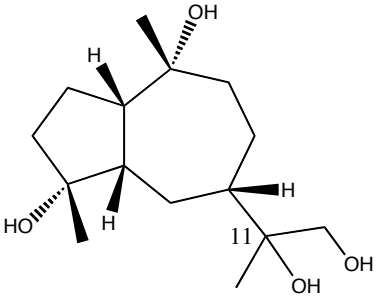 Xylaguaianol A (11*R**) Xylaguaianol B (11*S**)	*X.* sp. NC1214		Wei et al., 2015
3.8	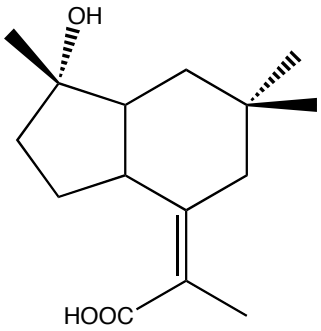 Xylarenic acid	*X.* sp. NCY2	Antibacterial Antitumor	Hu et al., 2008
3.9	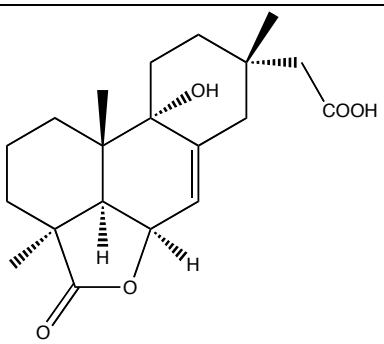 Xylarenolide	*X.* sp. 101		Li et al., 2010

3.10	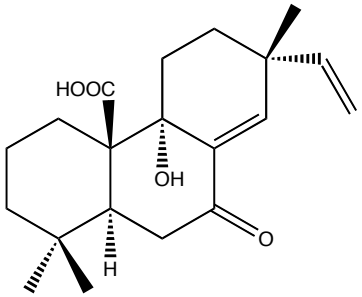 Sphaeropsidin C	*X.* sp. BCC 4297		Isaka et al., 2011
3.11	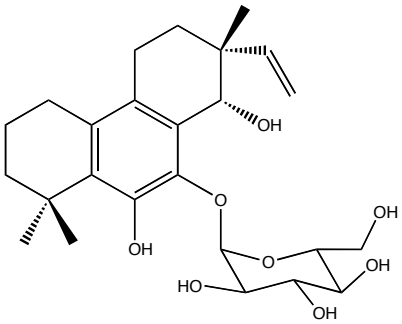 Xylopimarane	*X.* sp. BCC 4297	Antibacterial Cytotoxic	Isaka et al., 2011 Deyrup et al., 2007
3.12	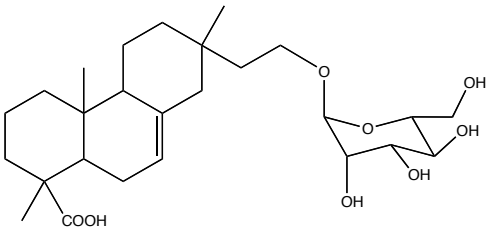 16-α-D-mannopyranosyloxyisopimar-7-en-19-oic acid	*X. polymorpha*	Cytotoxic	Shiono et al., 2009
3.13	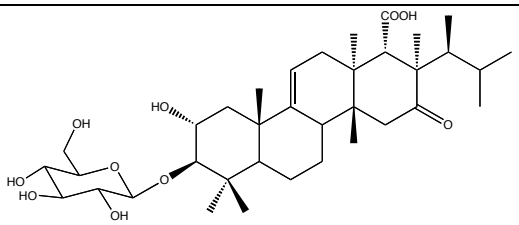 Kolokoside A	*X.* sp. NRRL 4019		Deyrup et al., 2007
3.14	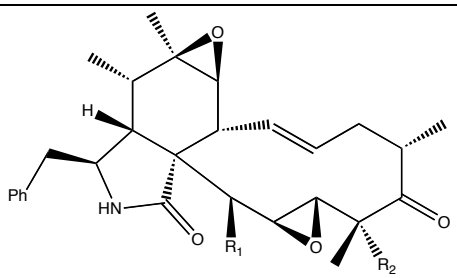 R_1 = AcO, R_2 = OH, 19,20-epoxycytochalasin Q R_1 = H, R_2 = OH, deacetyl 19,20-epoxycytochalasin Q	*X. obovata*	Cytotoxic	Dagne et al., 1994 Chen et al., 2011

3.15	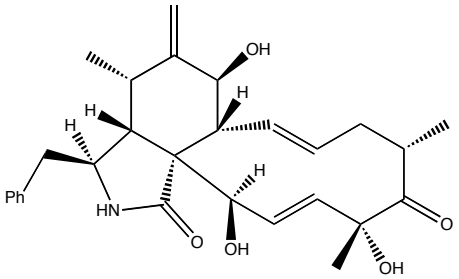 Deacetylcytochalasin D	*X.* sp. BCC9653	Pongcharoen et al., 2007
3.16	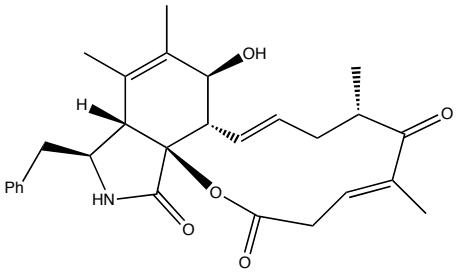 Cytochalasin Z_{27}	*X.* sp. XC-16	Zhang et al., 2014
3.17	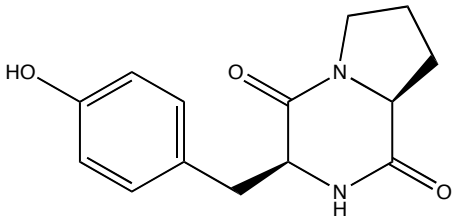 Cyclo(L-Pro-L-Tyr)	*X.* sp. BCC9653	Pongcharoen et al., 2007
3.18	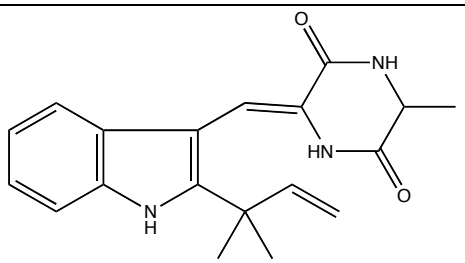 Neoechinulin A	*X. euglossa*	Wang et al., 2005
3.19	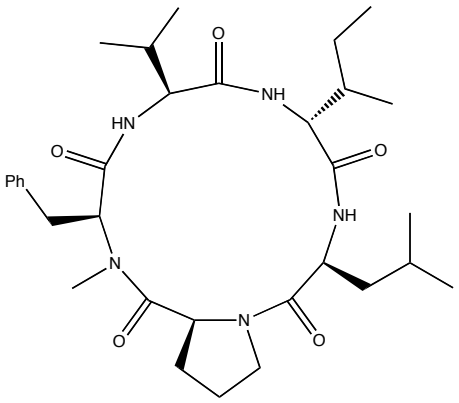 Cyclo(*N*-methyl-L-Phe-L-Val-D-Ile-L-Leu-L-Pro)	*X.* sp. No.7S-1–3-1 Antifungal	Wu et al., 2011

3.20	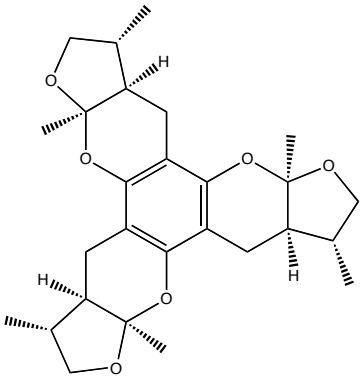 Xyloketal A	*X.* sp. No. 2508	Lin et al., 2001
3.21	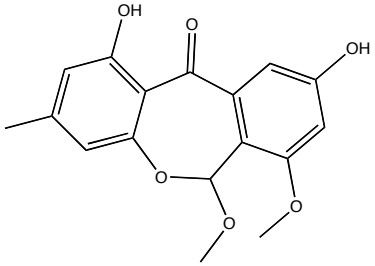 Arugosin J	*X.* sp	Hammerschmidt et al., 2015
3.22	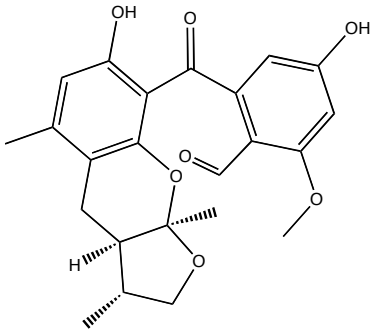 Xylarugosin	*X.* sp	Hammerschmidt et al., 2015
3.23	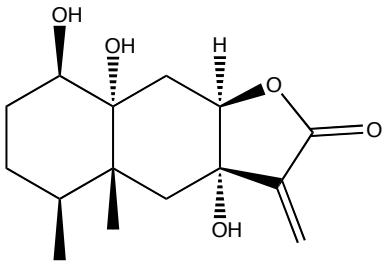 Eremophilanolide	*X.* sp. BCC 21097	Isaka et al., 2010
3.24	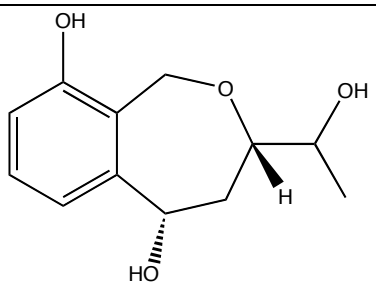 Xylarinol B	*X. polymorpha*	Lee et al., 2009

3.25	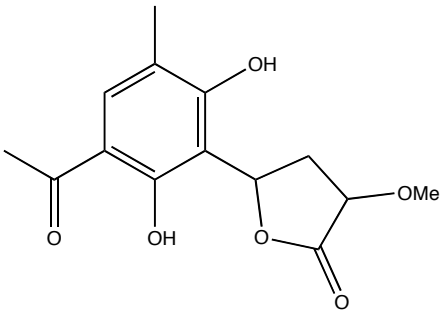 Globoscin	*X. globosa*		Adeboya et al., 1995
3.26	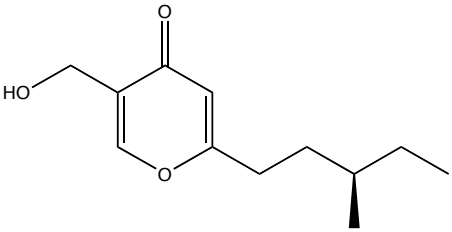 Xylaropyrone	*X. feejeensis* MU 18		Siriwach at al., 2011
3.27	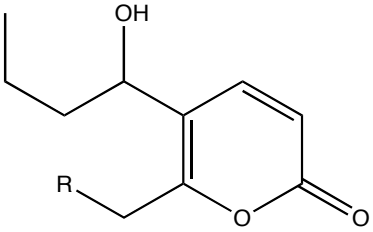 R = H, Xylariolide D R = OH, Taiwapyrone	*X.* sp. NCY2	Antibacterial MIC > 10 μg/mL	Hu et al., 2010
3.28	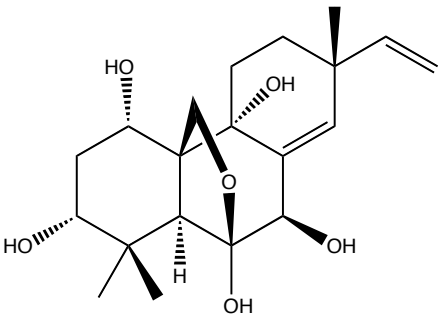 Xylallantin A	*X. allantoidea* BCC 23163	Cytotoxic	Isaka et al., 2014
3.29	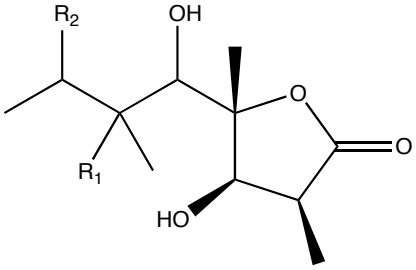 R_1 = H, R_2 = H, Xylariolide A R_1 = OH, R_2 = H, Xylariolide B R_1 = H, R_2 = OH, Xylariolide C	*X.* sp. NCY2	Antibacterial MIC > 10 μg/mL	Hu et al., 2010

3.30	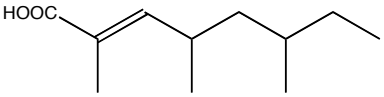 Xylarinic acid B	*X. polymorpha*	Antifungal	Jang et al., 2007
3.31	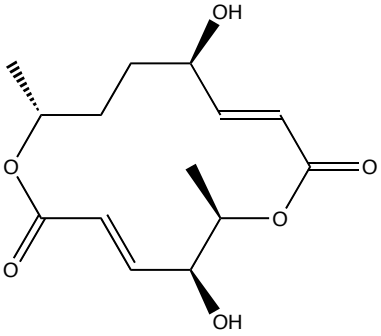 Clonostochydiol	*X. obovata*		Abate et al., 1997
3.32	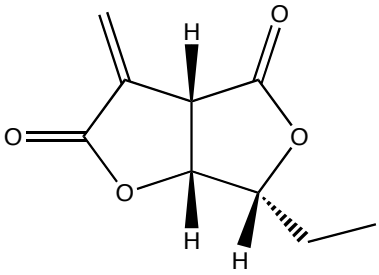 Xylobovide	*X. obovata*	Phytotoxic	Abate et al., 1997
3.33	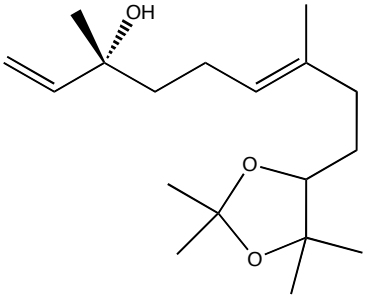 3,7-dimethyl-9-(-2,2,5,5-tetramethyl-1,3-dioxolan-4-yl)nona-1,6-dien-3-ol	*X.* sp.	Cytotoxic, antibacterial	Lin et al., 2016

3.2. A new eremophilane sesquiterpene from the fungus *Xylaria* sp. V-27 and inhibition activity against degranulation in RBL-2H3 cells

3.2.1. Introduction

Eremophilane sesquiterpenoids are group of secondary metabolites of both fungi and higher plants. Eremophilane-type sesquiterpene is common in *Xylaria* species and a lot of sesquiterpenes isolated so far from this genus have demonstrated interesting biological activities such as cytotoxicity (McDonald et al., 2004, Isaka et al., 2010), HIV-1 integrase inhibition (Singh et al., 1999), selective ligands for NPY Y5 receptor (Smith et al., 2002), α-glucosidase inhibition (Song et al., 2012), and antimalarial activities (Isaka et al., 2014).

In this thesis, a new eremophilane sesquiterpene, 13,13-dimethoxyintegric acid (**1-d**) has been isolated from a fungus *Xylaria* sp. V-27 obtained from a dead branch, together with known compound integric acid (**2-d**). The structure of **1-d** was established by means of spectroscopic analyses. **1-d** and **2-d** had growth restoring activity against the mutant yeast strain [*Saccharomyces cerevisiae* (*zds1*Δ *erg3*Δ *pdr1*Δ *pdr3*Δ)] and inhibited degranulation of rat basophilic leukemia RBL-2H3 cells stimulated by IgE+DNP-BSA, thapsigargin and A23187.

3.2.2. Fermentation, extraction and isolation

The fungal strain *Xylaria* sp. V-27 was isolated from a dead branch collected in Yamagata, Japan. This strain was then cultured on the steamed unpolished rice medium for four weeks. After cultivation the organic extract was subjected to silica gel and octadecyl silica gel (ODS) column chromatography to afford a new compound, 13,13-dimethoxyintegric acid (**1-d**) and known compound, integric acid (**2-d**) as the most abundant constituent of the mycelial extract.

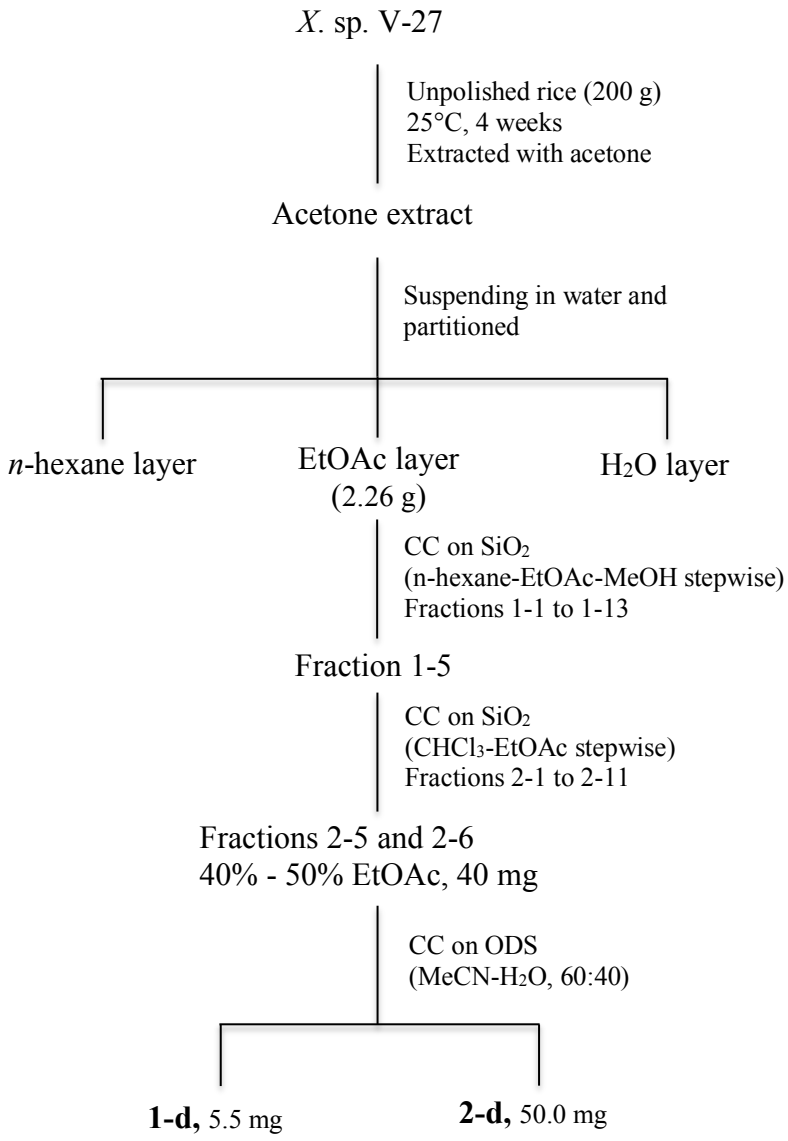

Scheme III.1. Isolation procedure of *X.* sp. V-27

3.2.3. Structure determination

Compounds **1-d** and **2-d** were isolated as white amorphous solid.

3.2.3.1. Compound 1-d

The molecular formula was determined to be $C_{27}H_{40}O_7$ by HRESIMS. The UV spectrum showed absorption maximum at 223 nm in MeOH. The IR spectrum exhibited absorption bands at 3356 and 1708 cm^{-1} which suggested the presence of hydroxy and carbonyl groups. Inspection of ^{1}H and ^{13}C NMR, DEPT and HMQC data revealed that **1-d** contained ester and carbonyl carbons (δ_C 167.0 and 198.8), a

carboxyl group (δ_C 178.0), three olefinic quaternary carbons (δ_C 143.2, 125.9 and 158.5), two olefinic methines (δ_C 129.9 and 149.7), a vinylidene (δ_C 116.5), an oxymethine (δ_H 5.50, and δ_C 72.8), an acetal methine (δ_H 4.82, and δ_C 104.7), an aliphatic quaternary carbon, three methines, six methylenes, two methoxy and four methyl groups (**Table III.2**).

Table III.2. ^{1}H and ^{13}C NMR Data of compound **1-d** ($CHCl_3$-d_1)

N°	δ_C	δ_H
1	72.8 t	5.50 (1H, m)
2	29.9 t	1.72 (1H, tt, 6.8, 3.4)
		2.16 (1H, m)
3	20.2 t	1.85 (1H, m)
		2.30 (1H, m)
4	53.6 d	2.45 (1H, dd, 13.1, 3.3)
5	38.5 s	
6	44.5 t	2.20-2.25 (m)
7	45.0 d	3.41 (1H, dd, 13.2, 6.2)
8	198.8 s	
9	129.9 d	6.04 (1H, s)
10	158.5 s	
11	143.2 s	
12	116.5 t	5.12 (1H, s)
		5.45 (1H, s)
13	104.7 d	4.82 (1H, s)
14	19.4 q	1.49 (3H, s)
15	178.0 s	
16	53.1 q	3.29 (3H, s)
17	54.1 q	3.35 (3H, s)
1’	167.0 s	
2’	125.9 s	
3’	149.7 d	6.56 (1H, dd, 10.0, 1.3)
4’	33.4 d	2.50 (1H, m)
5’	36.6 t	1.35 (1H, m)
		1.40 (1H, m)
6’	22.8 t	128.-1.33 (m)
7’	29.7 t	1.19-1.22 (m)
8’	14.1 q	0.88 (3H, t, 7.3)
9’	12.7 q	1.84 (3H, d, 1.3)
10’	20.0 q	1.01 (3H, d, 7.3)

^{1}H-^{1}H COSY and HMBC spectral data demonstrated that **1-d** is composed of a two cyclic sesquiterpene core attached with a long chain acid through an ester linkage.

The decalin moiety of the sesquiterpene was deduced to be an eremophilane based on COSY and HMBC correlations from the methyl proton (Me-14) to quaternary carbons at δ_C 38.5 (C-5) and δ_C 158.5 (C-10), methine carbons at δ_C 53.6 (C-4) and δ_C 44.5 (C-6), and from a methine proton at δ_H 6.04 (H-9) to methines at δ_C 72.8 (C-1) and δ_C 45.0 (C-7), and a quaternary carbon at δ_C 38.5 (C-5) (**Fig. III.2**).

The COSY and HMBC correlations from Me-9' to C-1' (δ_C 167.0), and C-3' (δ_C 149.7), and from Me-10' to C-3', suggested that there is a 2,4-dimethylocta-2-enoyl moiety in this molecule. Furthermore, the HMBC correlation between H-1 to C-1' and substantial downfield shift for H-1 revealed the location of the octanoyl was at C-1 (δ_C 72.8). The configuration of the trisubstituted double bond (C-2' and 3') was assigned as *E* on the basis of the NOE correlation between H-4' and Me-9'. In addition, the HMBC correlation from methine proton at δ_H 2.45 (H-4) to a carboxyl carbon at δ_C 178.0 (C-15) established the connectivity of the carboxyl group at C-4. The relative configurations of C-1, C-4, C-5, and C-7 in **1-d** were deduced from NOE experiments. NOE correlations from Me-14 to H-3', and from Me-14 to H-7 indicated that Me-14, H-7 and ester side chain moiety at C-1 were all β-oriented. Furthermore, NOE correlations were observed from H-4 to H-2a, suggesting that the carboxylic acid moiety was β-oriented. The relative configuration at C-4' remains uncertain.

Conclusion

Thus, the structure of **1-d** was identified as 13,13-dimethoxyintegric acid (A. Tchoukoua et al., 2017c)

3.2.3.2. Compound 2-d

2-d was determined to be integric acid through the analysis of the spectral data (MS, UV, $[\alpha]_D$, IR, ^1H and ^{13}C NMR), which were indistinguishable from those of integric acid (Singh et al., 1999).

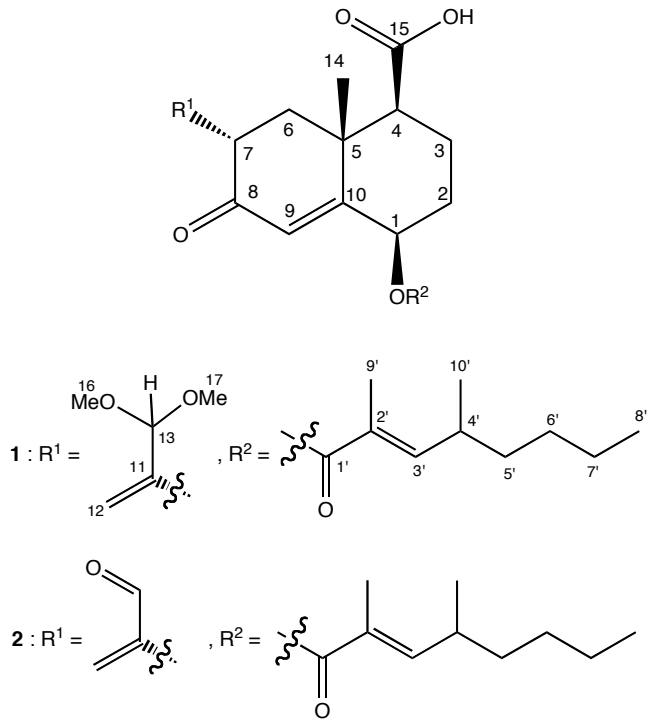

Fig. III.1. Structures of compounds **1-d** and **2-d**

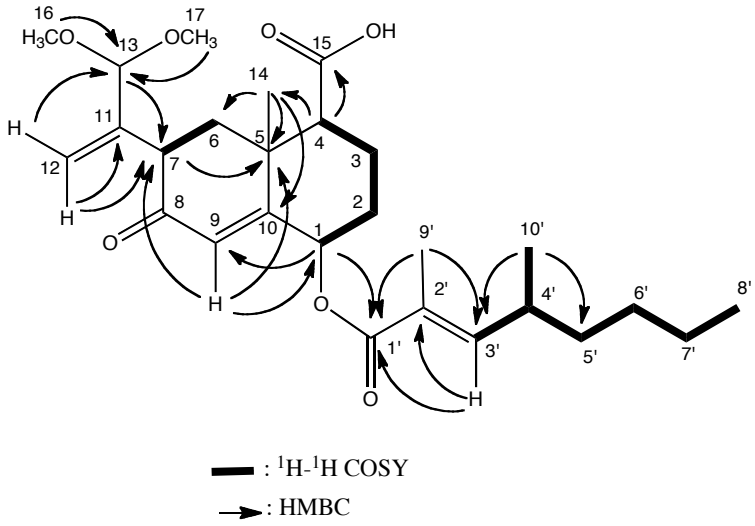

Fig. III.2. ^1H-^1H COSY and Key HMBC correlations for **1-d**.

3.3. Biological study

3.3.1. Growth restoring activity against YNS17 strain

13,13-dimethoxyintegric acid (**1-d**) and integric acid (**2-d)** gave rise to a faint growth zone around the inhibition zone dose dependently against YNS17 strain (**1-d**; 21.3 mm, **2-d**; 14.9 mm at 20 μg/disc) (**Fig. III.3**) and the phenotype of **1-d** and **2-d** were similar to those observed with Eremoxylarins A and B (Ogasawara et al., 2008). Compounds **1-d** and **2-d** at 10 μg/disc [No. 3 in Fig. III.3 (a) and (b)] showed the growth restoring zone.

(a) (b)

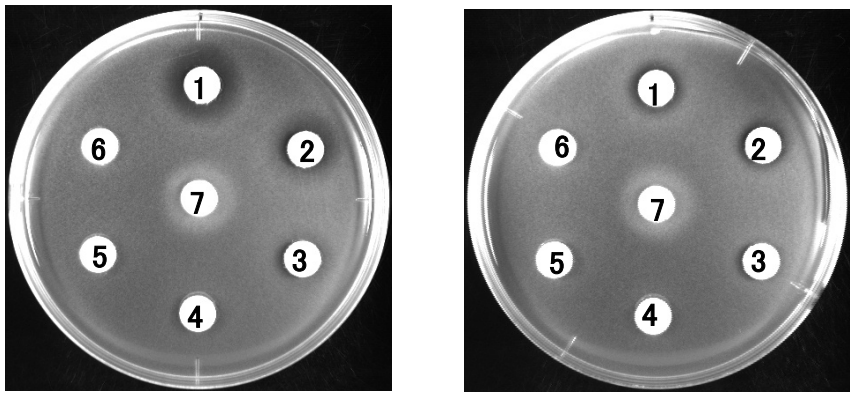

Fig. III.3.

Restored growth activity of **1-d** (a) and **2-d** (b) against the mutant strain of *Saccharomyces cerevisiae* (*zds1*Δ *erg3*Δ *pdr1*Δ *pdr3*Δ) with 0.3 M $CaCl_2$.

1: 40 μg/ disc, 2: 20 μg/ disc, 3: 10 μg/ disc, 4: 5 μg/ disc, 5: 2.5 μg/ disc, 6: 1.25 μg/ disc, 7: 0.02 μg/ disc (FK506)

3.3.2. Inhibition activity against degranulation in RBL-2H3 cells

Mast cells have been widely regarded as the key players of allergic reactions and the rat basophilic leukemia RBL-2H3 cell line is a commonly used β-hexosaminidase-releasing cell line as a mast cell line, although it is derived from basophils. Elevation of cytosolic Ca^{2+} levels is a common signal for RBL-2H3 degranulation. Although **1-d** has stronger activity of about four times than that of **2-d** against the mutant yeast, the cytotoxicity of **2-d** against RBL-2H3 cells (IC_{50} = 15.8 μM) was about ten times

stronger than that of **1-d** (IC_{50} = 138.4 μM) (**Fig. III.4**). Recently, it was reported that the growth restoring activity against YNS17 strain was parallel with the inhibition activity of degranulation against RBL-2H3 cells (Abe et al., 2016).

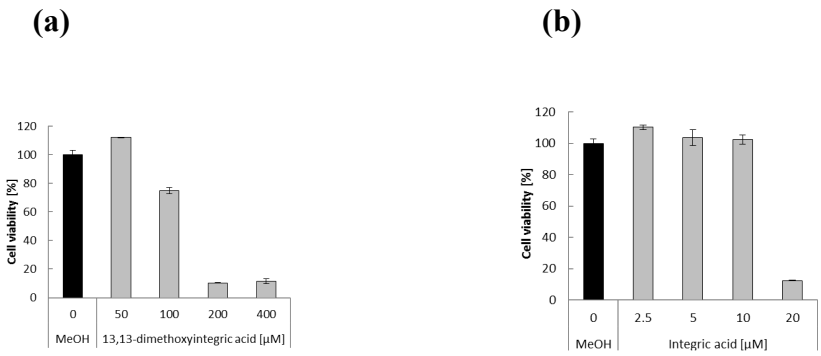

Fig. III.4.

Cell viability of RBL-2H3 cells by **1-d** (a) and **2-d** (b).

Cell viability after 48 h was determined using the MTT assay.

1-d inhibited degranulation of RBL-2H3 cells stimulated by IgE+DNP-BSA (IC_{50} = 42.2 μM), thapsigargin (IC_{50} = 21.2 μM) and A23187 (IC_{50} = 37.5 μM), respectively (**Fig. III.5 (a)**). **2-d** inhibited degranulation of RBL-2H3 cells stimulated by IgE+DNP-BSA (IC_{50} = 0.92 μM), thapsigargin (IC_{50} = 0.88 μM) and A23187 (IC_{50} = 1.02 μM), respectively (**Fig. III.5 (b)**). These cytotoxic and the inhibitory activities of degranulation against RBL-2H3 cells showed that the propenal unit on the structure plays an important role in the activities. Previous evidence has revealed that the propenal moiety is involved in HIV-1 integrase inhibitory activity (Singh et al., 1999). Calcineurin inhibition activity is also paralleled with these activities (**1-d**: IC_{50} = 40.5 μM, **2-d**: IC_{50} = 1.2 μM) (Ogasawara et al., 2008). Otherwise, the dimethoxy moieties in **1-d** may be favorable for the cell permeability of the compound into the mutant yeast than the aldehyde moiety in **2-d**.

(a)

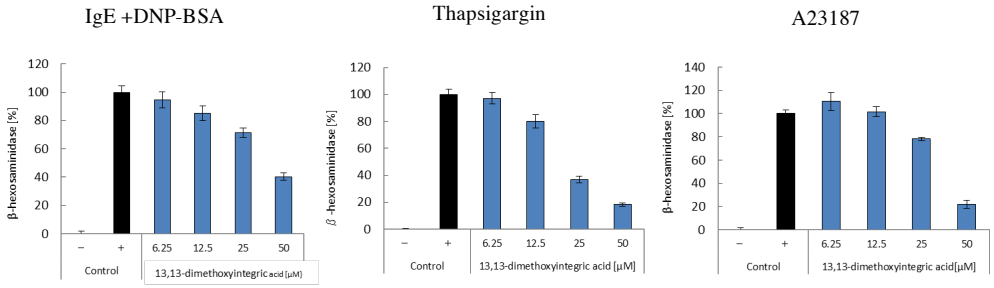

(b)

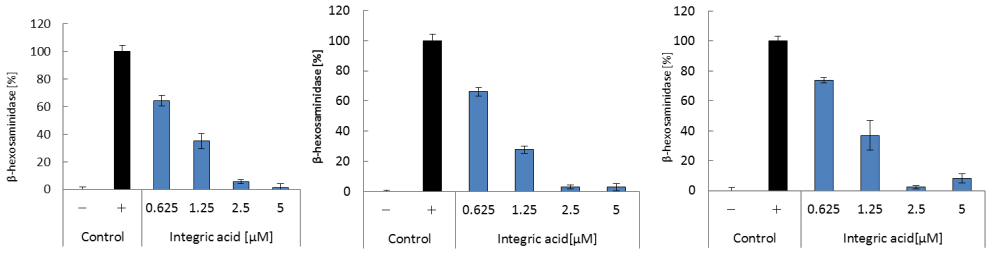

Fig. III.5.

Inhibition of degranulation against RBL-2H3 cells by **1-d** (a) and **2-d** (b).

RBL-2H3 cells were sensitized with IgE for 2 h, then added each sample for 30 min and stimulated with DNP-BSA as an antigen for 10 min. RBL-2H3 cells were also stimulated with thapsigargin for 20 min or A23187 for 30 min without the sensitization by IgE. The inhibition (%) of β-hexosaminidase release by the sample was measured as an absorbance at 405 nm.

3.4. A phytotoxic bicyclic lactone and other compounds from endophyte *Xylaria curta*

3.4.1. Introduction

Endophytic fungi recently have been recognized as an important screening resource, producing a wide range of novel and bioactive secondary metabolites (Kusari, Hertweck et al., 2012). Fungi in the genus *Xylaria* have been extensively investigated and many types of bioactive compounds have been isolated, such as antimalarial (Sawadsitang et al., 2015), cytotoxic (Shiono et al., 2009, Lin et al., 2016), antimicrobial (Tarman et al., 2012, Huang et al., 2014), anti-HIV (Singh et al., 1999), antioxidant (Liu et al., 2007), and phytotoxic (Shiono et al., 2005, Zhang et al., 2014, García-Méndez, et al., 2016) metabolites.

In this thesis, a new compound (3aS,6aR)-4,5-dimethyl-3,3a,6,6a-tetrahydro-2H-cyclopenta[*b*]furan-2-one (**2-e**), along with two known metabolites, myrotheciumone A (**1-e**) and 4-oxo-4*H*-pyron-3-acetic acid (**3-e**) was isolated from the ethyl acetate extract of fermentation broth of *Xylaria curta* 92092022. Compounds **1-e** and **2-e** showed moderate antibacterial and phytotoxic activities.

3.4.2. Fermentation, extraction and isolation

The fungal strain *X. curta* 92092022 was cultivated on sterilized unpolished rice (800 g) at 25 °C for 4 weeks. After cultivation, the organic extract was subjected to silica gel and octadecyl silica gel (ODS) column chromatography to afford a new compound **1-e** and known compounds **2-e** and **3-e**.

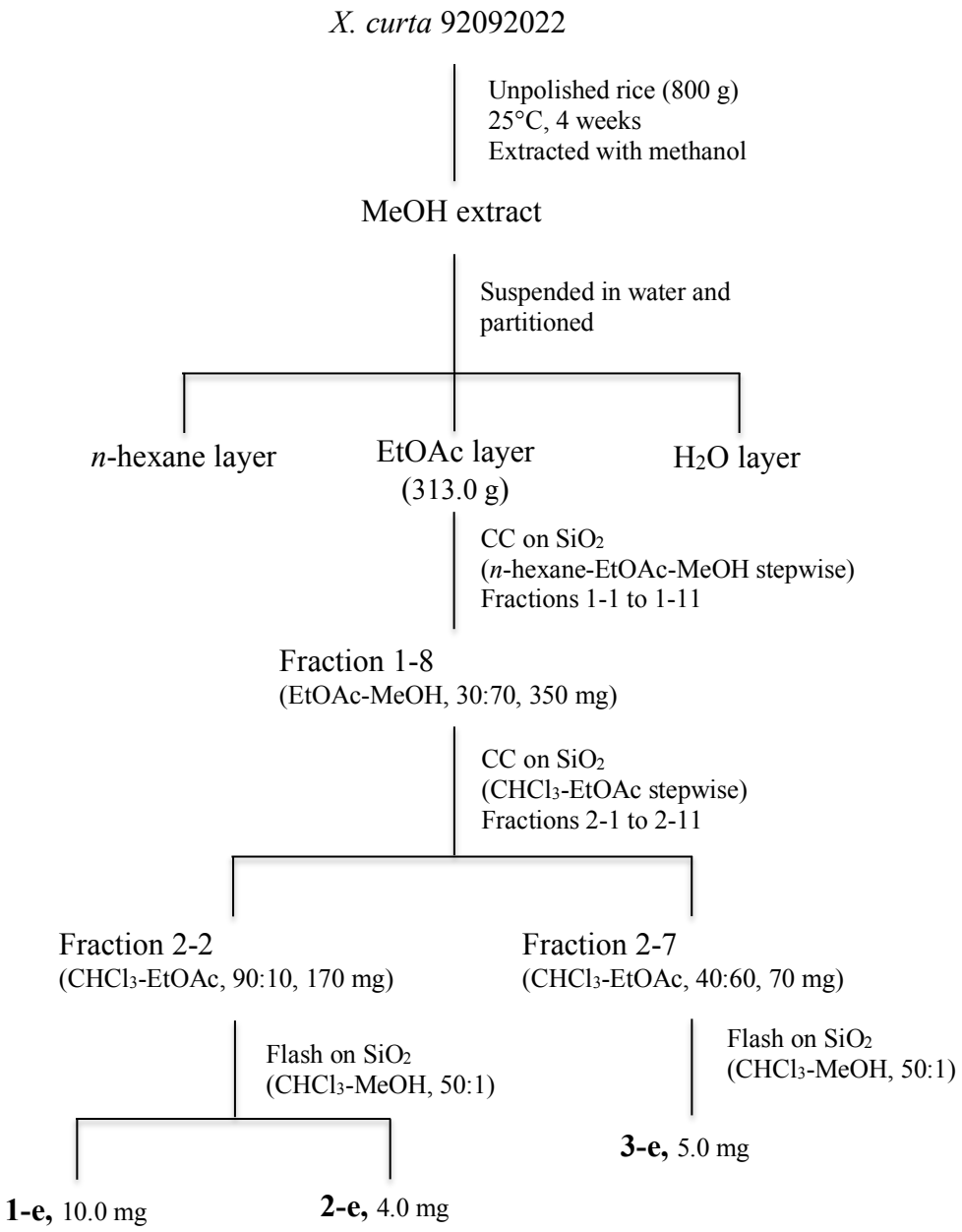

Scheme III.2. Isolation procedure of *X. curta*

3.4.3. Structure determination

Compounds **1-e, 2-e**, and **3-e** were isolated as white amorphous powder.

3.4.3.1. Compounds 1-e and 3-e

The structures of known compounds, myrotheciumone A (**1-e**) (Lin et al. 2014) and 4-oxo-4*H*-pyron-3-acetic acid (**3-e**) (Edwards et al. 2001; Zhang et al. 2008) were assigned by comparing their physicochemical properties and spectral data with those reported in the literature.

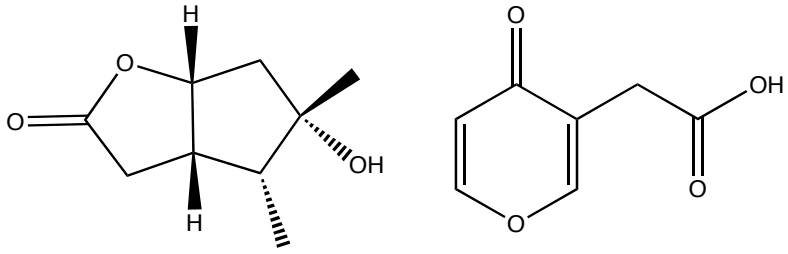

1-e **3-e**

Fig. III.6. Structures of compounds **1-e** and **3-e**

3.4.3.2. Compound 2-e

2-e was isolated as an amorphous powder. The molecular formula of **2-e** was determined by HRESITOFMS to be $C_9H_{12}O_2$. The IR spectrum of **2-e** showed the presence of a carbonyl (1758 cm^{-1}) group.

Table III.3. ^{1}H and ^{13}C NMR Data of **2-e** ($CHCl_3$-d_1)

No.	δ_H (*J* in Hz)	δ_C (*J* in Hz)
2	-	177.4
3	2.47 (1H, dd, *J* = 18.0, 2.0)	32.0
	2.67 (1H, dd, *J* = 18.0, 3.3)	
3a	3.33 (1H, m)	49.7
4	-	130.8
5	-	129.4
6	2.55 (1H, br. d, *J* = 17.3)	44.4
	2.66 (1H, br. d, *J* = 17.3)	
6a	5.03 (1H, t, *J* = 6.2)	82.3
7	1.58 (3H, s)	11.6
8	1.63 (3H, s)	13.8

The ^{13}C NMR spectrum ($CDCl_3$) showed nine resolved peaks, which were classified into two methyls, two sp^3 methylenes, two sp^3 methines, two sp^2 quaternary carbons and one carbonyl. Since the one carbonyl group and the one olefinic carbon account for two degrees of unsaturation, **2-e** must possess two rings. Furthermore, the robust absorption observed at 1758 cm^{-1} in the IR spectrum, together with the upfield shifted carbonyl signal at δ_C 177.4 and the downfield shifted proton signal at δ_H 5.03, indicated the presence of γ-lactone.

Detailed analyses of the ^{1}H–^{1}H COSY spectrum disclosed the presence of a partial structure shown as a bold line in **Fig. III.8**.

In HMBC spectrum the signals of H-6a and H-3a were correlated with the signal of C-2, and the signals of H-6 were correlated with the signals of C-4 and C-5, and the H-3a signal was correlated with the signals of C-4 and C-5. These data allowed us to construct the planar structure of **2-e**. Furthermore, the olefinic methyls were inferred to be connected to C-4 and C-5 based on the HMBC correlations of the Me-7 signal with the C-3a, C-4 and C-5 signals, and from the correlation of the Me-8 signal with the C-4, C-5 and C-6 signals (**Fig. III.8**).

Conclusion

Thus, the structure of **2-e** was identified as (3aS,6aR)-4,5-dimethyl-3,3a,6,6a-tetrahydro-2H-cyclopenta[*b*]furan-2-one (A. Tchoukoua et al., 2017d).

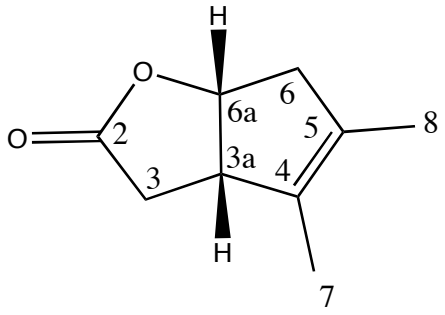

Fig. III.7. Structure of compound **2-e**

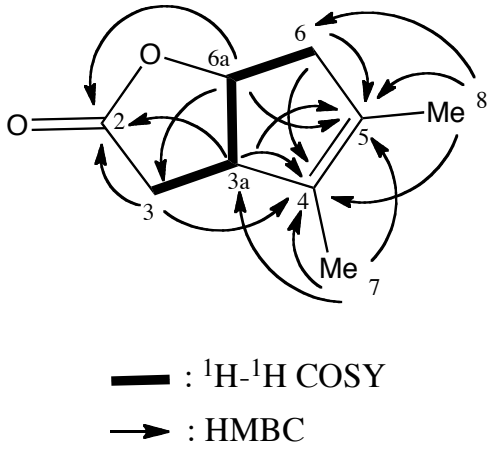

Fig. III.8. ^{1}H-^{1}H COSY and Key HMBC correlations for **2-e**.

3.5. Biological study

3.5.1. Antimicrobial activity

Compounds **1-e, 2-e, and 3-e** were evaluated by the agar diffusion method against Gram- positive and Gram-negative bacteria, yeast and fungus strains.

Table III.4. Antimicrobial activity of **1-e** – **3-e**

Diameter of the inhibition areas (mm) of samples				
Microorganisms	**1-e**	**2-e**	**3-e**	RA[a]
P. aeruginosa ATCC 15442	13	13	ND	18
S. aureus NBRC 13276	12	13	ND	32
A. clavatus F318a	ND	ND	ND	
C. albicans ATCC 2019	ND	ND	ND	

[a]RA : reference antibiotics were chloramphenicol (10 µg/disk) for *P. aeruginosa* and penicillin G (1.3 mg/disk) for *S. aureus*
ND: not detectable

3.5.2. Phytotoxic assay

Furthermore, we studied the potential phytotoxicity of **1-e**, **2-e,** and **3-e** against lettuce seedlings (*Lactuca sativa* L.). Aqueous solutions of **1-e** – **3-e**, ranging between 25 and 200 µg mL^{-1}, were assayed for their effects on seed germination, root length, and shoot length of the lettuce. Compound **1-e** inhibited root growth by 50% compared to the untreated controls at a concentration of 100 µg mL^{-1} [average length of roots: control (without compound) 3.0 ± 0.5 cm, in the presence of **1-e** (100 µg mL^{-1}) 1.5 ± 0.2 cm ($p < 0.05$)]. Compound **2-e** showed the most robust inhibitory effect on root growth. Compound **2-e** inhibited root growth by 50% at a concentration of 25 µg mL^{-1} [average length of roots: control (without compound) 3.2 ± 0.5 cm, in the presence of **2-e** (25 µg mL^{-1}) 1.6 ± 0.3 cm ($p < 0.05$)]. In addition, the highest concentration of **2-e** (200 µg mL^{-1}) strongly exerted an inhibitory effect on seed germination (90% inhibition). Furthermore, **3-e** showed no phytotoxicity in this study. Compound **1-e** displayed phytotoxic activity, which may depend on the hydrophilic character of the compound.

3.6. General conclusion

The diverse and widespread fungal genus *Xylaria* has been known to be a rich source of bioactive secondary metabolites.

The aim of this chapter was also the isolation of secondary metabolites produced by the endophytic fungi *Xylaria* sp. V-27 and *Xylaria curta* and to examine their pharmacological potential.

On the basis of chromatographic and spectroscopic analyses five compounds were isolated from both fungi, two of which were identified as new natural products (**1-d**, **2-e**).

Two eremophilane sesquiterpenes (**1-d**, **2-d**), two bicyclic lactones (**1-e**, **2-e**), and one γ-pyrone (**3-e**) were characterized.

Characteristic physical data of compounds isolated from *Xylaria* sp. V-27 and *Xylaria curta* were shown in the experimental section 3.7.3.1 and 3.7.3.2.

The eremophilane sesquiterpenes from *Xylaria* sp. indicated growth restoring activity against the mutant strain of *Saccharomyces cerevisiae* (*zds1*Δ *erg3*Δ *pdr1*Δ *pdr3*Δ) and inhibited degranulation of RBL-2H3 cells.

The novel lactone (**2-e**) isolated from *X. curta* was found to be another rare 5/5 rings-fusion system in a naturally occurring compound. It showed moderate antibacterial activity. Even though there have been only a few reports showing the effects of *Xylaria* sp. derived compounds on plant growth, the novel lactone showed phytotoxic activity against seed germination and lettuce radicle development. This observation suggests that the compound may protect the host plant from competition with neighbouring plants since some endophytes are able to enhance the allelophatic effects on the hosts in order to prevent the invasion of exotic plant species.

3.7. Experimental – III

3.7.1. General

See Experimental – I

3.7.2. Fungal material

Xylaria sp. V-27. The fungal strain *Xylaria* sp. V-27 was isolated from a dead branch collected in Yamagata, Japan.

Xylaria curta. The fungal strain *Xylaria curta* 92092022 was originally isolated from bark collected in Tawain (Hsieh et al., 2010). *X. curta* 92092022 was identified by its distinctive morphological characteristics.

3.7.3. Fermentation, Extraction and Isolation

Xylaria sp. V-27

The fungus was cultivated on sterile steamed unpolished rice for four weeks. After cultivation the organic extract was subjected to silica gel and octadecyl silica gel (ODS) column chromatography to afford a new compound, 13,13-dimethoxyintegric acid (**1-d**) and known compound, integric acid (**2-d**) as the most abundant constituent of the mycelial extract.

3.7.3.1. Characteristic physical data of *Xylaria* sp. V-27

Compound	Spectroscopic data
13,13-dimethoxyintegric acid (**1-d**)	Molecular formula: $C_{27}H_{40}O_7$ HRESIMS (positive-ion mode) m/z 499.2665 ($[M+Na]^+$ calcd for $C_{27}H_{40}O_7Na$ 499.2627) ^1H and ^{13}C NMR data, see Table III.2

Xylaria curta

The fungal strain was cultivated on sterilized unpolished rice for four weeks. After cultivation the organic extract was subjected to silica gel flash column chromatography to afford a new compound (**2-e**) and known compounds, myrotheciumone A (**1-e**) and grammicin (**3-e**).

3.7.3.2. Characteristic physical data of *Xylaria curta*

Compound	Spectroscopic data
(3aS,6aR)-4,5-dimethyl-3,3a,6,6a-tetrahydro-2H-cyclopenta[*b*]furan-2-one (**2-e**)	Molecular formula: $C_9H_{13}O_{12}$ HRESITOFMS (positive-ion mode) m/z 153.0928 ($[M+H]^+$ calcd for $C_9H_{13}O_2$ 153.0916) ^1H and ^{13}C NMR data, see Table III.3

3.7.4. Growth restoring activity against the mutant strain

Screening was performed according to previous described method (Ogasawara et al., 2008). Each sample was dissolved in MeOH and two-fold dilutions of them were used. Difco® yeast-peptone-dextrose (YPD) broth and YPD agar were purchased from Becton Dickinson Biosciences (Franklin Lakes, NJ, USA). The mutant yeast, YNS17 (*MAT*a *zds1::TRP1 erg3::HIS3 pdr1::hisG-URA3-hisG pdr3::hisG*) strains were derivatived of strain W303-1A. 8-mm paper discs containing each compound was placed on YPD agar medium containing YNS17 strain and 0.3 M $CaCl_2$. After 3 days of incubation at 28°C, the inhibitory activity of the Ca^{2+}-signaling transduction was determined by the diameter of the growth zone of the paper disc. FK506 (0.02 μg/disc) was used as a positive control. FK506 was kindly provided by Fujisawa Pharmaceutical Co., Ltd. (the present Astellas Pharma Inc., Tokyo Japan) (Ogasawara et al., 2008).

3.7.5. Cell culture and cytotoxicity

Rat basophilic leukemia RBL-2H3 cells (ATCC, Manasass, VA, USA) were maintained in DMEM supplemented with 10% heat-inactivated FBS (Biowest SAS, Nuaillé, France) and antibiotics [penicillin (50 units/ml)-streptomycin (50 μg/ml), Gibco, Thermo Fisher Scientific Inc., Waltham, MA, USA]. Cell viability was determined using MTT assay (Dojindo Lab., Kumamoto, Japan).

3.7.6. Measurement of the degranulation (β-hexosaminidase (β-HEX) assay)

RBL-2H3 cells were grown overnight in 96-well plates (3 x 10^5 cells/well) and sensitized with 0.5 μg/ml IgE (Yamasa Co., Tokyo, Japan) for 2 h. After washing

with 200 µl Tyrode buffer (137 mM NaCl, 2.7 mM KCl, 1.0 mM $MgCl_2$, 1.8 mM $CaCl_2$, 5.6 mM D-glucose, 20 mM HEPES, 1 mg/ml BSA, pH7.3), cells were incubated in 98 µl of Tyrode buffer and 2 µl of each sample for 30 min, then stimulated with 10 µl of 1 µg/ml DNP-BSA (Merck Millipore Co., Billerica, MA, US) as an antigen for 10 min. RBL-2H3 cells were also stimulated with 10 µl of 0.2 µM tapsigargin (Sigma-Aldrich Co., St. Louis, MO, USA) for 20 min or 10 µl of 20 µM A23187 (Sigma-Aldrich Co.) for 30 min without the sensitization by IgE. The supernatant (30 µl) was then transferred to a 96-well plate and incubated with 70 µl substrate (1.3 mg/ml 4-nitrophenyl-*N*-acetyl-β-D-glucosaminide, Sigma-Aldrich Co.) in 0.1 M citrate buffer (pH 4.5) at 37°C for 90 min. The reaction was stopped by adding 100 µl of stop solution (0.4 M glycine-NaOH). The absorbance was measured at 405 nm by a microplate reader. The inhibition (%) of β-hexosaminidase release by the sample was calculated using the following equation, and IC_{50} values were determined graphically. Inhibition (%) = [1-(T-N)/(C-N)] x 100%: Control (C) was Ig E+DNP-BSA (or thapsigargin or A23187) (+), test sample (-) and normal (N) was IgE+DNP-BSA (-) (or thapsigargin or A23187) (-), test sample (+) and test (T) was Ig E+DNP-BSA (or thapsigargin or A23187) (+), test sample (+). Quercetin was used as a reference compound (IC_{50} = 5.7 µM) (Abe et al., 2016).

3.7.7. Calcineurin assay

The calcineurin activity was measured using a commercial kit (AK-804, Biomol GmbH, Hamburg, Germany), in which free phosphate ion released from a substrate phosphopeptide (DLDVPIPGRFDRRVpSVAAE) was quantified by colorimetric analysis (650 nm) using the malachite green method. The calmodulin antagonist trifluoperazine was used as a positive control.

3.7.8. Antimicrobial activity

Test microorganisms were *Staphylococcus aureus* NBRC 13276, *Pseudomonas aeruginosa* ATCC 15442, *Aspergillus clavatus* F 318a, and *Candida albicans* ATCC 2019. Antimicrobial assays were carried out by the paper disk diffusion method using a published protocol (Shiono et al., 2005).

3.7.9. Phytotoxic assay

Each sample was dissolved in 0.5 mL of MeOH and then poured on filter paper in a Petri dish (φ 40 × 10 mm). After sample-loaded paper had been air dried, 1 mL of distilled water was poured on the sample-loaded paper or intact filter paper (negative control). And then, lettuce seeds (n = 10 in each Petri dish) were put on the filter paper and were incubated in a growth chamber in the dark at 25 °C for 5 days. The length of the hypocotyl and the root were measured.

Appendix – III

Selected spectra of chapter 3

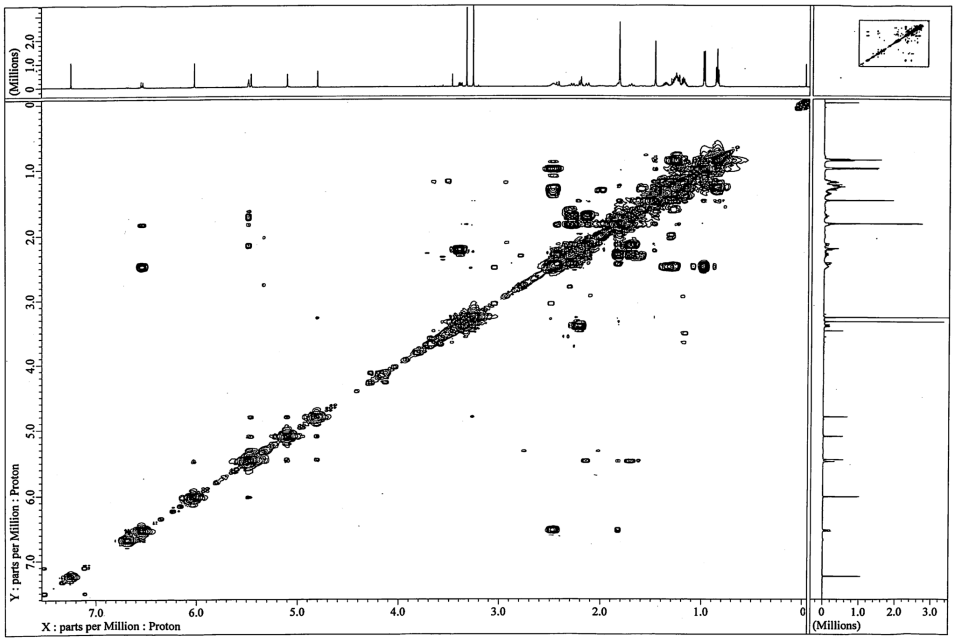

Fig. III.9. COSY spectrum of compound **1-d** (600 MHz, $CHCl_3$-d_1)

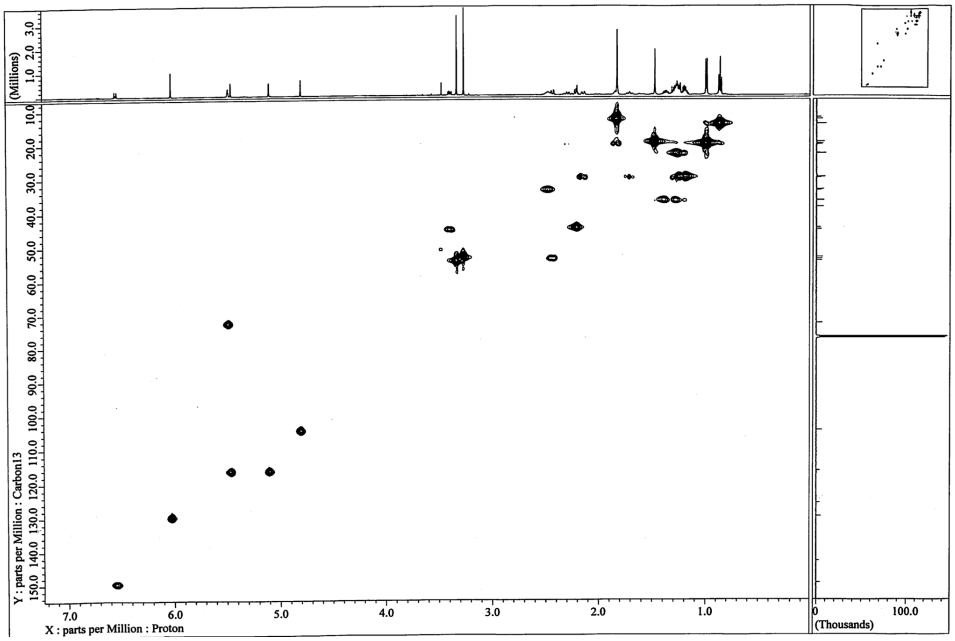

Fig. III.10. HMQC spectrum of compound **1-d** (600 MHz, $CHCl_3$-d_1)

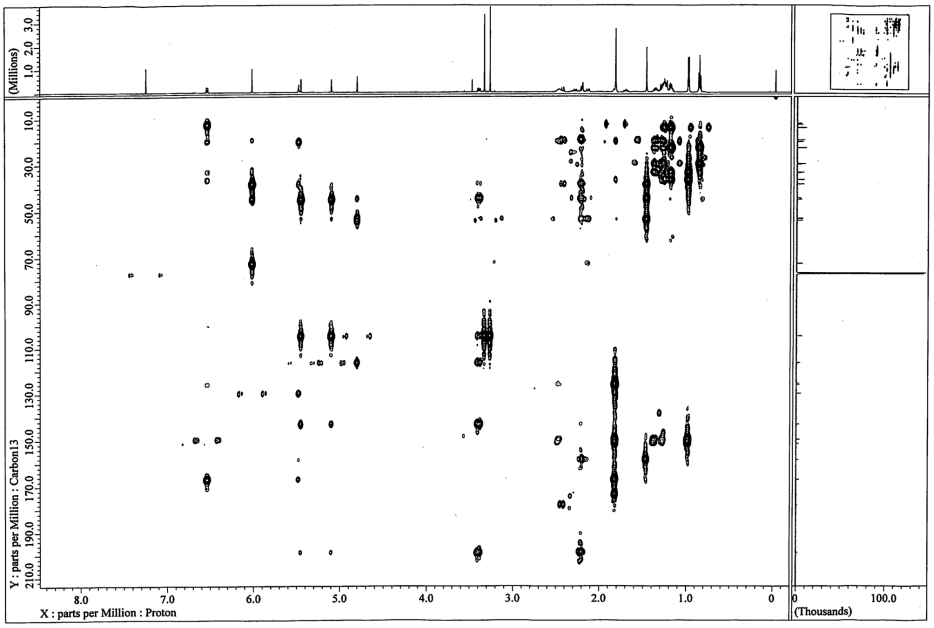

Fig. III.11. HMBC spectrum of compound **1-d** (600 MHz, $CHCl_3$-d_1)

3.8. References – III

Abe, T., Kobayashi, M., Okawa, Y., Inui, T., Yoshida, J., Higashio, H., Shinden, H., Uesugi, S., Koshino, H., Kimura, K., 2016. Yeast Ca^{2+}-signal transduction inhibitors isolated from Dominican amber prevent the degranulation of RBL-2H3 cells through the inhibition of Ca^{2+} -influx, *Fitoterapia,* **113**, 188–194.

Abate, D., Abraham, W. R., Meyer, H., 1997. Cytochalasins and phytotoxins from the fungus *Xylaraia obovata*. *Phytochemistry,* **44**, 1443–1448.

Adeboya, M., Edwards, R. L., Laessøe, T., Maitland, D. J., Whalley, A. S. J., 1995. Metabolites of the higher fungi. Part 28. Globoscinic acid and globoscin, a labile acid-lactone system from *Xylaria globosa* and *Xylaria obovata*. *J. Chem. Soc*., *Perkin Trans*., **1**, 2067–2672.

Bacon, C. W., and White, J. F., 2000. Microbial endophytes. Marcel Dekker, Inc., New York, N.Y.

Chen, Z., Huang, H., Chen, Y., Wang, Z., Ma, J., Wang, B., Zhang, W., Zhang, C., Ju, J., 2011. New cytochalasins from the marine-derived fungus *Xylaria* sp. SCSIO 156. *Helv. Chim. Acta,* **94**, 1671–1676.

Dagne, E., Gunatilaka, A. A. L., Asmellash, S., Abate, D., Kingston, D. G. I., Hofmann, G. A., Johnson, R. K., 1994. Two new cytotoxic cytochalasins from *Xylaria obovata*. *Tetrahedron,* **50**, 5615–5620.

Deyrup, S. T., Gloer, J. B., O'Donnell, K., Wicklow, D. T., 2007. Kolokosides A-D: triterpenoid glycosides from a Hawaiian isolate of *Xylaria* sp. *J. Nat. Prod*., **70**, 378–382.

Edwards, R. L., Maitland, D. J., Pittayakhajonwut, P., Whalley, A. J., 2001. Metabolites of the higher fungi. Part 33. Grammicin, a novel bicyclic $C_7H_6O_4$ furanopyranol from the fungus *Xylaria grammica* (Mont.) Fr., *J. Chem. Soc.*, **11**, 1296–1299.

García-Méndez, M. C., Macías-Ruvalcaba, N. A., Lappe-Oliveras, P., Hernández-Ortega, S., Macías-Rubalcava, M. L., 2016. Phytotoxic potential of secondary metabolites and semisynthetic compounds from endophytic fungus *Xylaria feejeensis* strain SM3e-1b isolated from *Sapium macrocarpum*. *J Agri Food Chem*., **64**, 4255–63.

Hammerschmidt, L., Ola, A., Müller, W. E. G., Lin, W., Mándi, A., Kurtán, T., Proksch, P., Aly, A. H., 2015. Two new metabolites from the endophytic fungus *Xylaria* sp. isolated from the medicinal plant *Curcuma xanthorrhiza. Tetrahedron Lett*., 56, 1193–1197.

Hsieh, H. M., Lin, C. R., Fang, M. J., Rogers, J. D., Fournier, J., Lechat, C., Ju, Y. M., 2010. Phylogenetic status of *Xylaria* subgenus *Pseudoxylaria* among taxa of the subfamily Xylarioideae (Xylariaceae) and phylogeny of the taxa involved in the subfamily. *Mol. Phylogenet. Evol*., **54**, 957–969.

Hu, Z.-Y., Li, Y.-Y., Lu, C.-H., Lin, T., Hu, P., Shen, Y.-M., 2010. Seven novel linear polyketides from *Xylaria* sp. NCY2. *Helv. Chim. Acta,* **93**, 925–933.

Hu, Z. Y., Li, Y. Y., Huang, Y. J., Su, W. J., Shen, Y. M., 2008. Three new sesquiterpenoids from *Xylaria* sp. NCY2. *Helv. Chim. Acta,* **91**, 46–52.

Huang, X., Sun, X., Lin, S., Xiao, Z., Li, H., Bo, D., She, Z., 2014. Xylanthraquinone, a new anthraquinone from the fungus *Xylaria* sp. 2508 from the South China Sea. *Nat. Prod. Res*., **28**, 111–114.

Isaka, M., Yangchum, A., Auncharoen, P., Srichomthong, K., Srikitikulchai, P., 2011. Ring B aromatic norpimarane glucoside from a *Xylaria* sp. *J. Nat. Prod*., **74**, 300–302.

Isaka, M., Chinthanom, P., Boonruangprapa, T., Rungjindamai, N., Pinruan, U., 2010. Eremophilane-type sesquiterpenes from the fungus *Xylaria* sp. BCC 21097. *J. Nat. Prod.*, **73**, 683–687.

Isaka, M., Yangchum, A., Supothina, S., Chanthaket, R., Srikitikulchai, P., 2014. Isopimaranes and eremophilanes from the wood-decay fungus *Xylaria allantoidea* BCC 23163. *Phytochem. Lett*., **8**, 59–64.

Jang, Y. W., Lee, I. K., Kim, Y. S., Lee, S. K., Lee, H. J., Yu, S. H., Yun, B. S., 2007. Xylarinic acids A and B, new antifungal polypropionates from the fruiting body of *Xylaria polymorpha*. *J. Antibiot*., **60**, 696.

Kirk, P. M., Cannon, P. F., Minter, D. W., Stalpers, J. A., 2008. 'Ainsworth & Bisby's Dictionary of the Fungi', 10th edn., CABI Publishing, Wallingford.

Kusari, S., Hertweck, C., Spiteller, M., 2012. Chemical ecology of endophytic fungi: origins of secondary metabolites. *Chem. Biol*., **19**, 792–798.

Lee, I. K., Jang, Y. W., Kim, Y. S., Yu, S. H., Lee, K. J., Park, S. M., OH, B. T., Chae, J. C., Yun, B. S., 2009. Xylarinols A and B, two new 2-benzoxepin derivatives from the fruiting bodies of *Xylaria polymorpha*. *J. Antibiot*., 62, 163–165.

Li, Y. Y., Hu, Z. Y., Lu, C. H., Shen, Y. M., 2010. Four new terpenoids from *Xylaria* sp. 101. *Helv. Chim. Acta,* **93**, 796–802.

Lin, Y., Wu, X., Feng, S., Jiang, G., Zhou, S., Vrijmoed, L. L. P., Jones, E. B. G., 2001. A novel *N*-cinnamoylcyclopeptide containing an allenic ether from the fungus Xylaria sp. (strain #2508) from the South China Sea. *Tetrahedron Lett*., **42**, 449–451.

Lin, T., Wang, G., Shan, W., Zeng, D., Ding, R., Jiang, X., Zhu, D., Liu, X., Yang, S., Chen, H., 2014. Myrotheciumones: bicyclic cytotoxic lactones isolated from an endophytic fungus of *Ajuga decumbens*. *Bioorg Med Chem Lett*. **24**, 2504–2507.

Lin, X., Yu, M., Lin, T., 2016. Secondary metabolites of *Xylaria* sp., an endophytic fungus from *Taxus mairei*. *Nat. Prod. Res*., **30**, 2442–2447.

Liu, X., Dong, M., Chen, X., Jiang, M., Lva, X., Yan, G., 2007. Antioxidant activity and phenolics of an endophytic *Xylaria* sp. from *Ginkgo biloba*. *Food Chem*., **105**, 548–554.

Lumbsch, H. T., Huhndorf, S., 2007. Outline of Ascomycota. *Myconet*., **13**, 1–58.

McDonald, L. A., Barbieri, L. R., Bernan, V. S., Janso, J., Lassota, P., Carter, G. T., 2004. 07H239-A, a new cytotoxic eremophilane sesquiterpene from the marine-derived Xylariaceous fungus LL-07H239. *J. Nat. Prod.*, **67**, 1565–1567.

Ogasawara, Y., Yoshida, J., Shiono, Y., Miyakawa, T., Kimura K., 2008. New eremophilane sesquiterpenoid compounds, eremoxylarins A and B directly inhibit calcineurin in a manner independent of immunophilin. *J. Antibiot.*, **61**, 496–502.

Petrini, O., Petrini, L. E., Rodrigues, K., 1995. Xylariaceous endophytes: an exercise in biodiversity. *Fitopatol Bras*., **20**, 531–539.

Petrini, L. E., Petrini, O., 1985. Xylariaceous fungi as endophytes. *Sydowia,* **38**, 216–234.

Pittayakhajonwut, P., Suvannakad, R., Thienhirun, S., Prabpai, S., Kongsaeree, P., Tanticharoen M., 2005. An anti-herpes simplex virus-type 1 agent from *Xylaria mellisii* (BCC 1005). *Tetrahedron Lett*., **46**, 1341–1344.

Pongcharoen, W., Rukachaisirikul, V., Isaka, M., Sriklung, K., 2007. Cytotoxic metabolites from the wood-decayed fungus *Xylaria* sp. BCC 9653. *Chem. Pharm. Bull*., **55**, 1647–1648.

Sawadsitang, S., Mongkolthanaruk, W., Suwannasai, N., Sodngam, S., 2015. Antimalarial and cytotoxic constituents of *Xylaria* cf. *cubensis* PK 108. *Nat. Prod. Res*., **29**, 2033–2036.

Schulz, B., Boyle, C., Draeger, S., Römmert, A.-K., and Krohn, K. (2002). Endophytic fungi: a source of novel biologically active secondary metabolites *Mycol. Res.*, **106**, 996–1004.

Shiono, Y., Murayama, T., Takahashi, K., Okada, K., Katohda, S., Ikeda, M., 2005. Three oxygenated cyclohexenone derivatives produced by an endophytic fungus. *Biosc. Biotechnol. Biochem*., **69**, 287–292.

Shiono, Y., Motoki, S., Koseki, T., Murayama, T., Tojima, M., Kimura, K., 2009. Isopimarane diterpene glycosides, apoptosis inducers, obtained from fruiting bodies of the ascomycete *Xylaria polymorpha*. *Phytochemistry,* **70**, 935–939.

Silva, G. H., Oliveira, C. M., Teles, H. L., Pauletti, P. M., Castro-Gamboa, I., Silva, D. H. S., Bolzani, V. S., Young, M. C. M., Costa-Neto, C. M., Pfenning, L. H., Berlinck, R. G. S., Araujo, A. R., 2010. Sesquiterpenes from *Xylaria* sp., an endophyte fungus associated with Piper aduncum (Piperaceae). *Phytochemistry, Lett*., **3**, 164–167.

Singh, S.B., Zink D., Polishook, J., Valentino, D., Shafiee, A., Silverman, K., Felock, P., Teran, A., Vilella, D., Hazuda, D. J., Lingham, R. B., 1999. Structure and absolute stereochemistry of HIV-1 integrase inhibitor integric acid. A novel eremophilane sesquiterpenoid produced by a *Xylaria* sp. *Tetrahedron Lett.* **40**, 8775–8779.

Siriwach, R., Kinoshita, H., Kitani, S., Igarashi, Y., Pansuksan, K., Panbangred, W., Nihira, T., 2011. Xylaropyrone, a new γ-pyrone from the endophytic fungus *Xylaria feejeensis* MU18. *J. Antibiot*., **64**, 217–219.

Smith, C. J., Morin, N. R., Bills, G. F., Dombrowski, A. W., Salituro, G. M., Smith, S. K., Zhao, A., Macneil, D. J., 2002. Novel sesquiterpenoids from the fermentation of *Xylaria persicaria* are selective ligands for the NPY Y5 receptor. *J. Org. Chem*., **67**, 5001–5004.

Song, Y., Wang, J., Huang, H., Ma, L., Wang, J., Gu, Y., Liu, L., Lin, Y., 2012. Four eremophilane sesquiterpenes from the mangrove endophytic fungus *Xylaria* sp. BL321. *Mar. Drugs*., **10**, 340–348.

Tarman, K., Palm, G. J., Porzel, A., Merzweiler, K., Arnold, N., Wessjohann, L. A., Unterseher, M., Lindequist, U., 2012. Helicascolide C, a new lactone from an Indonesian marine algicolous strain of *Daldinia eschscholzii* (Xylariaceae, Ascomycota). *Phytochem. Lett.*, **5**, 83–86.

Tchoukoua, A., Suzuki, T., Ariefta, N. R., Koseki, T., Okawa, Y., Kimura, K.-I., Shiono, Y., 2017c. A new eremophilane sesquiterpene from the fungus *Xylaria* sp. V-27 and inhibition activity against degranulation in RBL-2H3 cells. *J. Antibiotics,* **00**, 1–4. doi:10.1038/ja.2017.120.

Tchoukoua, A., Ota, T., Akanuma, R., Ju, Y.-M., Supratman, U., Murayama, T., Koseki, T., Shiono, Y., 2017d. A phytotoxic bicyclic lactone and other compounds from endphyte *Xyalria curta*. *Nat. Prod. Res*., **31**, 2113–2118.

Wang, X. N., Tan, R. X., Wang, F., Steglich, W., Liu, J. K., 2005. The first isolation of a phlegmacin type pigment from the Ascomycete *Xylaria euglossa*. *Z. Naturforsch*., **60b**, 333–336.

Wei, H., Xu, Y.-M., Espinosa-Artiles, P., Liu, M. X., Luo, J.-G., U'Ren, J. M., Arnold, A. E., Gunatilaka, A. A. L., 2015. Sesquiterpenes and other constituents of *Xylaria* sp. NC1214, a fungal endophyte of the moss *Hypnum* sp. *Phytochemistry,* **118**, 102–108.

Wu, W., Dai, H., Bao, L., Ren, B., Lu, J., Luo, Y., Guo, L., Zhang, L., Liu, H., 2011. Isolation and structural elucidation of proline-containing cyclopentapeptides from an endolichenic *Xylaria* sp. *J. Nat. Prod*., **74**, 1303–1308.

Zhang, Y. L., Ge, H. M., Li, F., Song, Y. C., Tan, R. X., 2008. New phytotoxic metabolites from *Pestalotiopsis* sp. HC02, a fungus residing in *Chondracris rosee* gut. *Chem. Biodivers*., **5**, 2402–2407.

Zhang, Q., Xiao, J., Sun, Q. Q., Qin, J. C., Pescitelli, G., Gao, J. M., 2014. Characterization of cytochalasins from the endophytic *Xylaria* sp. and their biological functions. *J. Agric. Food Chem*., **62**, 10962–10969.